Aus der Klinik und Poliklinik für Frauenheilkunde und Geburtshilfe

der Ludwig-Maximilians-Universität München

Direktor: Prof. Dr. med. Sven Mahner

.....

Immunogenomic Infiltration is Associated with the Prognosis of Cervical Cancer

Dissertation

zum Erwerb des Doktorgrades der Medizin

an der Medizinischen Fakultät der

Ludwig-Maximilians-Universität München

vorgelegt von

Qun Wang

aus

China

Jahr
2022

Mit Genehmigung der Medizinischen Fakultät der

Ludwig-Maximilians-Universität München

Erster Gutachter:	apl. Prof. Dr. rar. nat. Udo Jeschke
Zweiter Gutachter:	Prof. Dr. Artur Mayehofer
Dritter Gutachter:	apl. Prof. Dr. Doris Mayr
ggf. weitere Gutachter:	_____
	_____
Mitbetreuung durch den promovierten Mitarbeiter:	Dr. Helene Hildegard Heidegger
Dekan:	Prof. Dr. med. Thomas Gudermann
Tag der mündlichen Prüfung:	02.06.2022

Affidavit

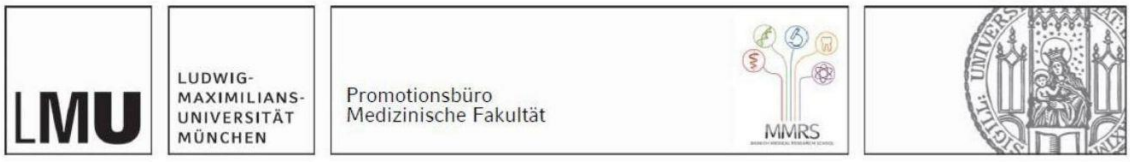

Affidavit

Wang, Qun
Surname, first name

Maistraße 11
Street

80337, München, Deutschland
Zip code, town, country

I hereby declare, that the submitted thesis entitled:

Immunogenomic Infiltration is Associated with the Prognosis of Cervical Cancer

.....

is my own work. I have only used the sources indicated and have not made unauthorized use of services of a third party. Where the work of others has been quoted or reproduced, the source is always given.

I further declare that the submitted thesis or parts thereof have not been presented as part of an examination degree to any other university.

Shan Dong, 30.06.2022
place, date

Qun Wang
Signature doctoral candidate

Table of content

List of abbreviations

APOD	apolipoprotein D
ATC	adoptive cell therapy
BMP6	Bone Morphogenetic Protein 6
CSK	C-Terminal Src Kinase
ROC	the Receiver Operator Characteristic curve
CART	chimeric antigen receptor T cell
CCL22	C-C motif chemokine ligand 22
CESC	Cervical Squamous Cell Carcinoma and Endocervical Adenocarcinoma
CD68	Cluster of Differentiation 68
DETF	differentially expressed TFs
DEG	different expressed genes
DFS	disease free survival
EGFR	Epidemal Growth Factor receptor
ELISA	enzyme-linked immunosorbent assay
EMT	epidermal - stromal transformation
FOXP3	forkhead box P3
FDA	food and drug administration
FIGO	International Federation of Gynecology and Obstetrics
FPKM	Fragments Per Kilobase of transcript per Million mapped reads
GEPIA	Gene Expression Profiling Interactive Analysis
GRN	Granulin Precursor
HPV-16	human papillomavirus type 16
HDAC1	Histone Deacetylase 1
IL-1β	Interleukin 1 Beta
IL3RA	Interleukin 3 Receptor Subunit Alpha
IL-4	Interleukin 4
IL-10	Interleukin 10
IL17RD	Interleukin 17 Receptor D
IRG	immune related genes
LEPR	Leptin Receptor
LPS	lipopolysaccharides
MDSC	Myeloid inhibitory cells

NFATC1	nuclear factor of activated T cells 1
NSCLC	non-small-cell lung cancer
OS	overall survival
PARP	poly-ADP-ribose polymerase
PBS	phosphate-buffered saline
PBMC	Peripheral blood mononuclear cell
PD1	programmed cell death protein 1
PD-L1	programmed death-ligand
SCC	squamous cell carcinoma
SIRG	immune related genes associated with survival rate
TAM	tumor associated macrophages
TAF	tumor-associated fibrocytes
TCGA	the Cancer Genome Atlas
TGF	transforming Growth Factor beta
TFRC	Transferrin Receptor
Th1	T helper type 1 cell
Th2	T helper type 2 cell
TIMER	Tumor IMmune Estimation Resource
Treg	regulatory T cells

1. Introduction

1.1 Tumor Microenvironment

Currently, it is regarded that tumor metastasis is formed by two steps. First, tumor cell proliferates and newborn blood vessels appear, then tumor cells break through the barrier of extra cellular of matrix and invade towards outside. Subsequently, tumor cells shape solid tumor at secondary site.

Tumor Microenvironment at primary tumor site is consist of TAMs, TAFs (Tumor-associated fibrocytes) , MDSC (Myeloid inhibitory cells), mastocyte and so on. These cells could promote tumor metastasis by secreating multiple cytokines and chemokines. Some specific tumor microenvironments can promote metastasis by affecting tumor cell proliferation, the expression level of metastasis related genes, inducing angiogenesis and degradation of chemokine extracellular matrix.

As to tumor microenvironment at secondary tumor site, since Stephen Paget proposed the hypothesis of “seed and soil”, numerous clinical and basic research have proved that tumor metastasis is the result of the interaction between the metastatic tumor cell (seed) and their organ microenvironment (soil) [1]. Especially, immunomicroenvironment that consist of immunocytes and inflammatory factors act in the progression of tumor. For example, a subgroup of CD11b+ macrophages could supervise emigrating tumor cells and promote the invasion [2]. Moreover, cancer cells could inhibit cytotoxic T-cell function to downregulate immune response [3]. In addition, immunotherapy, including adoptive cell therapy (ATC), targeted therapy, has acquired magnificent progression. For example, a creative ATC named chimeric antigen receptor T cell (CART) therapy has been successfully applied to hematological malignancies [4]. However, not all tumors have been found their specific antigens. Tumor immunotarget therapy is to use cytokines such as interferon and interleukin, immune checkpoint inhibitors such as PD-1/PD-L1 and CTL-4, and tumor vaccines or other various mechanisms to stimulate or enhance the body's own immune response to resist tumors [5,6]. However, partial patients are resistant to the therapies because of individual heterogeneity, or multiple immune escape mechanisms, or low immune cell infiltration in the tumors [7].

1.2 Targeted therapy

Presently, as the development of molecular biology and genetics, researchers reveal that malignant tumor presents biological defects with complex specificity, including the mutation of oncogenes and anti-oncogenes, the decoration of chromosome and so on. Targeted therapy avails the target molecules of tumor tissues or cells with specific structure to kill tumor cells specificly with drugs that can combine with the target molecules.Targeted therapies are developing toward to be personalized and genome-driven [8].

Bevacizumab, as a monoclonal antibody of VEGFR, is first to attempt to target newborn tumor vessels in colon cancer [9]. Subsequently, Trastuzumab and Neratinib are admitted to treat breast cancer by targeting HER2 [10]. Vemuafenib, as a mutant inhibitor of BRAF, works for 80% Melanoma patients with muted BRAFV600E [11]. Erbtinib and Gefitinib are a kind of EGFR-TKLs, can shrink the tumor in 61% NSCLC patients [12]. Imatinib Mesylate is BCR-ABL TKI, which can increases the PFS and OS of CML patients, compared to traditional medicine [13.] Sorafenib can extend the OS of HCC patients by targeting VEGFR [14]. Bortezomib, capable of combining the proteasome subunit of 20S protein, increases complete remission to 43% [15]. In cervical cancer, target therapy mainly acts in the respects of anti-angiogenesis, block EGFR (Epidemal Growth Factor receptor), inhibit PARP (poly-ADP-ribose polymerase), and inhibit immune check points. For example, Bevacizumab combined with traditional chemotherapy in the treatment of cervical cancer can improve the anticancer effect, but the side effects are also heavy [16]. Pazopanib, inhibitors of VEGFR and EGF have effects in cervical cancer of late stage [17]. Cediranib, as a tyrosine excitation of VEGFR, can extend the PFS of metastastic or recurrent cervical cancer patients when combined with traditional drugs[18]. Trastuzumab, as a monocolonal antibody of EGFR, can increase the sensibility of chemotherapeutics to HeLa cells [19]. Gefitinib and Erlotinib, as tyrosine kinase inhibitors, can increase cumulative survival rate of late staged cervical cancer patients, accompanied with lighter side effect [20]. Immune checking points are the signals for inhibiting immune. By adjusting the strength and range of immune activities, the normal tissue can be protected from damage. Immue check point therapy is to adjust regulatory T cells to elavate immune response to treat tumors. However, less reports are concerned with cervical cancer.

Polymethyl methacrylate (PMMA), a synthetic polymer, the Food and Drug Administration has approved it as some human clinical applications like bone cement. PMMA 4 particles promote macrophages in vitro to produce higher level of TNF-alpha, and acquire better performance of anti-tumor effect in vivo [21]. RAW 264.7 macrophages can release pro-inflammatory and anti-inflammatory factors TH1, TH2 and TH17 under the induction of a novel synthetic fluoroquinolone derivative 6-fluoroquinolone derivative 6-fluoro-8-nitro-4-oxo-1,4-dihydroquinoline-3-carboxylate (6FN). The growth of HeLa cells was observed to have a significant inhibitory effect [22]. Indomethacin is used as a prostaglandin inhibitor.The therapeutic strategy of the combination of OK-432 and Ind. enhances the immunopotentiation mediated by macrophages, leading to a better effect in antitumor [23]. Peritoneal macrophages collected from cervical cancer patients, when treated with sizofiran (SPG) and rIFN-gamma simutaneously, show a potent tumoricidal effect [24]. Furthermore, sizofiran -immunotherapy assisted with radiotherapy enhances the cytotoxicity of macrophages for cervical cancer patients [25]. The vaccination of synthetic long peptide (SLP) can promote through T cells secrete a sufficient amount of cytokines to convert M2-like macrophages into M1-like macrophages stimulated by cytokines. which is elementary for shrinking cervical tumor tissue [26]. Antibodies in sera of recombinant vaccinia virus expressing bovine papillomavirus E2 gene can activate macrophage-mediated cytotoxicity and effectively kill papilloma tumor cells [27].

Moreover, target therapy is susceptible to be drug resistant. There are multiple mechnisms to cause drug resistance. First, the strengthed drug transshipment. A decrease in uptake of drugs by tumor cells , strengthened responsibility to the drug, and enhanced expression of drug transfer bump are closedly associated with drug resistance. In some solid tumor, such as colon cancer, kidney cancer and liver cancer, the expresion of ABCB1 is upregulaed. The highly expressed ABCB1 could weaken the effect of medicine by pumping medicine out of the cells [28] Some targeted drugs like imatinib, erlotinib, and sunitinib could be released out of cells by being combined with ABCB1 and ABCG2, which resulting in drug resistance [29]. Second,the change of targeted genes. The mutation or the changed expression level of targeted genes are ssociated with drug resistance. For example, the most important reason for NSCLC patients to get resistant when treated with EGFR-TKI is the mutation of EGFR T790M [30]. The third reason is the activation of targeted gene bypass, which will cause compensatory so that drug resistance could appear. In lung carcinoa cells resistant to EGFR-TKI, researchers find the proliferation of c-Met bypass [31]. Fourth, drug - adapted epidermal - stromal transformation (EMT). The lack of MED12 could induce NSCLC cell to produce EMT by activating TGF-b pathway so that EGFR targeted therapy gets drug resistant [32]. Last but not the least, the change of tumor microenvironment. TME is closely associated with drug resistance. The mechanisms of drug resistance contains not only the change in the cancer cells but also that of the environment around cancer cells. Tumor associated mesenchymal cells and fibroblasts could produce drug resistance by activating PI3K-AKT and MEK-ERK pathway [33]. HGF secreated by stromal cells could increase the phosphorylation of its cognite receptors c-MET so that cell lines with BRAF-V600E mutation could be resistant to BRAF inhibitors. Similarly, enhancing the expression of PDGF-C in tumor associated fibroblasts could enhance the drug resistance [34]. Developing drugs with multiple targets or the combination application of drugs with single target is urgent. Therefore, further researches to identify more effective immune checking points are necessary.

1.3 Immune related genes and prognostic prediction

Immune related genes have not only the potential to be immune checking points but also to predict the prognosis of cancer patients. A predictive model consisted of 10 IRGs (immune related genes) could predict the prognosis for head and neck cancer [35]. Seven IRGs are conducted to be a predictive model of Colon Adenocarcinoma [36]. A predictive model is built by Six IRGs for lung squamous cell carcinoma [37]. Thirteen IRGs are screened out to conduct a prognostic formula for bladder cancer [38]. A prognostic index has been constructed grounded in percent-splice-in values in squamous cervical cancer (SCC) [39]. Genomic alterations have been explored and a venture index pattern that can supervise HPV- correlated bladder disease has been developed [40]. A venture mark pattern has been created grounded in variously embodied glycolysis-correlated genes, and the pattern is capable of anticipating the analysis of cervical cancer masses [41]. Currently, A 4-gene prognostic venture mark pattern has been set in cervical cancer [42]. Apart from the contemporary researches, it also exists multiple other researches on the prognostic pattern [43,44]. However, less reports are concerned with cervical cancer. Therefore,

further researches to identify an efficient model to predict individual prognosis of cervical cancer patients and immunotherapy targets are necessary.

We have explored twenty immune genes crucially correlated with the survival rate of cervical cancer patients. DUOX1, IL17RD, CSK, NFATC4, TGFA, CD79,LEPR, N2RF1, EPGN, GRN, and TRAV26-1 have still no related reports in the field of cervical cancer. APOD is expressed less in cervical cancer, while TFRC is expressed more in cervical cancer, contrasted with normal cervix [45] [46]. A former study has identified that cervical cancer is significantly associated with the polymorphism of rs1041981 of LTA [47]. There is a significant association between the rare allele (A) of SNP rs2239704 of the 5′ UTR of the LTA gene and increased risk of cervical cancer [48]. F2RL1 is up-regulated in cell lines of cervical cancer and crucially associated with poor OS [49,50]. Increased HGF in lesions of cervical cancer is significantly related to a poor prognosis [51]. HDAC1/DNMT3A-containing complex participate in supressing cancer stem cells in cervical cancer [52]. HGF and BMP6 can promote cervical cancer cells as to migration and invasion [53] [54]. CD123(+) dendritic cells is significantly less in cervical cancer patients ' peripheral blood, contrasted with the control [55]. A higher proportion of Nrp1+ T-regs suppresses the immune response to distant cervical cancer cells [56]. The facts mentioned above are consistant with our current findings. However, Tyk2 is proved to be up-expressed in squmous cervical cancer cells [57], which is opposite from our study. Low-through-put experiment, like western blotting analysis, is required to verify accurately. PTPN6 is proved to be desperately correlated with HPV infection to cervical cancer patients, which can be interpreted as cell defense reaction [58].

To probe molecular mechanism behind the clinical importance, we established a transcription factor-mediated network that could adjust hub IRGs. Among the different expressed transcription factors associated with survival rate (SDETFs), FIGO stage and tumor size is significantly correlated with FOXP3 [59]. FOXP3 is correlated with lymphatic angiogenesis of cervical cancer [60]. FOXP3 is proved to be high expression in cervical cancer, and it benefits to the proliferation, invasiveness, and inhibiting the apoptosis of cervical cancer cells [61]. Totally, to cervical cancer patients, FOXP3 is a risk contributor for the survival rate, which is accordant with our present findings. CBX7 restrains cervical cancer cells to proliferate [62]. LTA restrains CD4+ T-cells to proliferate in a FOXP3+ Treg-dependent manner in chronic hepatitis C patients, suggesting that LTA works at FOXP3 [63]. Hence, former researches supply restricted data over the mechanism of 10 IRGs in the respect of cervical cancer patients‘ survival rate.

Discoveries which are associated with the function the total macrophage have on cervical cancer has long been a point of controversy. It has been found that the quantity of macrophage in infiltrating carcinoma is larger compared to that of squamous intraepithelial lesion of cervix [64]. What’s more, the quantity of macrophage is larger in squamous intraepithelial lesion than regular cervical tissue [65]. On the contrary, a research indicated that existence of the significant infiltration of macrophages showed no association with the grade of tumor and the condition of the lymphoglandula but was negatively correlated with the phrase of the tumor [66]. Nevertheless, Davidson et al. have demonstrated that the

density of the macrophage is irrelevant to the survival rate of patients who suffer from cervical cancer [67]. Moreover, some studies have shown that CD68 macrophages that stand for all activated macrophages could not be regarded as a predictive symbol[68,69]. The link between M2-like macrophages and CC is specific. When compared with M2-like TAMs in normal cervical specimens, the content of M2-like TAMs can be found to be significantly higher in cervical squamous cell carcinoma tissues [70]. This indicates that the high index of CD163+ is clearly closely related to FIGO and lymphatic metastasis [71]. CD204+M2 macrophage tumor infiltration density values are at a high level in cervical adenocarcinoma, and compared with normal organisms, it is found to affect the length of lifespan. [72].

1.4 Macrophage

Targeted therapy focus not only tumor cells and T cells, but also some immunosuppressive cells, such as Treg cells and tumor associated macrophages (TAMs) [9,73].

The sources of macrophages are mainly two: tissue-resident macrophages, and infiltrating macrophages.

When embryonic organs are formed, macrophages residing on tissues are mainly macrophages derived from yolk sacs and epithelial tissues or epithelium of precursors of the fetal liver in a normal state. Macrophages will persist into adulthood and exist as resident self-sustaining [74]. The functions and properties they exhibit are related to the location of their organization [75,76]. After birth, monocytes derived from the bone marrow or spleen can replenish macrophages in tissues on their own in the event of injury and infection. The location of these macrophages is in the interstitial position. For example, when alveolar macrophages are replaced by postpartum monocytes, new macrophages are generated with the same expression profile as alveolar macrophages. This phenomenon suggests that the function of macrophages is related to the environment in which the tissue is located [77]. The function of tissue-resident macrophages in maintaining balance in the body is affected by pathological or physiological inflammation [74,78]. For example, by assisting the mediation of macrophages, the transformation of lymphocytes can be inhibited by seminal plasma. It was also found that the presence of seminal plasma also interferes with the adhesion, diffusion, and phagocytic activity of Peritoneal macrophages of Aspergillus microcess [79]. In addition, with SPG and IFN-γ, strongly active tumor cells can be obtained, and the inhibitory effect on PGE2 will increase with the increase of TNF, IFN-γ, and IL-1 secretion [80].

Studies involving the nature of infiltrating macrophages have revealed that circulating monocytes can concentrate most pro-inflammatory mediators at the tumor site, or in tissues that produce inflammation or infection. When in the stage of inflammation, there are mainly two types of inflammatory macrophages, which promote inflammation and inhibit inflammation, or become M1-like or M2-like. These two types of macrophages are closely related to the following factors, including growth factors, metabolic capacity, local aerobic capacity, tissue cells, and tissue mechanisms [81]. In the course of specific

practice, the influencing factors received during macrophage production are specific. It mainly includes four aspect factors, M2a, M2b, M2c, and M2d [82].

Th1 cytokines IFN γ, IL-2, IL-3, IL-12, TNF-α, these four factors will affect the polarization of M1-like macrophages. For example, induction can be performed by LPS and TLR as agonists. Pro-inflammatory factors are secreted by M1-like macrophages, mainly composed of the following factors, IL-1β, IL-6, IL-12, IL-23, iNOS and tumor necrosis factor α (TNF-α), chemokine ligand 9 (CXCL-9), CXCL-10, and also include MHC I and MHC II. Therefore, it can be concluded that M1-like macrophages have an effective inhibitory effect on inflammation as well as tumors. In contrast, Th2 cytokines can induce the production of M2-like macrophages, which may mainly include the following factors, such as IL-4, IL-10, TGF-13, TNF-α, TGF-β β, GM-CSF, immune complexes, and TLRs. In the process of increasing the value of cervical cancer cells, it is affected by TAM, and the value-added, metastasis and lethality of cervical cancer cells are all related to it. At the same time, TAM can also play a reshaping role in cervical cancer, involving fibrosis and the effective generation of blood vessels. According to studies, TAM functions more closely to M2-like macrophages [85].

Generally, macrophages are differentiated into two types: M1 (classically activated) and M2 (alternatively activated) macrophages [86]. M1 macrophages are stimulated by Th1 factors. They are anti-tumor. Oppositely, M2 macrophages are stimulated by Th2 factors. They are pro-tumor [87]. Recently, three different subtypes of M2 macrophages (M2a, M2b, and M2c) have been described. M2a macrophages are polarized by IL-4 and act in tissue remodeling and reducing inflammation [88,89]. M2b macrophages are stimulated by Fc γ receptor plus LPS or IL-1β and act in antigen presentation that causes Th2 cell differentiation that is detrimental for cancer immunotherapy [86,91] while some studies suggest that Th2 cells could work well in eliminating cancer as soon as they are transferred [92,93]. M2c is stimulated by some anti-inflammatory stimuli, such as IL-10 or TGF and associated with immunoregulation, matrix deposition and tissue remodeling [94]. Studies have shown that M2 subtypes play a role in tumors. M2a synergistically promote migratory and invasive responses of breast cancer cells [95]. M2b could promote hepatoma carcinoma progression [96]. Pellino-1 inhibit tumor growth in vivo by inhibiting IL-10-induced M2c macrophage polarization [97].

TAMs are shaped by various activation modes and labelled with various markers in different tumors [98]. As far as cervical cancer, the formation mechanism of TAMs principally associate with tumor-derived molecules, the anaerobism mini-environment and molecules which come from other sources. With regard to the generation of TAMs, researchers discovered in 1982 that monocytic functions the chemotaxis, the inhibitory effect of the T cell mitosogen response is affected by phagocytosis and auxiliary function when hyaline leukocytes were precultured in cervical cancer sera. According to the reasonable speculation of the study, it can be found that containing some components in the cancer serum can play an immunosuppressive function, mainly by inhibiting the function of monocytes in the cancer-containing components. [96]. What's more,it was also found that When treating M1-like macrophages using supernatants from CC cell lines, M2-like phenotypes such as CD163, TLR-3, -7, -9, and IL-10 can be found increased [97,98].

In a similar way, cervical cancer cells which are co-incubated reduce the macrophage M1-like polarization partly by the means of downregulating necroptosis [99]. Molecules from seminal plasma: COX-2 can be activated by seminal plasma (SP) to achieve high expression of prostaglandin E2 receptors in cervical adenocarcinoma cells [80,81]. Cervical cells produce higher concentrations of IL-6 when stimulated in vitro by normal seminal plasma [82]. In addition, it plays an important role in the polarization of M2-like macrophages, prostaglandin E2 and IL-6 [79]. The results suggest that seminal plasma (SP) may have an impact on the differentiation of monocytes through the effects on prostaglandins or IL-6 in cervical cancer. However, more experimental verification of the effect of the molecules in SP on macrophages is expected to be performed.

Molecules from anaerobic microenvironment: Overexpression of Nrp-1 in cervical cancer in the absence of oxygen can lead to the aggregation of cervical TME of hypoxic types and the transformation of polarized macrophages into M2-like phenotypes. [83]. Nevertheless, these researches did not illustrate which composition resulted in the M2-like induction. As the investigation moves forward, researchers have discovered that CC cell-derived factors play role in the polarity as well as the activation of monocytes.

Molecules from anaerobic microenvironment: Overexpression of Nrp-1 in cervical cancer in the absence of oxygen can lead to the aggregation of cervical TME of hypoxic types and the transformation of polarized macrophages into M2-like phenotypes. [83]. Nevertheless, these researches did not illustrate which composition resulted in the M2-like induction. As the investigation moves forward, researchers have discovered that CC cell-derived factors play role in the polarity as well as the activation of monocytes.

Heusinkveld et.al through the study of the interaction between CD4(+)Th1 cells, the main discovery is that the M2-like macrophages induced by cervical cancer cells can be stimulated by high levels of stimulation to obtain lymphoid homecoming marker CCR7, and under the activation of lymphoid homecoming markers, M1-like macrophages can be obtained, and a tumor suppression environment can be achieved under this condition [100]. The specific composition of Th1 is unclear for macrophages.

Saito T et. By studying the degree of rIFN-γ its inhibitory effect on tumor growth with dose changes when treating cervical cancer. In addition, rIFN-γ has been found to have a strong inhibitory effect on the growth of human adherent ascites cells against ovarian cancer and melanoma cells [101]. However, there is no solid evidence to verify this inhibitory effect, and rIFN-γ has an effect on the spread of TAM, thereby playing a role in eliminating tumors in CC.

TAMs mediates immune tolerance so that they could enhance the effects of some anti-tumor drugs. For example, the clearance of TAM in hepatoma could enhance the effect on inhibiting angiogenesis and metastasis of Sorafenib [102]. However, some studies show that the Fc γ receptor of TAMs participate in antibody dependent cellular cytotoxicity. Therefore, the clearance of TAMs will block the response of effector T cells resulting in decreasing pharmaceutic effect [103]. What is the distribution of subtypes of macrophages in TAMs in various cancers and how to regulate tumor-promoting TAMs to anti-tumor types are essential to be studied.

1.5 Cervical cancer

The fourth important factor in the occurrence of cervical cancer death resulting from cancers in female around the world and the third most common type of cancer. It is also the most prevalent kind of cancer in the developing cancers. Among global women, new cases are about 466000 each year. The occurrence of cervical cancer is associated with many factors, such as the infection of HPV, fecundity, lower age of first delivery, messy sex, poorer economy status, smoking, and long-term oral contraceptive [104,105]. Squamous cell carcinoma (SCC) and adenocarcinoma occupy the most histological subtypes of cervical cancer, accounting for 70% and 25%, respectively [106].

Continuous HPV infection will promote the form of pre-metastatic niche of cervical cancer. The highly risky types HPV 16/18 can activate the signal transduction of interleukin-6 or the pathway of signal transduction and activator of transcription 3 (STAT3) to promote the progression of cervical cancer. On one side, in the HPV genome, E6 could activate STAT3 to promote cervical cancer cells to produce IL-6. STAT3 in activated fibroblasts could further promote senescence of normal stromal fibroblasts by autocrine and paracrine pathways. Eventually, pre-metastatic niche is reconstructed, which accelerates the growth and malignant transformation of cervical epithelial cells. The process of activating STAT3 can polarize M1 to M2 macrophages, while M2 macrophages, as a kind of anti-inflammation cells, can promote the proliferation of cancer cells [107]. For example, in adenocarcinoma of the cervix, the amount of CD204+ M2 macrophages is significantly negatively associated with disease free survival rate (DFS), which indicates that the higher amount of CD204+ M2 macrophages could predict worse prognosis of cervical cancer patients [108]. Meanwhile, the activation of STAT3 could also promote the growth of tumor-associated blood and lymphatic angiogenesis[109]. On the other side, oncoprotein E6 of HPV could induce cervical cancer cells secrete factors to attract tumor associated fibroblasts by the pathway of IL-6 or transcription factor activation to promote the metastasis of tumor cells [110].

Although recent improvements in therapeutic options, including chemoradiotherapy and surgery, have increased the survival rate of patients with primary cervical cancer, the 5-year survival rate of the patients who suffer from local or distant metastasis is reduced to 50% [111,112]. At present, immunotherapy has made a breakthrough in the treatment of cervical cancer. In particular, the monoclonal antibody pembrolizumab has been developed into a drug that FDA approved for second-line therapy in patients with cervical cancer who are positive for PD-L1 or who have high microsatellite instability or mismatch repair gene defects. The Listeria monocytogenes live inactivated vaccine vector (ADXS11-001) can be genetically engineered to generate the fusion protein of HPV-16 E7 to stimulate the immune response to E7. However, the overall remission rate is low [113,114]. Therefore, efforts to further screen out patients with good response to immunotherapy and to search for new targeted molecules would be crucial.

1.6 CCL22

Huang et al. studied the effects of overexpression of the CCL22 gene on cancer cells in the head and neck [115]. CCL22 can be found in macrophages of glossal squamous cell carcinoma [116]. In addition, CCL22 was also found to be present in rectal cancer M2-like macrophages[117]. As a kind of secreted protein of monocyte-derived macrophages and DCs, the C-C motif chemokine ligand 22 (CCL22) gene participates in chemotactic activity for various immunocytes including monocytes and chronically activated T lymphocytes [118-120]. CCL22 could be up-regulated by cytokines secreted from Th2 cells, and down-regulated by cytokines from Th1 cells. Furthermore, some kinds of cancer cells also produce CCL22 [121]. CCR4 is the receptor of CCL22. CCR4 is expressed on the surface of Th2 and Treg cells [122]. CCL22 could also inhibit immune activities to microbial infections and cancer progression by attracting Th2 cells and Treg cells [123]. For example, CCL22 could attract entering the mass of adjustable T (T-reg) in tumor cells and decrease immune cells in ovarian cancer [124]. High leveled CCL22 expressed in M2 macrophages confers colorectal cancer to be resistant to 5-fluorouracil [125]. Studies have shown that the expression of the mRNA of the CCL22 gene found in tissues of cervical cancer is relatively high relative to the normal part [126]. Li et al. conducted a meticulous study of CCL22 and found that the relatively independent influencing factor for postoperative recovery after breast cancer treatment was the secretion content of CCL22 [127]. Other studies have shown a strong association between the CCL22 gene, derived from serum macrophages, and the risk of glioma development [128]. Another important factor affecting the postoperative recovery of patients with stage II/III gastric cancer is CCL22 [129]. However, its prognostic value and mechanism to promote cervical cancer progression remains unclear.

1.7 JAK/STAT pathway and cervical cancer

JAK/STAT pathway is mainly consisted with transducing protein of JAKs and STATs. JAKs, including JAK1 and JAK2, belong to tyrosine protein kinases, which can bind to a variety of cytokines and activate STAT. STATs is a kind of transcription factor, STAT3 is more common, STAT3 is a nuclear transcription factor. Among the treatment options for cervical cancer, the most important treatment direction is the important therapeutic role of the JAK/STAT pathway, which involves the important role of STAT3 and STAT5 in tumor proliferation, cycle and spread. In cervical cancer cells, the JAK/STAT signaling pathway activated by Bcl-2 signaling promotes the growth activity of tumor cells, the spread of tumor cells, and the adverse effects on other cells [130]. There is an important association between overexpression of the STAT-3 gene in cervical cancer and HPV infection [131]. After cervical cancer treatment is completed, the expression of STAT-3 is considered the worst effect of prognosis [132]. The most important factor affecting the severity of cervical cancer is the increased content of the STAT5 protein [133]. In addition, comparison with normal control groups reveals that THE EXPRESSION OF STAT-3 is affected by over expression of STAT-5 [131]. Therefore, it can be concluded that the signaling pathway that plays a key role in the occurrence of cervical cancer is the signaling of JAK-

STAT [134]. In addition, the increase in the value of cervical cancer cells can be effectively controlled by the upregulation of par2 (F2RL1) gene content, which is consistent with the current research results, that is, the overexpression of the F2RL1 gene is involved in the process of JAK-STAT signaling.

1.8 Aims

The current doctoral thesis aims to investigate the association between tumor immunomicroenvironment and postoperative recovery in patients with cervical cancer. Specifically, manuscript 1 aims to create a risk assessment model that includes the detection of 10 genes to predict overall the patient's probability of survival who suffer from squamous cell carcinoma of the cervix (SCC). Meanwhile, immune-related genes that are closely related to survival are screened out, which provide potential therapeutic targets. Manuscript 2 focus on an immune-related gene CCL22 to study the prognostic role of CCL22 and the mechanism behind it in cervical cancer.

2. Summary

In conclusion, the current doctoral thesis highlights the prognostic significance of the immune-related genes in cervical cancer. In manuscript 1, by the method of bioinformatics, a risk score model consisting of 10 immune-related genes was constructed, which could predict prognosis moderately and steadily in squamous cell cervical cancer (SCC) patients with FIGO stage I, regardless of the age and grade. Meanwhile, 22 immune-related genes associated with the survival of cervical cancer were identified which provided potential therapeutic targets. Moreover, JAK-STAT pathway was the hot pathway of the 22 immune-related genes. However, the results of high-through method are inaccurate. More experiments need to be performed. In manuscript 2, CCL22 positive infiltrating cells were associated with overall survival rate of cervical cancer patients. The number of infiltrating CCL22+ cells was positively correlated with that of infiltrating FOXP3+ T-reg cells. CCL22 was secreted by M2 macrophages. However, the mechanism of CCL22 in promoting cervical cancer still need to be studied further.

3. Zusammenfassung

In der vorliegenden Dissertation wird die prognostische Bedeutung der immunbezogenen Gene bei Gebärmutterhalskrebs erläutert. In Manuskript 1 wurde durch die Methode der Bioinformatik ein Risikoscore-Modell aus 10 immunbezogenen Genen konstruiert, das die Prognose von Patientinnen mit Plattenepithelkarzinom des Gebärmutterhalses (SCC) im FIGO-Stadium I unabhängig von Alter und Grad vorhersagen kann. Inzwischen wurden 22 immunbezogene Gene identifiziert, welche mit dem Überleben von Gebärmutterhalskrebs in Verbindung stehen und potenzielle therapeutische Ziele darstellen. Darüber hinaus war der JAK-STAT-Signalweg der wichtigste der 22 immunbezogenen Gene. Die Ergebnisse der High-Through-Methode sind jedoch ungenau, so dass weitere Versuche durchgeführt werden müssen. In Manuskript 2 wurden CCL22-positive infiltrierende Zellen mit der Gesamtüberlebensrate von Patientinnen mit Zervixkarziom in Verbindung gebracht. Die Anzahl der infiltrierenden CCL22+-Zellen korrelierte positiv mit der Anzahl der infiltrierenden FOXP3+-T-Zellen. CCL22 wurde von M2-Makrophagen sezerniert. Der genaue Mechanismus von CCL22 bei der Förderung von Gebärmutterhalskrebs muss jedoch noch weiter untersucht werden.

4.Your contribution to the publications

4.1 Contribution to paper I

I am the independent first author of this paper. I am responsible for performing R language script, analyzing data and writing manuscript.

4.2 Contribution to paper II

I am the independent first author of this paper. I am responsible for performing experiments, analyzing data and writing manuscript.

5. Paper 1

International Journal of *Molecular Sciences*

MDPI

Article

Immunogenomic Identification for Predicting the Prognosis of Cervical Cancer Patients

Qun Wang [1], Aurelia Vattai [1], Theresa Vilsmaier [1], Till Kaltofen [1], Alexander Steger [2], Doris Mayr [3], Sven Mahner [1], Udo Jeschke [1,4,*] and Helene Hildegard Heidegger [1]

[1] Department of Obstetrics and Gynecology, University Hospital, LMU Munich, 80377 Munich, Germany; wqyxdz888@163.com (Q.W.); aurelia.vattai@med.uni-muenchen.de (A.V.); Theresa.Vilsmaier@med.uni-muenchen.de (T.V.); till.kaltofen@med.uni-muenchen.de (T.K.); sven.mahner@med.uni-muenchen.de (S.M.); Helene.heidegger@med.uni-muenchen.de (H.H.H.)
[2] Klinik für Innere Medizin I, Technische Universität München, 80333 Munich, Germany; alexander.steger@tum.de
[3] Department of Pathology, LMU Munich, 80377 Munich, Germany; doris.mayr@med.uni-muenchen.de
[4] Department of Obstetrics and Gynaecology, University Hospital Augsburg, Stenglinstr. 2, 86156 Augsburg, Germany
* Correspondence: udo.jeschke@med.uni-muenchen.de or Udo.Jeschke@uk-augsburg.de

Abstract: Cervical cancer is primarily caused by the infection of high-risk human papillomavirus (hrHPV). Moreover, tumor immune microenvironment plays a significant role in the tumorigenesis of cervical cancer. Therefore, it is necessary to comprehensively identify predictive biomarkers from immunogenomics associated with cervical cancer prognosis. The Cancer Genome Atlas (TCGA) public database has stored abundant sequencing or microarray data, and clinical data, offering a feasible and reliable approach for this study. In the present study, gene profile and clinical data were downloaded from TCGA, and the Immunology Database and Analysis Portal (ImmPort) database. Wilcoxon-test was used to compare the difference in gene expression. Univariate analysis was adopted to identify immune-related genes (IRGs) and transcription factors (TFs) correlated with survival. A prognostic prediction model was established by multivariate cox analysis. The regulatory network was constructed and visualized by correlation analysis and Cytoscape, respectively. Gene functional enrichment analysis was performed by Gene Ontology (GO) and Kyoto Encyclopedia of Genes and Genomes (KEGG). A total of 204 differentially expressed IRGs were identified, and 22 of them were significantly associated with the survival of cervical cancer. These 22 IRGs were actively involved in the JAK-STAT pathway. A prognostic model based on 10 IRGs (*APOD*, *TFRC*, *GRN*, *CSK*, *HDAC1*, *NFATC4*, *BMP6*, *IL17RD*, *IL3RA*, and *LEPR*) performed moderately and steadily in squamous cell carcinoma (SCC) patients with FIGO stage I, regardless of the age and grade. Taken together, a risk score model consisting of 10 novel genes capable of predicting survival in SCC patients was identified. Moreover, the regulatory network of IRGs associated with survival (SIRGs) and their TFs provided potential molecular targets.

Keywords: cervical cancer; tumor immune; bioinformatics analysis; TCGA; KEGG

check for updates

Citation: Wang, Q.; Vattai, A.; Vilsmaier, T.; Kaltofen, T.; Steger, A.; Mayr, D.; Mahner, S.; Jeschke, U.; Heidegger, H.H. Immunogenomic Identification for Predicting the Prognosis of Cervical Cancer Patients. *Int. J. Mol. Sci.* **2021**, *22*, 2442. https://doi.org/10.3390/ijms22052442

Academic Editor: Fabio Grizzi

Received: 3 February 2021
Accepted: 24 February 2021
Published: 28 February 2021

Publisher's Note: MDPI stays neutral with regard to jurisdictional claims in published maps and institutional affiliations.

Copyright: © 2021 by the authors. Licensee MDPI, Basel, Switzerland. This article is an open access article distributed under the terms and conditions of the Creative Commons Attribution (CC BY) license (https://creativecommons.org/licenses/by/4.0/).

1. Introduction

Cervical cancer is primarily caused by the infection of high-risk human papillomavirus (hrHPV), and it ranks the fourth most common cancer in females globally [1]. There are approximately 527,000 new cases of cervical cancer and 265,000 related deaths annually [2]. Among all pathological types of cervical cancer, squamous cell carcinoma (SCC) and adenocarcinoma account for 80–85% and 15–20%, respectively [3]. Presently, although the development of surgery, radiation therapy, and chemotherapy, the rates of recurrence and metastasis in patients with late-stage cervical cancer are still up to 40.3% and 31%, respectively [4]. The prognosis of patients with metastatic cervical cancer remains poor,

with a median survival of 8–13 months [5]. Therefore, it is urgently necessary to identify effective predictive biomarkers and molecular mechanisms involved in the prognosis of cervical cancer, which may help find better predictive and therapeutic targets.

Increasing attention has been paid to research on immunotherapy for cervical cancer. Zhou J et al. have shown that IFNα-expressing amniotic fluid-derived mesenchymal stem cells can suppress HeLa cell-derived tumors in a mouse model [6]. An HPV vaccine containing some HPV16 E7 peptides presents an anti-tumor effect in tumor-free mice [7]. Jung KH et al. have enhanced the efficacy of T cells by optimizing the maturation and function of dendritic cells with lipopolysaccharide (LPS) and interferon (IFN)γ, adding interleukin (IL)-21 during priming, and depleting memory T cells, and the reliable expansion of T cells specific for oncoproteins E6 and E7 has been achieved [8]. Currently, the treatment for immune checkpoints, such as cytotoxic T lymphocyte 4 (CTLA-4), programmed death protein 1 (PD-1), and its ligand (PD-L1), has shown initial success against cervical cancer [9]. Since the great potential in immunotherapy, more molecular mechanisms need to be explored to improve the immunotherapy. Transcriptome profiling, as a high-throughput research approach, has been applied to many cancer studies. For example, i n non-small cell lung cancer and thyroid cancer, the prognostic value of immune-related genes (IRGs) has been analyzed with the data acquired from sequencing [10,11]. However, the clinicopathological correlation and prognostic significance of IRGs in cervical cancer remain largely undetermined.

In the present study, we identified 204 differentially expressed IRGs between cervical tumor and para-tumor tissues, and an individualized prognostic prediction model based on risk scores was constructed for patients with early-stage SCC. Functional enrichment analysis showed that the IRGs associated with survival (SIRGs) were mainly involved in the receptor-ligand activity and JAK-STAT signaling pathway. The receiver operating characteristic (ROC) curve and risk curve verified the moderate efficacy of the predictive model. The area under the curve (AUC) was 0.738. The overall survival (OS) in the high-risk group was significantly lower, compared with the low-risk group ($p = 2.702 \times 10^5$). Moreover, Kaplan-Meier analysis showed that the model worked steadily, regardless of age and grade. The risk curve showed that the higher the risk score, the more the deaths, and the shorter the OS. Besides, according to univariate and multivariate cox regression analyses, the risk score could be an independent risk factor (HR = 3.170, 95% CI [1.701–5.910], $p = 0.0001$) adjusted by age, grade, stage, and histological type. Interactive transcription factors (TFs) for IRGs associated with survival were also explored. These results could offer not only a promising prediction model for cervical cancer prognosis but also molecular targets to study the immunity mechanism for cervical cancer progression.

2. Results

2.1. Identification of Differentially Expressed Genes (DEGs)

A total of 2240 DEGs, including 1412 down-regulated and 1928 up-regulated ones (Supplementary Materials Figure S1a and Figure 1a), were identified by comparing the gene expression data between three para-tumor tissue specimens and 286 primary cervical tumor tissue specimens. By comparing the IRGs obtained from the Immunology Database and Analysis Portal (ImmPort) database [12] with the DEGs, 204 IRGs overlapped with DEGs were selected, including 115 down-regulated, and 89 up-regulated ones (Figure S1b and Figure 1b). Gene Ontology (Go) analysis revealed that these differentially expressed IRGs were significantly associated with tumor-related biological processes. Moreover, "epithelial cell proliferation", "receptor complex" and "growth factor binding" were the most frequent biological terms in biological processes, cellular components, and molecular functions, respectively (Table 1). Cytokine-cytokine receptor interaction was the most frequently identified function of potential pathways by Kyoto Encyclopedia of Genes and Genomes (KEGG) (Figure 1c).

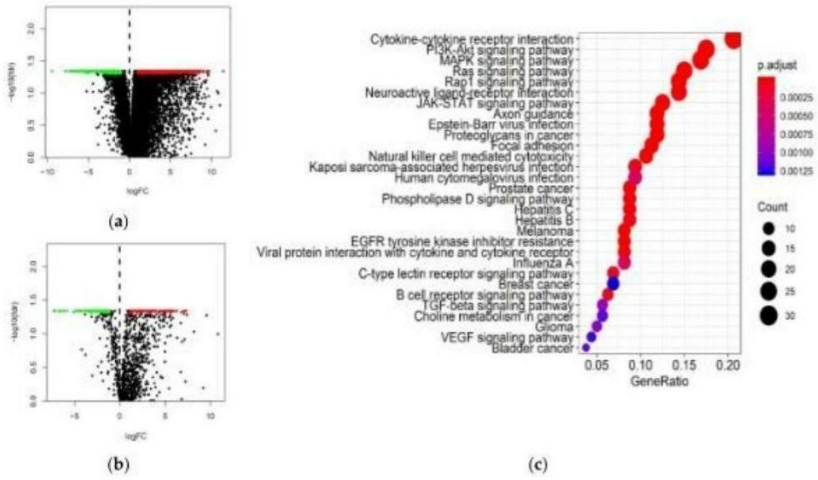

Figure 1. DEGs. (**a**) Volcano plot of DEGs between primary cervical cancer and para-tumor tissues. (**b**) Volcano plot of differentially expressed IRGs. Green dots, down—regulated genes; red dots, up-regulated genes, black dots, no DEGs. (**c**) The results of KEGG analysis. IRGs, Immune—related genes.

Table 1. GO analysis.

ID	Description	*p*-Adjust	Count
GO:0050673	epithelial cell proliferation	1.78×10^{-18}	36
GO:0050678	regulation of epithelial cell proliferation	1.78×10^{-18}	34
GO:0050679	positive regulation of epithelial cell proliferation	2.34×10^{-16}	25
GO:0018108	peptidyl-tyrosine phosphorylation	1.52×10^{-15}	30
GO:0018212	peptidyl-tyrosine modification	1.55×10^{-15}	30
GO:0032103	positive regulation of response to external stimulus	7.98×10^{-14}	27
GO:0001667	ameboidal-type cell migration	1.22×10^{-13}	31
GO:0010631	epithelial cell migration	1.26×10^{-13}	28
GO:0090132	epithelium migration	1.39×10^{-13}	28
GO:0090130	tissue migration	1.93×10^{-13}	28
GO:0060326	cell chemotaxis	2.54×10^{-12}	23
GO:0010632	regulation of epithelial cell migration	6.51×10^{-12}	24
GO:0043410	positive regulation of MAPK cascade	9.99×10^{-12}	30
GO:0050900	leukocyte migration	1.07×10^{-11}	29
GO:0043235	receptor complex	1.08×10^{-11}	23
GO:0009897	external side of plasma membrane	3.19×10^{-7}	15
GO:0060205	cytoplasmic vesicle lumen	1.02×10^{-6}	18
GO:0031983	vesicle lumen	1.02×10^{-6}	18
GO:0034774	secretory granule lumen	2.17×10^{-6}	17
GO:0031012	extracellular matrix	3.89×10^{-6}	20
GO:0062023	collagen-containing extracellular matrix	6.87×10^{-6}	18
GO:0098552	side of membrane	3.49×10^{-5}	16
GO:0022624	proteasome accessory complex	9.42×10^{-5}	5
GO:0005912	adherens junction	0.00042719	17
GO:0045121	membrane raft	0.000466985	13
GO:0098857	membrane microdomain	0.000466985	13
GO:0098589	membrane region	0.000619958	13
GO:0031093	platelet alpha granule lumen	0.001187147	6
GO:0005925	focal adhesion	0.001187147	14

Table 1. *Cont.*

ID	Description	*p*-Adjust	Count
GO:0019838	growth factor binding	4.90×10^{-18}	22
GO:0048018	receptor ligand activity	3.61×10^{-17}	33
GO:0030545	receptor regulator activity	1.93×10^{-16}	33
GO:0019199	transmembrane receptor protein kinase activity	1.44×10^{-15}	16
GO:0008083	growth factor activity	2.21×10^{-14}	20
GO:0005126	cytokine receptor binding	1.90×10^{-11}	20
GO:0019955	cytokine binding	2.16×10^{-11}	15
GO:0005178	integrin binding	1.19×10^{-10}	15
GO:0004713	protein tyrosine kinase activity	2.39×10^{-10}	15
GO:0042562	hormone binding	2.39×10^{-10}	13
GO:0050431	transforming growth factor beta binding	1.42×10^{-9}	8
GO:0005539	glycosaminoglycan binding	3.49×10^{-9}	17
GO:0004714	transmembrane receptor protein tyrosine kinase activity	4.41×10^{-9}	10
GO:0005125	cytokine activity	6.15×10^{-9}	15
GO:0003707	steroid hormone receptor activity	1.06×10^{-8}	10

Note: Green bar, biological process. Blue bar, cellular components. Pink bar, molecular function.

2.2. Identification of Differentially Expressed SIRGs

Since survival time and status are important for the prognostic evaluation, it seems to be feasible to evaluate the prognosis of patients based on the expressions of genes associated with survival. First, we identified 22 differentially expressed SIRGs among 212 cervical cancer cases with complete OS data. GO analysis revealed that tumor-related biological process was the most frequently implicated term (Table 2). JAK-STAT signaling pathway was the most frequently identified pathway analyzed by KEGG (Figure 2a). A forest plot of hazard ratios indicated that 10 genes were significant protective factors, and 12 genes were significant adverse factors (Figure 2b). Protein-protein interaction (PPI) network analysis demonstrated that TYK2, CSK, PTPN6, and IL3RA were the hub genes, which were screened out based on the criteria of correlation coefficient 0.3 and the number of interactive genes no less than 3 (Figure 2c). These hub genes were actively involved in the JAK-STAT signaling pathway (Figure 2d).

Table 2. GO analysis.

ID	Description	*p* Adjust	Count
GO:0018108	peptidyl-tyrosine phosphorylation	9.23×10^{-5}	7
GO:0018212	peptidyl-tyrosine modification	9.23×10^{-5}	7
GO:0050679	positive regulation of epithelial cell proliferation	0.001681	5
GO:0050673	epithelial cell proliferation	0.002676	6
GO:0050730	regulation of peptidyl-tyrosine phosphorylation	0.002676	5
GO:0050769	positive regulation of neurogenesis	0.002676	6
GO:0042063	gliogenesis	0.002676	5
GO:0002833	positive regulation of response to biotic stimulus	0.002676	3
GO:0046850	regulation of bone remodeling	0.002676	3
GO:0001818	negative regulation of cytokine production	0.002676	5
GO:0030665	clathrin-coated vesicle membrane	0.01508	3
GO:0043235	receptor complex	0.01508	4
GO:0030662	coated vesicle membrane	0.0269	3
GO:0030136	clathrin-coated vesicle	0.0269	3
GO:0016323	basolateral plasma membrane	0.028616	3
GO:0008083	growth factor activity	7.32×10^{-5}	5
GO:0048018	receptor ligand activity	0.000263	6
GO:0030545	receptor regulator activity	0.000263	6
GO:0004713	protein tyrosine kinase activity	0.010353	3
GO:0005154	epidermal growth factor receptor binding	0.012091	2
GO:0004715	non-membrane spanning protein tyrosine kinase activity	0.016435	2

Note: Green bar, biological process. Blue bar, cellular components. Pink bar, molecular function.

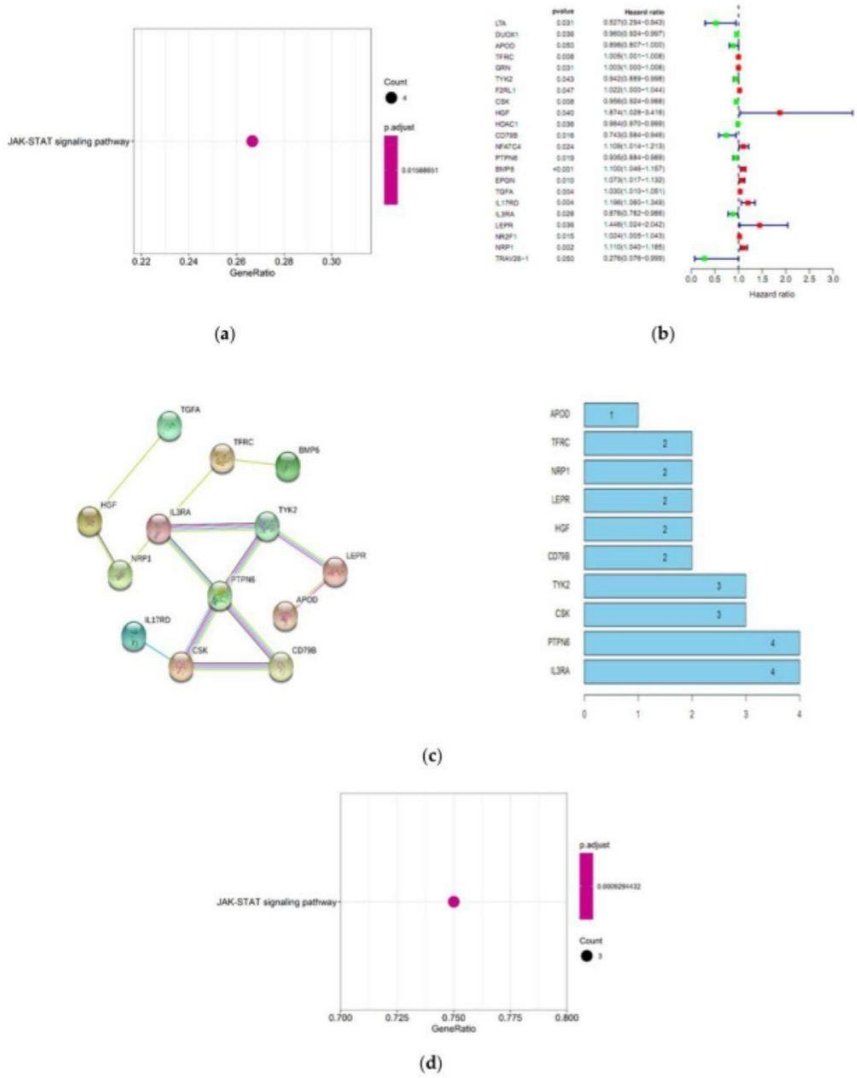

Figure 2. Identification of SIRGs. (**a**) The most significant KEGG pathways for SIRGs. (**b**) A forest plot of hazard ratios. The left is the list of SIRGs and their prognostic values showing as name, *p*-value, and the hazard ratio (95% CI), and the right is the relevant forest plot; Green bar, protective factor; red bar, adverse factor. (**c**) PPI network. The left is the PPI network, and the right is the number of interactive genes for each gene. (**d**) The most significant KEGG pathways for the hub SIRGs. SIRGs, immune-related genes associated with survival.

2.3. Construction of the Prognostic Model

A total of 10 IIRGs were screened out from the 22 SIRGs using the multivariate COX analysis, which were independent factors for the survival status and time of 212 cervical cancer cases. Table 3 shows their correlation coefficients. A prognostic model was established as follows:

Table 3. The IRGs involved in the predictive model.

Gene	Coef [1]	HR [2]	HR.95L	HR.95H	*p*-Value
APOD	−0.06584	0.936277	0.847164	1.034765	0.196953
TFRC	0.004018	1.004026	0.999878	1.008191	0.057172
GRN	0.00648	1.006501	1.003542	1.009469	1.61E−05
CSK	−0.04999	0.951235	0.91998	0.983551	0.003357
HDAC1	−0.01997	0.980231	0.963732	0.997013	0.021143
NFATC4	0.129489	1.138247	1.011662	1.280671	0.03134
BMP6	0.055054	1.056598	0.992466	1.124874	0.084843
IL17RD	0.124096	1.132124	0.971935	1.318714	0.110877
IL3RA	−0.22745	0.79656	0.688675	0.921347	0.00219
LEPR	0.520483	1.68284	1.112013	2.546688	0.013808

[1] Coef: coefficient; [2] HR: hazard ratio.

Risk score = [Expression level of APOD × (−0.06584)] + [Expression level of TFRC × 0.004018] + [Expression level of GRN × 0.00648)] + [Expression level of CSK × (−0.04999)] + [Expression level of HDAC1 × (−0.01997)] + [Expression level of NFATC4 × 0.129489 + [Expression level of BMP6 × 0.055054] + [Expression level of IL17RD × 0.124096]+ [Expression level of IL3RA × (−0.22745)] + [Expression level of LEPR × 0.520483].

2.4. Efficacy Verification of the Prognostic Model

To verify the efficacy of the prognostic model, we performed a Kaplan-Meier survival analysis for the 212 cases. The OS rate of the high-risk group was significantly lower compared with the low-risk group ($p < 0.001$). The result showed that the prognostic model could distinguish different clinical outcomes from cervical cancer patients (Figure 3a). Besides, we also performed an ROC analysis (Figure 3b). The AUC was 0.738, suggesting moderate accuracy for the prognosis in cervical cancer. Moreover, the model still worked in subgroup analyses of age (Figure S2a) and grade (Figure S2b), while it could only work in subgroup analyses of SCC (Figure S2c) and FIGO I stage (Figure S2d) subgroups, suggesting that the model was steady in patients with early-stage SCC, regardless of age or grade. The risk curve showed that patients could be divided into the high-risk group and low-risk group according to the median risk score, and the survival time of the high-risk group was lower compared with the low-risk group. Moreover, the number of death was greater in the high-risk group compared with the low-risk group (Figure 3c,d). The DEGs involved in the prognostic model were shown in the heat map, which was consistent with the trend shown by the correlation coefficients (Figure 3e, Table 3).

Univariate analysis and multivariate analysis indicated that the risk score could be an independent predictor (HR = 3.170, 95% CI [1.701–5.910], $p = 0.001$) after other clinicopathological characteristics, such as age, grade, and Figo stage, were adjusted (Table 4).

Therefore, the predictive model could be a reliable and steady method to judge the clinical outcomes for SCC patients with FIGO I stage. For example, the 5-year survival rate of the low-risk group and high-risk group were about 80% and 55%, respectively.

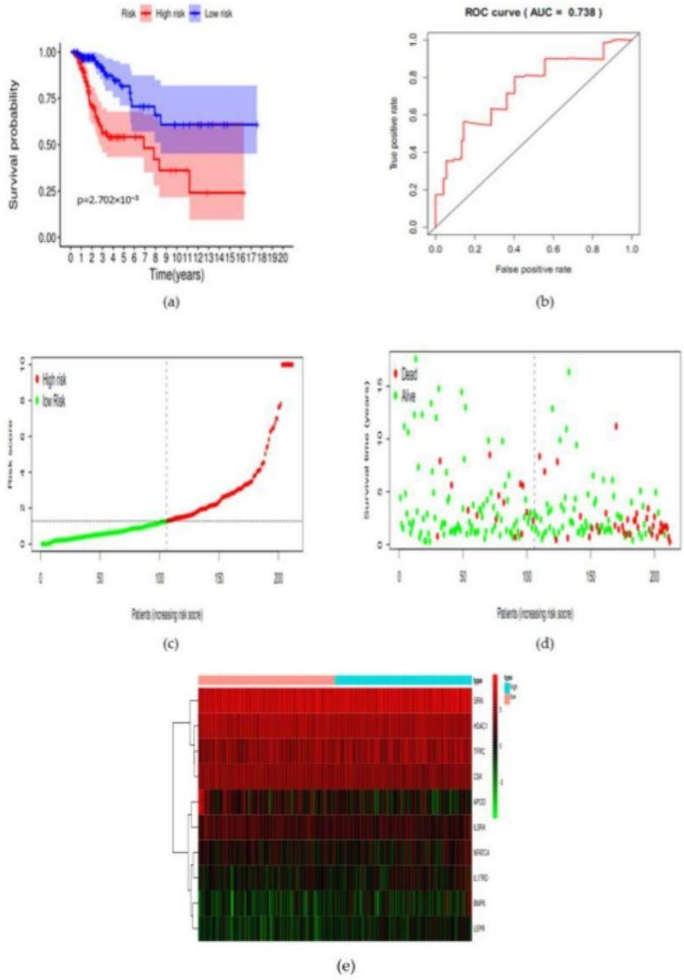

Figure 3. Verification of the efficacy of the prognostic model. (**a**) Kaplan-Meier plots demonstrated that the prognostic model could distinguish different clinical outcomes from cervical cancer patients ($p < 0.05$). Blue represents the low-risk group; red represents the high-risk group. (**b**) The ROC for verifying the accuracy of the predictive model and AUC for the risk score model displayed moderately accuracy in the cancer Genome Atlas (TCGA) dataset. (**c**) Value of risk score in cervical cancer patients. Both the horizontal axis and the vertical axis represent risk score. From left to right, the risk score is increasing; red dot represents the high- risk case; green dot represents the low-risk case; (**d**) survival status and time in the two risk groups. From left to right, the risk score is increasing. The vertical axis represents the survival time. (**e**) Heatmap of the differentially expressed SIRGs involved in the prognostic model. From left to right, the risk score is increasing. Blue represents a high-risk case. Red represents a low-risk case.

Table 4. Univariate and multivariate cox regression analyses.

Clinicopathological	Univariate Analysis			Multivariate Analysis		
Characteristics	**HR**	**95% CI**	***p*-Value**	**HR**	**95% CI**	***p*-Value**
Age > 45 years	1.048	0.608–1.807	0.865	–	–	–
Grade 3–4	1.043	0.597–1.822	0.883	–	–	–
FIGO stage			**0.001** *			**0.016** *
I	–	–	–	–	–	–
II–III	0.884	0.473–1.654	0.701	0.742	0.395–1.394	0.353
IVA	5.121	1.956–13.408	**0.001** *	2.778	1.019–7.575	**0.046** *
IVB	3.139	1.095–9.000	**0.033** *	2.891	1.006–8.306	**0.049** *
Histological type (squamous carcinoma vs. adenocarcinoma)	1.513	0.545–4.204	0.427	–	–	–
High risk	3.369	1.846–6.147	**0.001** *	3.170	1.701–5.910	**0.001** *

* $p < 0.05$.

2.5. The Clinical Significance of IIRGs

We analyzed the differences of IIRGs in clinicopathological characteristics, including age, grade, FIGO stages, of the 212 cases to determine the relationship between the risk score and clinical parameters. The expressions of IL17RD and TFRC were significantly higher in the group of patients aged over 45 years (Figure 4a,b). The expression of HDCA1 was significantly lower in the group of grades 3&4 compared with the group of grades 1&2 (Figure 4c).

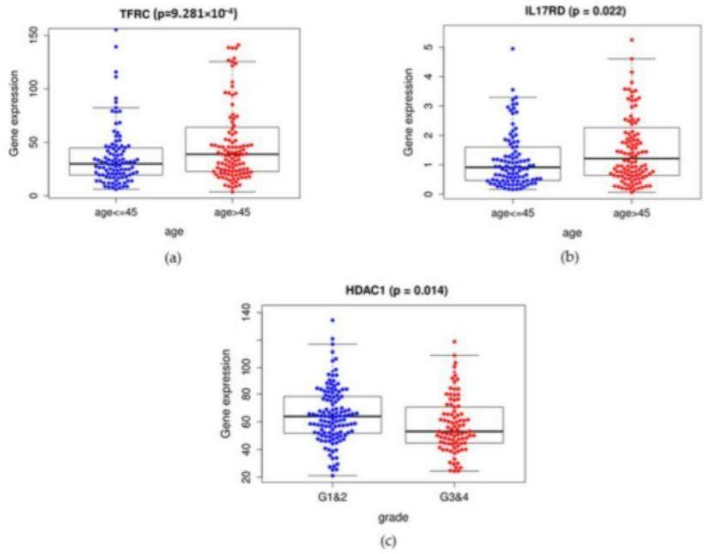

Figure 4. The clinical significance of IIRGs. The box plots showed that the expressions of TFRC, IL17RD, and HDAC1 were significantly different in subgroups of age and grade. (**a**,**b**) Blue represents the group of age ≤ 45years, and red represents the group of age > 45 years. (**c**) Blue represents the group of grades 1 and 2, and red represents the group of grades 3 and 4.

2.6. TFs Regulatory Network

To explore the potential molecular mechanisms of SIRGs, we investigated the TFs associated with 22 SIRGs. We selected differentially expressed 74 TFs by intersecting the list of TFs with DEGs (Figure 5a). Among these 74 TFs, five TFs were significantly associated with survival (Figure 5b). Based on the criteria of correlation coefficient = 0.3, and $p = 0.001$, a regulatory network was constructed using these five TFs and SIRGs (Figure 5c).

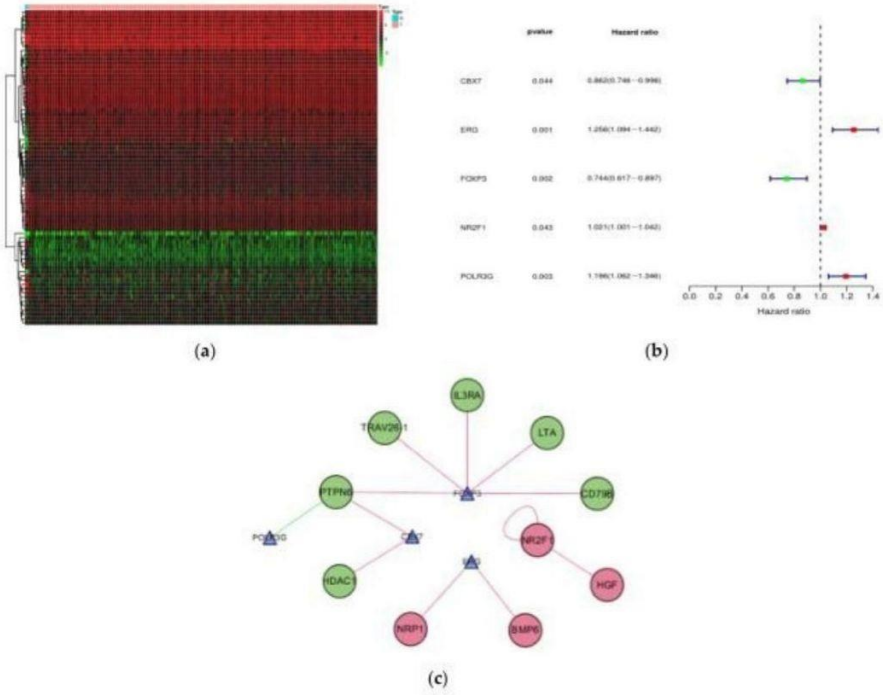

(a) (b)

(c)

Figure 5. The construction of a regulatory network between SDETFs and SIRGs. (**a**) Heatmap of the SDETFs. (**b**) A forest plot of hazard ratios. The left is the list of SDETFs and their prognostic values showing as name, *p*-value, and the hazard ratio (95% CI), and the right is the relevant forest plot. Green bar, protective factor; red bar, adverse factor. (**c**) A regulatory network between SDETFs and SIRGs. Triangle, TFs; Roundness, SIRGs; Red roundness, the overexpressed SIRGs; Green roundness, down-expressed SIRGs. Red line, the TFs up-regulate SIRGs; Green line, the TFs down-regulate SIRGs.

3. Discussion

Cervical cancer is caused by the persistent infection of hrHPV [13–15]. Although surgery, chemoradiotherapy, anti-angiogenic medicine, and even the new immunotherapy have been applied for cervical cancer treatment, the prognosis remains poor at the late stage [4,9,16]. Therefore, research on effective prognostic biomarkers and new molecular mechanisms has drawn increasing attention. Kidd EA et al. have found that the standardized uptake value for F-18 fluorodeoxyglucose is a sensitive predictive biomarker for the survival of cervical cancer patients [17]. Luo W et al. have identified a 6-lncRNA signature, which can be regarded as novel diagnostic biomarkers for cervical cancer [18]. Li X et al. have identified a histone family gene signature for predicting the prognosis of cervical cancer patients [19]. These studies have provided an elemental knowledge of

the pathogenesis of cervical cancer at the genetic level. However, the prognostic role of immunogenomics in cervical cancer remains largely undetermined. In the present study, we performed a comprehensive analysis of IRGs in cervical cancer, which might enhance our knowledge of their clinical value and help us understand potential molecular mechanisms. Moreover, these IRGs might act as valuable clinical biomarkers or therapeutic targets. Besides, we constructed a prognostic model that could help assess potential clinical outcomes of cervical cancer patients.

Tumor immune microenvironment can promote the progression of cervical cancer, including cancer cell proliferation, invasion, metastasis, immunosuppression and tissue remodeling, fibrosis, and angiogenesis. For example, CXCL12 induces mononuclear phagocytes to release HB-EGF, triggering anti-apoptotic and proliferative signals in Hela cells [20]. D-dopachrome tautomerase (D-DT), a homolog of macrophage migration inhibitory factor (MIF), can promote the invasion of cervical cancer cells when it is overexpressed [21]. An altered balance in IL-12p70 and IL-10 production can weaken T cell proliferation in cervical cancer [22]. These studies suggest the importance of immunity in cervical cancer progression. Therefore, it is necessary to identify differentially expressed IRGs. Genome profile alterations cause tumorigenesis. We identified alternations in immunogenomic profiles to study the effect of alternations on the immune microenvironment and clinical prognosis. Gene functional enrichment analysis suggested that these genes were mainly involved in growth factor (GF) activity. GFs actively act in the pathogenesis of cervical cancer. Notably, these GFs are correlated to proliferation, aggression, and migration [23–25]. Therefore, these GFs could also be used to monitor metastasis, assess survival, and identify potential drug targets as clinical biomarkers.

Among the 20 SIRGs, no related reports have explored the roles of DUOX1, GRN, CSK, CD79, NFATC4, EPGN, TGFA, IL17RD, LEPR, N2RF1, and TRAV26-1 in cervical cancer. APOD is down-regulated in cervical cancer compared with normal cervix [26]. TFRC expression is up-regulated in cervical cancer compared with normal cervix [27]. A previous study has found that there is a significant correlation between cervical cancer and the polymorphism of rs1041981 in the LTA gene [28]. The rare allele (A) of SNP rs2239704 in the 5′ UTR of the LTA gene is significantly associated with increased risks of cervical cancer [29]. F2RL1 is overexpressed in cervical cancer cell lines and significantly correlated with poor OS [30,31]. HGF overexpression in lesions of cervical cancer has been reported to be related to a poor prognosis [32]. HDAC1/DNMT3A-containing complex is associated with the suppression of cancer stem cells in cervical cancer [33]. HGF can induce migration and invasion of cervical cancer cells [34].] BMP6 may participate in invasion and metastasis in cervical cancer [35]. The proportion of CD123(+) dendritic cells is significantly lower in the peripheral blood of cervical cancer patients compared with the controls [36]. A higher frequency of Nrp1(+) T-regs frequency suppresses the immune response against distant cervical cancer cells [37]. The above-mentioned results are consistent with our current findings. However, Tyk2 is confirmed to be overexpressed in SCC [38], which is different from our study. Low-throughput experiments, such as Western blotting analysis, are required to verify the factual expression. PTPN6 is positively correlated with HPV infection in cervical cancer with the explanation of cell defense reaction [39].

To explore molecular mechanisms underlying the potential clinical importance, we constructed a TF-mediated network that could regulate hub IRGs. Among the SDETFs, Foxp3 is significantly associated with FIGO stage and tumor size [40]. Foxp3 is associated with lymphangiogenesis of cervical cancer [41]. FoxP3 has been confirmed to be highly expressed in cervical cancer, and it facilitates the proliferation and invasiveness and inhibits the apoptosis of cervical cancer cells [42]. In conclusion, Foxp3 is a risk factor for the survival of cervical cancer, which is consistent with our current findings. CBX7 inhibits the proliferation of cervical cancer cells [43]. LTA inhibits the proliferation of CD4(+) T-cells in a FoxP3(+) Treg-dependent manner in patients with chronic hepatitis C, suggesting that LTA acts on FoxP3 [44]. Therefore, previous studies provide limited information about the mechanisms of 10 IRGs in the survival of cervical cancer.

The effects of the JAK/STAT pathway and the persistent activation of STAT3 and STAT5 during the process of tumor cell proliferation, cycling, and invasion have made it a favorite treatment target. In cervical cancer, the activated JAK/STAT signaling pathway by Bcl-2 promotes cell viability, migration, and invasion [45]. There is a strong association between HPV infection and STAT-3 overexpression in cervical cancer [46]. The expression of STAT3 has been proposed as a poor prognostic factor in cervical cancer [47]. STAT5 protein is up-regulated and associated with the severity of cervical cancer [48]. Moreover, overexpression of STAT-5 elevates the STAT-3 expression compared with the normal controls [46]. Therefore, JAK/STAT signaling may play an important role in cervical carcinogenesis. Moreover, up-regulation of PAR2 (F2RL1) induces the proliferation of cervical cancer cells by activating STAT3 [31], which is consistent with our current results that overexpression of F2RL1 was involved in the JAK/STAT signaling pathway.

In the present study, we created an immune-based prognostic signature to monitor the immune status and assess the prognosis for cervical cancer patients. Previously, Wu HY et al. (2020) have constructed a prognostic index based on percent-splice-in values in SCC [49]. Eun Jung Kwon et al. (2020) have explored genomic alterations and developed a risk index model that can monitor HPV- related bladder cancer [50]. Cai LY has created a risk score model based on differentially expressed glycolysis-related genes, and the model can predict the prognosis of cervical cancer patients [51]. Recently, Zhao S et al. (2020) have constructed a 4-gene prognostic risk score model in CESC by identifying DEGs [52]. Beyond the above-mentioned studies, there are also many studies about the prognostic model [53,54]. Compared with the previous studies, our prognostic model could assecss immune-genomic profiles. Moreover, we constructed a TF-mediated regulatory network, which provided a more detailed mechanism of IIRGs. Our prognostic index, based on 10 differentially expressed IIRGs in cervical cancer, demonstrated favorable clinical viability. Our data showed that the risk score model performed moderately and steadily in prognostic predictions in patients with early-stage cervical cancer.

We must point out that only three control specimens were acquired in the present study. Although it met the minimum requirements for the biological repeat, insufficient control samples tended to cause larger errors. Therefore, more other experiments are still necessary to validate the transcriptome results.

4. Materials and Methods

4.1. Gene Expression Data and Clinical Data Collection

FPKM transcriptome RNA-sequencing data and clinical data of cervical samples were downloaded from TCGA data portal (https://portal.gdc.cancer.gov/) on 1 December 2020. FPKM transcriptome RNA-sequencing data were derived from 289 samples, including three para-tumor tissue specimens (Table 5) and 286 primary cervical tumor tissues. As to para-tumor slides, the percentage of tumor cells, lymphocytes, necrosis, infiltrated monocytes, infiltrated neutrophil was 0, and the percentage of normal cells was 100%. The percentage of stroma cells of TCGA-FU-A3EO was 0, while that of the other two para-tumor tissue specimens was missing. As to tumor slides, the percentage of tumor cells was 80% (70%, 90%), the percentage of infiltrated lymphocytes was 7.5% (2%, 40%), the percentage of infiltrated monocytes was 0% (0%, 10%), the percentage of necrosis was 2% (0, 5%), the percentage of infiltrated neutrophil was 1% (0%, 20%), and the percentage of normal cells was 0% (0%, 5%). The para-tumor slides were collected from Christiana Healthcare, International Genomics Consortium, and Montefiore Medical Center, respectively. The samples were obtained from 253 patients with SCC and 31 patients with cervical adenocarcinoma. As to the clinical data, there were 212 cases with clinical data including age, grade, FIGO stage, survival status, and OS no less than 90 days. The clinical characteristics of the 212 cases were shown in Table 6.

Table 5. The clinical data of three para-tumor samples.

Serial Number	Age	pathological Pattern	Survival Time	Survival State	Grade	TNM	FIGO
TCGA-HM-A3JJ	45	Squamous cancer	659 days	dead	G3	T1b1N1M0	IB1
TCGA-FU-A3EO	55	Adenocarcinoma	490 days	alive	G2	T2b1N0M0	IIB
TCGA-MY-A5BF	68	Squamous cancer	634 days	alive	-	T2a2N0M0	IIA2

Table 6. The characteristic of 212 clinical samples.

Characteristics	Number of Cases (%)
Histological type	
Adenocarcinoma	22 (10.4)
Squamous cancer	190 (89.6)
Age (year)	
≤45	100 (47.2)
>45	112 (52.8)
Grade	
1–2	122 (57.5)
3–4	90 (42.5)
T stage	
I	116 (54.7)
II-III	82 (38.7)
IVa	5(2.4)
IVb	9(4.2)
Survival status	
Alive	159 (75.0%)
dead	53 (25.0%)
Duration of disease (year)	
≤5	176 (83.0)
>5	36 (17.0)

The list of IRGs was downloaded from the ImmPort database, which is a powerful public database with hundreds of downloads per month [12].

4.2. Analysis of DEGs

To identify the DEGs between three para-tumor and 289 cervical tumor tissue specimens, an R language script was made, and a limma package (http://www.bioconductor.org/packages/release/bioc/html/limma.html) on 2 January 2020 was downloaded and performed by the R software. The mean value of each gene expressed in para-tumor samples and cervical tumor samples was calculated by the script, and repeated genes were deleted by limma package. Wilcoxon-test was applied to compare the difference in expression. The false discovery rate (FDR) <0.05 and log2 |fold change| > 1 were set as the cutoff values to identify the DEGs. Differentially expressed IRGs were extracted by intersecting the results of DEGs and the list of IRGs by using the R language. The DEGs were presented using the pheatmap package and volcano plot script by R software.

The DEGs and differentially expressed IRGs were then subjected to clusterProfiler package in R for GO and KEGG pathway enrichment analysis to determine their potential functions and pathways.

4.3. Screening of Differentially Expressed SIRGs

IRGs significantly associated with survival of 212 tumor cases were identified from all the differentially expressed IRGs through univariate cox analysis ($p < 0.05$). These IRGs were defined as SIRGs. Forest map script was performed by R software.

The SIRGs were then subjected to cluster-Profiler package for GO and KEGG pathway enrichment analysis to determine their potential functions and pathways [13].

4.4. Construction of the Prognostic Model

R language script was made to perform multivariate cox analysis of SIRGs acquired by univariate cox analysis. Those IRGs in the model were defined as IIRGs. The risk score, as the indicator of the prognostic model, was calculated as the sum of the product of each IIRG expression and its regression coefficient. According to the median risk score of 1.276, all the 212 cases were divided into the high-risk group and low-risk group.

4.5. Construction of the Regulatory Network of SIRGs and Their TFs

The list of TFs related to cancer was downloaded from the Cistrome database (http://cistrome.org/) on 3 January 2020. This public database has collected the set of cis-acting targets of a trans-acting factor on a genome-wide scale. The TFs were intersected with DEGs, and the differentially expressed TFs (DETFs) were obtained by R language. Moreover, univariate cox analysis was carried out to identify DETFs significantly associated with survival (SDETFs).

Spearman correlation analysis between SDETFs and SIRGs in tumor tissues from the same samples was performed by R software. The correlation coefficient >0.3 and $p < 0.001$ were set as the standard for screening the correlated SDETFs (CSDETFs) with SIRGs. Therefore, the CSDETFs were acquired. Cytoscape software version 3.7.1 was applied to display the regulation relationship between CSDETFs and SIRGs.

4.6. Validaion of the Risk Score Model

Survival analysis was performed between the high-risk group and low-risk group in terms of age (age $\leq$ 45, and age > 45), grade (1–2, and grade3–4), cancer type (cervical adenocarcinoma and SCC), and FIGO stage (I, II–III, IVa, and IVb) by SPSS. A p value of less than 0.05 was considered statistically significant.

4.7. Statistical Analysis

The screening analysis of DEGs was performed by the Wilcoxon-test. Correlation analysis between SDETFs and SIRGs was carried out by Spearman correlation. DEG expression in each clinicopathological characteristic was tested by theWilcoxon-test. AUC of the survival ROC curve was calculated by the ROC package in R software. A p value of less than 0.05 was considered statistically significant [14].

5. Conclusions

Collectively, we adopted the bioinformatic method to comprehensively analyze the differentially expressed IRGs in cervical cancer and identified 204 tumor-associated IRGs. Among them, we also identified 22 SIRGs and constructed an individual predictive model with moderate accuracy and stability for prognostic prediction in SCC patients with FIGO I. We further explored the KEGG pathway and regulatory network between survival-associated TFs and SIRGs. However, the exact mechanism underlying how these genes affected the prognosis of cervical cancer should be verified by more accurate experiments.

Supplementary Materials: The following are available online at https://www.mdpi.com/1422-0067/22/5/2442/s1.

Author Contributions: H.H.H., U.J.: project development, data collection. Q.W.: experiments, manuscript writing. H.H.H., T.V., T.K., A.S., and A.V.: data collection, manuscript editing. H.H.H., and Q.W.: data analyses. D.M., U.J., and S.M.: supervision, data analyses. Q.W.: experiments, methodology. All authors have read and agreed to the published version of the manuscript.

Funding: The China Scholarship Council (CSC) funded this study for Qun Wang.

Data Availability Statement: The authors confirm that the data supporting the findings of this study are available within the article and its supplementary materials.

Acknowledgments: The results shown here are in part based upon data generated by the TCGA Research Network: https://www.cancer.gov/tcga on 1 January 2020.

Conflicts of Interest: Sven Mahner reports grants and personal fees from AstraZeneca, personal fees from Clovis, grants, and personal fees from Medac, grants, and personal fees from MSD. He also reports personal fees from Novartis, grants and personal fees from PharmaMar, grants and personal fees from Roche, personal fees from Sensor Kinesis, grants, and personal fees from Tesaro, grants and personal fees from Teva, outside the submitted work. All other authors declare no conflict of interest.

References

1. Torre, L.A.; Bray, F.; Siegel, R.L.; Ferlay, J.; Lortet-Tieulent, J.; Jemal, A. Global cancer statistics, 2012. *CA Cancer J. Clin.* **2015**, *65*, 87–108. [CrossRef] [PubMed]
2. Di, J.; Rutherford, S.; Chu, C. Review of the Cervical Cancer Burden and Population-Based Cervical Cancer Screening in China. *Asian Pac. J. Cancer Prev.* **2015**, *16*, 7401–7407. [CrossRef]
3. Ahn, K.; Kweon, S.; Kim, D.W.; Lee, H. Different expression of GSK3beta and pS9GSK3beta depending on phenotype of cervical cancer: Possible association of GSK3beta with squamous cell carcinoma and pS9GSK3beta with adenocarcinoma. *Obs. Gynecol. Sci.* **2019**, *62*, 157–165. [CrossRef] [PubMed]
4. Hass, P.; Eggemann, H.; Costa, S.D.; Ignatov, A. Adjuvant hysterectomy after radiochemotherapy for locally advanced cervical cancer. *Strahlenther. Onkol.* **2017**, *193*, 1048–1055. [CrossRef] [PubMed]
5. van Meir, H.; Kenter, G.G.; Burggraaf, J.; Kroep, J.R.; Welters, M.J.; Melief, C.J.; Van Der Burg, S.H.; IE Van Poelgeest, M. The need for improvement of the treatment of advanced and metastatic cervical cancer, the rationale for combined chemo-immunotherapy. *Anticancer Agents Med. Chem.* **2014**, *14*, 190–203. [CrossRef] [PubMed]
6. Zhou, J.; Liang, T.; Wang, D.; Li, L.; Cheng, Y.; Guo, Q.; Zhang, G. IFNalpha-Expressing Amniotic Fluid-Derived Mesenchymal Stem Cells Migrate to and Suppress HeLa Cell-Derived Tumors in a Mouse Model. *Stem. Cells Int.* **2018**, *2018*, 1241323. [CrossRef]
7. Yang, Y.; Che, Y.; Zhao, Y.; Wang, X. Prevention and treatment of cervical cancer by a single administration of human papillomavirus peptide vaccine with CpG oligodeoxynucleotides as an adjuvant in vivo. *Int. Immunopharmacol.* **2019**, *69*, 279–288. [CrossRef] [PubMed]
8. McCormack, S.E.; Cruz, C.R.Y.; Wright, K.E.; Powell, A.B.; Lang, H.; Trimble, C.; Keller, M.D.; Fuchs, E.; Bollard, C.M. Human papilloma virus-specific T cells can be generated from naive T cells for use as an immunotherapeutic strategy for immunocompromised patients. *Cytotherapy* **2018**, *20*, 385–393. [CrossRef] [PubMed]
9. Nishio, H.; Iwata, T.; Aoki, D. Current status of cancer immunotherapy for gynecologic malignancies. *Jpn. J. Clin. Oncol.* **2020**, *51*, 167–172. [CrossRef]
10. Li, B.; Cui, Y.; Diehn, M.; Li, R. Development and Validation of an Individualized Immune Prognostic Signature in Early-Stage Nonsquamous Non-Small Cell Lung Cancer. *JAMA Oncol.* **2017**, *3*, 1529–1537. [CrossRef]
11. Lin, P.; Guo, Y.N.; Shi, L.; Li, X.J.; Yang, H.; He, Y.; Li, Q.; Dang, Y.; Weei, K.; Chen, G. Development of a prognostic index based on an immunogenomic landscape analysis of papillary thyroid cancer. *Aging* **2019**, *11*, 480–500. [CrossRef] [PubMed]
12. Bhattacharya, S.; Andorf, S.; Gomes, L.; Dunn, P.; Schaefer, H.; Pontius, J.; Berger, P.; Desborough, V.; Smith, T.; Campbell, J.; et al. ImmPort: Disseminating data to the public for the future of immunology. *Immunol. Res.* **2014**, *58*, 234–239. [CrossRef]
13. Yu, G.; Wang, L.G.; Han, Y.; He, Q.Y. clusterProfiler: An R package for comparing biological themes among gene clusters. *OMICS* **2012**, *16*, 284–287. [CrossRef] [PubMed]
14. Heagerty, P.J.; Lumley, T.; Pepe, M.S. Time-dependent ROC curves for censored survival data and a diagnostic marker. *Biometrics* **2000**, *56*, 337–344. [CrossRef] [PubMed]
15. Morris, B.J. The advent of human papillomavirus detection for cervical screening. *Curr. Opin. Obs. Gynecol.* **2019**, *31*, 333–339. [CrossRef] [PubMed]
16. Tewari, K.S.; Sill, M.W.; Long, H.J., 3rd; Penson, R.T.; Huang, H.; Ramondetta, L.M.; Lisa, M.L.; Ana, O.; Thomas, J.R.; Mario, M.L.; et al. Improved survival with bevacizumab in advanced cervical cancer. *N. Engl. J. Med.* **2014**, *370*, 734–743. [CrossRef]
17. Kidd, E.A.; Siegel, B.A.; Dehdashti, F.; Grigsby, P.W. The standardized uptake value for F-18 fluorodeoxyglucose is a sensitive predictive biomarker for cervical cancer treatment response and survival. *Cancer* **2007**, *110*, 1738–1744. [CrossRef]
18. Luo, W.; Wang, M.; Liu, J.; Cui, X.; Wang, H. Identification of a six lncRNAs signature as novel diagnostic biomarkers for cervical cancer. *J. Cell Physiol.* **2019**, *235*, 993–1000. [CrossRef]
19. Li, X.; Tian, R.; Gao, H.; Yang, Y.; Williams, B.R.G.; Gantier, M.P.; McMillan, N.A.J.; Xu, D.; Hu, Y.; Gao, Y. Identification of a histone family gene signature for predicting the prognosis of cervical cancer patients. *Sci. Rep.* **2017**, *7*, 16495. [CrossRef] [PubMed]
20. Rigo, A.; Gottardi, M.; Zamo, A.; Mauri, P.; Bonifacio, M.; Krampera, M.; Damiani, E.; Pizzolo, G.; Vinante, F. Macrophages may promote cancer growth via a GM-CSF/HB-EGF paracrine loop that is enhanced by CXCL12. *Mol. Cancer* **2010**, *9*, 273. [CrossRef]
21. Wang, Q.; Wei, Y.; Zhang, J. Combined Knockdown of D-dopachrome Tautomerase and Migration Inhibitory Factor Inhibits the Proliferation, Migration, and Invasion in Human Cervical Cancer. *Int. J. Gynecol. Cancer* **2017**, *27*, 634–642. [CrossRef]
22. Heusinkveld, M.; de Vos van Steenwijk, P.J.; Goedemans, R.; Ramwadhdoebe, T.H.; Gorter, A.; Welters, M.J.; Hall, T.V.; Berg, S.H. M2 macrophages induced by prostaglandin E2 and IL-6 from cervical carcinoma are switched to activated M1 macrophages by CD4+ Th1 cells. *J. Immunol.* **2011**, *187*, 1157–1165. [CrossRef]

23. Souza, J.L.; Martins-Cardoso, K.; Guimarães, I.S.; de Melo, A.C.; Lopes, A.H.; Monteiro, R.Q.; Almeida, V.H. Interplay Between EGFR and the Platelet-Activating Factor/PAF Receptor Signaling Axis Mediates Aggressive Behavior of Cervical Cancer. *Front. Oncol.* **2020**, *17*, 557280. [CrossRef] [PubMed]
24. Li, L.; Zhang, R.; Yang, H.; Zhang, D.; Liu, J.; Li, J.; Guo, B. GDF15 knockdown suppresses cervical cancer cell migration in vitro through the TGF-β/Smad2/3/Snail1 pathway. *FEBS Open Bio.* **2020**, *10*, 2750–2760. [CrossRef] [PubMed]
25. Faulkner, S.; Griffin, N.; Rowe, C.W.; Jobling, P.; Lombard, J.M.; Oliveira, S.M.; Walker, M.M.; Hondermarck, H. Nerve growth factor and its receptor tyrosine kinase TrkA are overexpressed in cervical squamous cell carcinoma. *FASEB Bioadv.* **2020**, *2*, 398–408. [CrossRef]
26. Gu, Z.; Wang, H.; Xia, J.; Yang, Y.; Jin, Z.; Xu, H.; Shi, J.; De Domenico, I.; Tricot, G.; Zhan, F. Decreased ferroportin promotes myeloma cell growth and osteoclast differentiation. *Cancer Res.* **2015**, *75*, 2211–2221. [CrossRef]
27. Song, J.Y.; Lee, J.K.; Lee, N.W.; Jung, H.H.; Kim, S.H.; Lee, K.W. Microarray analysis of normal cervix, carcinoma in situ, and invasive cervical cancer: Identification of candidate genes in pathogenesis of invasion in cervical. *Int. J. Gynecol. Cancer* **2008**, *18*, 1051–1059. [CrossRef]
28. Castro, F.A.; Haimila, K.; Sareneva, I.; Schmitt, M.; Lorenzo, J.; Kunkel, N.; Kumar, R.; Försti, A.; Kjellberg, L.; Hallmans, G.; et al. Association of HLA-DRB1, interleukin-6 and cyclin D1 polymorphisms with cervical cancer in the Swedish population–a candidate gene approach. *Int. J. Cancer* **2009**, *125*, 1851–1858. [CrossRef]
29. Bodelon, C.; Madeleine, M.M.; Johnson, L.G.; Du, Q.; Galloway, D.A.; Malkki, M.; Petersdorf, E.W.; Schwartz, S.M. Genetic variation in the TLR and NF-kappaB pathways and cervical and vulvar cancer risk: A population-based case-control study. *Int. J. Cancer* **2014**, *134*, 437–444. [CrossRef] [PubMed]
30. Hugo de Almeida, V.; Guimaraes, I.D.S.; Almendra, L.R.; Rondon, A.M.R.; Tilli, T.M.; de Melo, A.C.; Sternberg, C.; Monteiro, R.Q. Positive crosstalk between EGFR and the TF-PAR2 pathway mediates resistance to cisplatin and poor survival in cervical cancer. *Oncotarget* **2018**, *9*, 30594–30609. [CrossRef] [PubMed]
31. Shanshan, H.; Lan, X.; Xia, L.; Huang, W.; Meifang, Z.; Ling, Y. Inhibition of protease-activated receptor-2 induces apoptosis in cervical cancer by inhibiting signal transducer and activator of transcription-3 signaling. *J. Int. Med. Res.* **2019**, *47*, 1330–1338. [CrossRef] [PubMed]
32. Leo, C.; Horn, L.C.; Einenkel, J.; Hentschel, B.; Hockel, M. Tumor hypoxia and expression of c-met in cervical cancer. *Gynecol. Oncol.* **2007**, *104*, 181–185. [CrossRef] [PubMed]
33. Liu, D.; Zhou, P.; Zhang, L.; Gong, W.; Huang, G.; Zheng, Y.; He, F. HDAC1/DNMT3A-containing complex is associated with suppression of Oct4 in cervical cancer cells. *Biochemistry* **2012**, *77*, 934–940. [CrossRef] [PubMed]
34. Lu, J.; Li, X.; Tu, K.; Guan, Y.; Fung, K.P.; Liu, F. Verticillin A suppresses HGF-induced migration and invasion via repression of the c-Met/FAK/Src pathway in human gastric and cervical cancer cells. *Onco. Targets Ther.* **2019**, *12*, 5823–5833. [CrossRef] [PubMed]
35. Liu, C.Y.; Chao, T.K.; Su, P.H.; Lee, H.Y.; Shih, Y.L.; Su, H.Y.; Chu, T.-Y.; Yu, M.-H.; Lin, Y.-W.; Lai, H.-C. Characterization of LMX-1A as a metastasis suppressor in cervical cancer. *J. Pathol.* **2009**, *219*, 222–231. [CrossRef]
36. Ye, F.; Yu, Y.; Hu, Y.; Lu, W.; Xie, X. Alterations of dendritic cell subsets in the peripheral circulation of patients with cervical carcinoma. *J. Exp. Clin. Cancer Res.* **2010**, *29*, 78. [CrossRef]
37. Battaglia, A.; Buzzonetti, A.; Martinelli, E.; Fanelli, M.; Petrillo, M.; Ferrandina, G.; Scambia, G.; Fattorossi, A. Selective changes in the immune profile of tumor-draining lymph nodes after different neoadjuvant chemoradiation regimens for locally advanced cervical cancer. *Int. J. Radiat. Oncol. Biol. Phys.* **2010**, *76*, 1546–1553. [CrossRef]
38. Zhu, X.; Lv, J.; Yu, L.; Zhu, X.; Wu, J.; Zou, S.; Jiang, S. Proteomic identification of differentially-expressed proteins in squamous cervical cancer. *Gynecol. Oncol.* **2009**, *112*, 248–256. [CrossRef]
39. Tao, X.H.; Shen, J.G.; Pan, W.L.; Dong, Y.E.; Meng, Q.; Honn, K.V.; Jin, R. Significance of SHP-1 and SHP-2 expression in human papillomavirus infected Condyloma acuminatum and cervical cancer. *Pathol. Oncol. Res.* **2008**, *14*, 365–371. [CrossRef] [PubMed]
40. Zhang, H.; Zhang, S. The expression of Foxp3 and TLR4 in cervical cancer: Association with immune escape and clinical pathology. *Arch. Gynecol. Obstet.* **2017**, *295*, 705–712. [CrossRef]
41. Tang, J.; Yang, Z.; Wang, Z.; Li, Z.; Li, H.; Yin, J.; Deng, M.; Zhu, W.; Zeng, C. Foxp3 is correlated with VEGF-C expression and lymphangiogenesis in cervical cancer. *World J. Surg. Oncol.* **2017**, *15*, 173. [CrossRef]
42. Luo, Q.; Zhang, S.; Wei, H.; Pang, X.; Zhang, H. Roles of Foxp3 in the occurrence and development of cervical cancer. *Int. J. Clin. Exp. Pathol.* **2015**, *8*, 8717–8730. [PubMed]
43. Li, R.; Yan, Q.; Tian, P.; Wang, Y.; Wang, J.; Tao, N.; Li, N.; Lin, X.; Ding, L.; Liu, J.W.; et al. CBX7 Inhibits Cell Growth and Motility and Induces Apoptosis in Cervical Cancer Cells. *Mol. Ther. Oncolytics.* **2019**, *15*, 108–116. [CrossRef] [PubMed]
44. Zhai, N.C.; Chi, X.M.; Li, T.Y.; Song, H.X.; Li, H.J.; Jin, X.; Ian, N.C.; Su, L.S.; Niu, J.Q.; Tu, Z.K. Hepatitis C virus core protein triggers expansion and activation of CD4(+)CD25(+) regulatory T cells in chronic hepatitis C patients. *Cell Mol. Immunol.* **2015**, *12*, 743–749. [CrossRef]
45. Wang, X.; Xie, Y.; Wang, J. Overexpression of MicroRNA-34a-5p Inhibits Proliferation and Promotes Apoptosis of Human Cervical Cancer Cells by Downregulation of Bcl-2. *Oncol. Res.* **2018**, *26*, 977–985. [CrossRef] [PubMed]
46. Sobti, R.C.; Singh, N.; Hussain, S.; Suri, V.; Bharti, A.C.; Das, B.C. Overexpression of STAT3 in HPV-mediated cervical cancer in a north Indian population. *Mol. Cell Biochem.* **2009**, *330*, 193–199. [CrossRef] [PubMed]

47. Takemoto, S.; Ushijima, K.; Kawano, K.; Yamaguchi, T.; Terada, A.; Fujiyoshi, N.; Nishio, S.; Tsuda, N.; Ijichi, M.; Kakuma, T.; et al. Expression of activated signal transducer and activator of transcription-3 predicts poor prognosis in cervical squamous-cell carcinoma. *Br. J. Cancer* **2009**, *101*, 967–972. [CrossRef] [PubMed]
48. Sobti, R.C.; Singh, N.; Hussain, S.; Suri, V.; Bharadwaj, M.; Das, B.C. Deregulation of STAT-5 isoforms in the development of HPV-mediated cervical carcinogenesis. *J. Recept. Signal Transduct. Res.* **2010**, *30*, 178–188. [CrossRef]
49. Wu, H.Y.; Li, Q.Q.; Liang, L.; Qiu, L.L.; Wei, H.W.; Huang, B.Y.; Chen, G.; He, R.Q.; Huang, Z.G.; Hou, W.; et al. Prognostic alternative splicing signature in cervical squamous cell carcinoma. *IET Syst. Biol.* **2020**, *14*, 314–322. [CrossRef] [PubMed]
50. Eun, J.K.; Mi, H.H.; Jeon, Y.J.; Yun, H.K. Identification and Complete Validation of Prognostic Gene Signatures for Human Papillomavirus-Associated Cancers: Integrated Approach Covering Different Anatomical Locations. *J. Virol.* **2020**, JVI.02354-20.
51. Cai, L.Y.; Hu, C.; Yu, S.S.; Liu, L.X.; Yu, X.B.; Chen, J.H.; Liu, X.; Lin, F.; Zhang, C.; Li, X.Y. Identification and validation of a six-gene signature associated with glycolysis to predict the prognosis of patients with cervical cancer. *BMC Cancer* **2020**, *20*, 1133. [CrossRef] [PubMed]
52. Zhao, S.; Yu, M.X. Identification of MMP1 as a Potential Prognostic Biomarker and Correlating with Immune Infiltrates in Cervical Squamous Cell Carcinoma. *DNA Cell Biol.* **2020**, *39*, 255–272. [CrossRef] [PubMed]
53. Chen, Q.; Hu, L.; Huang, D.; Chen, K.; Qiu, X.; Qiu, B. Six-lncRNA Immune Prognostic Signature for Cervical Cancer. *Front. Genet.* **2020**, *11*, 533628. [CrossRef] [PubMed]
54. Chen, H.; Deng, Q.; Wang, W.; Tao, H.; Gao, Y. Identification of an autophagy-related gene signature for survival prediction in patients with cervical cancer. *J. Ovaian Res.* **2020**, *13*, 131. [CrossRef] [PubMed]

5. Paper 2

cancers

MDPI

Article

Higher CCL22+ Cell Infiltration is Associated with Poor Prognosis in Cervical Cancer Patients

Qun Wang [1], Elisa Schmoeckel [2], Bernd P. Kost [1], Christina Kuhn [1], Aurelia Vattai [1], Theresa Vilsmaier [1], Sven Mahner [1], Doris Mayr [2], Udo Jeschke [1,*] and Helene Hildegard Heidegger [1]

1 Department of Obstetrics and Gynecology, University Hospital, LMU Munich, 80377 Munich, Germany; wqyxdz888@163.com (Q.W.); bernd.kost@med.uni-muenchen.de (B.P.K.); chrinstina.kuhn@med.uni-muenchen.de (C.K.); aurelia.vattai@med.uni-muenchen.de (A.V.); Theresa.vilsmaier@med.uni-muenchen.de (T.V.); sven.mahner@med.uni-muenchen.de (S.M.); Helene.heidegger@med.uni-muenchen.de (H.H.H.)

2 Department of Pathology, LMU Munich, 80377 Munich, Germany; elisa.schmoeckel@med.uni-muenchen.de (E.S.); doris.mayr@med.uni-muenchen.de (D.M.)

* Correspondence: udo.jeschke@med.uni-muenchen.de

Received: 20 November 2019; Accepted: 11 December 2019; Published: 12 December 2019

check for updates

Abstract: The chemokine CCL22 recruits regulatory T (T-reg) cells into tumor tissues and is expressed in many human tumors. However, the prognostic role of CCL22 in cervical cancer (CC) has not been determined. This study retrospectively analyzed the clinical significance of the expression of CCL22 and FOXP3 in 230 cervical cancer patients. Immunohistochemical staining analyses of CCL22 and FOXP3 were performed with a tissue microarray. Double immunofluorescence staining, cell coculture, and ELISA were used to determine CCL22 expressing cells and mechanisms. The higher number of infiltrating CCL22+ cells ($CCL22^{high}$) group was associated with lymph node metastasis ($p = 0.004$), Fédération Internationale de Gynécologie et d'Obstétrique (FIGO) stages ($p = 0.010$), therapeutic strategies ($p = 0.007$), and survival status ($p = 0.002$). The number of infiltrating CCL22+ cells was positively correlated with that of infiltrating FOXP3+ cells ($r = 0.210$, $p = 0.001$). The $CCL22^{high}$ group had a lower overall survival rate (OS), compared to the $CCL22^{low}$ group ($p = 0.001$). However, no significant differences in progression free survival (PFS) were noted between the two groups. $CCL22^{high}$ was an independent predictor of shorter OS (HR, 4.985; $p = 0.0001$). The OS of the combination group $CCL22^{high}FOXP3^{high}$ was significantly lower than that of the combination group $CCL22^{low}FOXP3^{low}$ regardless of the FIGO stage and disease subtype. $CCL22^{high}FOXP3^{high}$ was an independent indictor of shorter OS (HR, 5.284; $p = 0.009$). The PFS of group $CCL22^{high}FOXP3^{high}$ was significantly lower than that of group $CCL22^{low}FOXP3^{low}$ in cervical adenocarcinoma, but $CCL22^{high}FOXP3^{high}$ was not an independent indicator (HR, 3.018; $p = 0.068$). CCL22 was primarily expressed in M2-like macrophages in CC and induced by cervical cancer cells. The findings of our study indicate that cervical cancer patients with elevated CCL22+ infiltrating cells require more aggressive treatment. Moreover, the results provide a basis for subsequent, comprehensive studies to advance the design of immunotherapy for cervical cancer.

Keywords: CCL22; FOXP3; cervical cancer; macrophage; T-reg

1. Introduction

Cervical cancer is the second most prevalent tumor in developing countries and the fourth most common cause of cancer-related deaths among women. Over half a million new cervical cancer cases, and an estimated 265,700 deaths are reported each year worldwide [1,2]. Several factors

including economic conditions, genetic factors, endocrine [3], and immunity play significant role in the progression of cervical cancer. High-risk human papilloma virus is the primary cause of cervical cancer (CC) [4]. Immunosuppression states like infection with HIV [5] or taking immunosuppressive drugs [6] increases susceptibility to HPV infection and which subsequently causes cervical cancer. The current cervical cancer treatments include surgery, chemotherapy, and radiotherapy, but these are not effective for the management of advanced local cervical cancer, metastatic and recurrent tumors [7]. Recently, immunotherapy, particularly the immune checkpoint inhibitors, has achieved a great breakthrough. For example, the use of Pembrolizumab, a PD-1 inhibitor, in the later-staged and recurrent CC was authorized [8]. However, not all CC patients are sensitive to Pembrolizumab. Additional immune-related molecules should, therefore, be identified to explain the pathogenesis and improve the treatment of cervical cancer.

The role and mechanism of immune cells in the development of cervical cancer has not been adequately studied. Previous studies showed that the number of FOXP3+ regulatory T-cells that could suppress the innate and adaptive immunity systems [9,10] was higher in cervical cancer compared to other types of tumors [11] and suppressed immune responses [12]. On the one hand, it was reported that cervical cancer cells could secrete indoleamine 2,3-dioxygenase (IDO) to recruit FOXP3+ regulatory T-cells [12]. On the other hand, cervical cancer cells can secrete a series of molecules such as PEG2, IL-6, CCL2, and IL-10 that differentiate and activate M2-like macrophages [13–16]. M2-like macrophages have been widely accepted to play a role in the poor prognostic effect in CC [17]. M2-like macrophages promoted the CC cell proliferation by the GM-CSF/HB-EGF paracrine loop [18]. The number of M2-like macrophages was related to invasion patterns [19] and lymph node metastasis [20]. M2-like macrophages participate in immune suppression in cancer [21], yet, its underlying mechanism in CC has not been sufficiently elucidated. Previous studies on cervical cancer indicated that M2-like macrophages could decrease the presence of HPV16 E7 specific CD8+ T cells by diminishing HLA-DR expression and increasing the expression of either IL-10 or CSF1R [22–24]. Activated macrophages may inhibit the number of CD4+ T cells by producing neopterin [25]. M2-like macrophages could decrease the percentage of HPV specific regulatory T cells by blocking IL-10 signaling [26]. However, the association of CCL22 from cervical cancer cells or macrophages and regulatory T cells is still elusive.

The C-C motif chemokine ligand 22 (*CCL22*) gene is a secreted protein that exerts chemotactic activity for monocytes, dendritic cells, natural killer cells, and for chronically activated T lymphocytes [27–30]. Accumulating studies indicate that CCL22 plays a tumor-promoting role in human cancer. In ovarian cancer, for instance, CCL22 was found to induce regulatory T (T-reg) cells into tumor mass and inhibit T cell immunity [31]. High expression of CCL22 in M2 macrophages confers resistance to 5-fluorouracil in colorectal cancer [32]. A previous study showed that the *CCL22* mRNA expression level was higher in CC tissue than in a normal cervix [33]. However, the function of CCL22 in cervical cancer remains unknown.

The present study determined the functional role of CCL22 in infiltrating macrophages in cervical cancer. The expression level of CCL22 and the FOXP3+ regulatory T-cell marker was measured using a tissue microarray (TMA) with immunohistochemical staining. We further evaluated the correlation between clinical characteristics and CCL22 and FOXP3 expression. The findings of our study indicated that the number of CCL22+ cells was positively correlated with that of FOXP3+ cells ($r = 0.210$, $p = 0.001$). Moreover, group $CCL22^{high}$ had a significantly lower overall survival rate (OS), compared to the $CCL22^{low}$ group ($p = 0.001$). There was, however, no significant difference in progression free survival (PFS). The OS of the combination group $CCL22^{high}FOXP3^{high}$ was significantly lower than that of group $CCL22^{low}FOXP3^{low}$ regardless of the FIGO stage and disease subtype ($p < 0.05$). The PFS of group $CCL22^{high}FOXP3^{high}$ was significantly lower than that of group $CCL22^{low}FOXP3^{low}$ in cervical adenocarcinoma ($p < 0.05$). A double immunofluorescence staining indicated that M2-like macrophages primarily secreted CCL22. These results suggest that CCL22 secreted by M2 macrophages could recruit T-reg cells in cervical cancer and reduce the patient survival rate.

2. Results

2.1. CCL22 Was Overexpressed in Cervical Squamous Cell Carcinoma and Endocervical Adenocarcinoma (CESC)

The GEPIA database was used to identify the expression profile of CCL22 (http://gepia.cancer-pku.cn/) [34]. Transcript expression analysis for CCL22 was carried out in a total of 319 samples including 13 normal and 306 CESC tissues across TCGA normal and GTEx data. Next, using the ANOVA method, 1 as the Log2FC cutoff value, 0.01 as the cutoff value of the significance level, the expression difference of CCL22 in CESC tissue was obtained (Figure 1). The CCL22 mRNA level in CESC tissue was much higher than that in normal cervical tissues.

TIMER database was also used to identify the correlation between T-regs, TAM2, and CCL22 (https://cistrome.shinyapps.io/timer/) [35]. MRC1 (also named CD206) and FOXP3 represent M2 macrophage and regulatory T-cells, respectively [12,36]. Correlation analysis for MRC1, FOXP3, and CCL22 was carried out in the CESC dataset from TCGA. The results showed that CCL22 was positively correlated with MRC1 and FOXP3 ($r = 0.329$, $p = 4.45 \times 10^{-9}$; $r = 0.385$, $p = 4.31 \times 10^{-12}$, respectively). MRC1 was positively correlated with FOXP3 ($r = 0.43$, $p = 0.001$). The UALCAN database was used to analyze the survival rate in groups with differently expressed CCL22 in the CESC dataset from TCGA (http://ualcan.path.uab.edu/index.html) [37]. The result showed that although there was no significant difference, and the OS of the high CCL22 expression group was lower than that of the low CCL22 expression group in the long run ($p = 0.069$) (Figure S1).

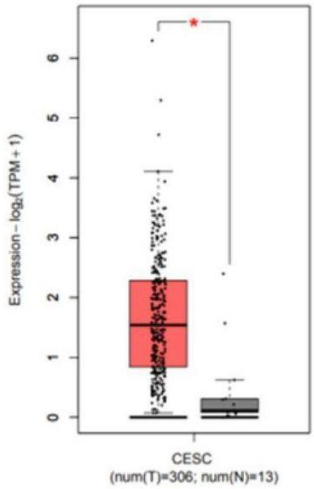

Figure 1. Transcripts expression level of CCL22 in CESC tissue explored using the GEPIA database. Red and grey colors denote the expression level in tumor tissue and normal tissue, respectively. CESC, cervical squamous cell carcinoma and endocervical adenocarcinoma. The asterisk (*) indicate significant higher CCL22 expression in tumor tissue compared to normal tissue.

2.2. The Association between the IRS of CCL22 in CC Cells, Infiltrating CCL22+ Cell and FOXP3+ Cell Counts with Clinical Characteristics

Tissue microarray by immunohistochemistry was performed to test the number of CCL22+ and FOXP3+ cells in a retrospective cohort of 230 cervical cancer cases, including 187 cases of squamous carcinoma and 43 cases of adenocarcinoma. As shown in Figures 2 and 3, the immunoreactivity of CCL22 and FOXP3 protein were detected. The IRS of CCL22 expressed in cervical cancer cells was evaluated and the number of CCL22+ and FOXP3+ cells was counted. We found that CCL22 expressed in CC cells was significantly associated with the disease subtypes ($p < 0.05$). The higher number of CCL22+ cells was significantly associated with lymph node metastasis ($p < 0.05$), FIGO stages ($p < 0.05$), therapeutic strategies ($p < 0.05$), and survival status ($p < 0.05$). The group with lower number of CCL22 (+) cells had 42.7% (88/206) lymph node metastasis, 55.8% (115/206) FIGO stage I to II, 38.3% (79/206) cases treated by surgery, and 11.2% (23/206) in death. The group with the higher number ($n > 11$) of CCL22 (+) cells had 12.5% (3/24) of cancer with lymph node metastasis, 83.3% (20/24) FIGO stage I to II, 70.8% (17/24) cases treated by surgery, and 37.5% (9/24) of cancer with death. The higher number of FOXP3+ was significantly associated with grading ($p < 0.05$). The number of FOXP3+ cells was significantly associated with disease subtypes ($p < 0.05$). The higher number ($n > 29$) of FOXP3+ cells was noted in 94.1% (32/34) with squamous carcinoma, while a lower number of FOXP3+ cells was observed in 79.1% (155/196) with squamous carcinoma (Table 1).

Table 1. The association between the number of CCL22+ cells and FOXP3+ cells and clinicopathological characteristics.

Clinicopathological Characteristics	Total (%)	IRS of CCL22 in CC Cells		p	Quantity of CCL22+ (n%)		p	Quantity of FOXP3+ (n%)		p
		Low (IRS < 4)	High (IRS ≥ 4)		Small ($n \leq 11$)	Large ($n > 11$)		Small ($n \leq 29$)	Large ($n > 29$)	
All cases	230	134 (58.3%)	96 (41.7%)	–	206 (89.6%)	24 (10.4%)	–	196 (85.2%)	34 (14.8%)	–
Age (year)										
≤50	132 (57.4%)	80 (59.7%)	52 (54.2%)	0.403	114 (55.3%)	18 (75.0%)	0.065	115 (58.7%)	17 (50.0%)	0.345
>50	98 (42.6%)	54 (40.3%)	44 (45.8%)		92 (44.7%)	6 (25.0%)		81 (41.3%)	17 (50.0%)	
Tumor Size (cm)										
<2	2 (0.9%)	2 (1.5%)	0 (0%)		2 (1.0%)	0 (0%)		2 (1.0%)	0 (0%)	
2–4	120 (52.2%)	75 (56%)	45 (46.9%)	0.080	103 (50.0%)	17 (70.8%)	0.090	102 (52%)	18 (52.9%)	0.905
>4	107 (46.5%)	57 (42.5%)	51 (53.1%)		101 (49.0%)	7 (29.2%)		92 (46.9%)	16 (47.1%)	
PN										
Without lymph node metastasis	139 (60.4%)	81 (60.4%)	58 (60.4%)	0.996	118 (57.3%)	21 (87.5%)	0.004 *	122 (62.2%)	17 (50.0%)	0.178
With lymph node metastasis	91 (39.6%)	53 (39.6%)	38 (39.6%)		88 (42.7%)	3 (12.5%)		74 (37.8%)	17 (50.0%)	
PM										
Without metastasis	219 (95.2%)	127 (94.8%)	92 (95.8%)	0.709	195 (94.7%)	24 (100%)	0.115	187 (95.4%)	32 (94.1%)	0.752
With metastasis	11 (4.8%)	7 (5.2%)	4 (4.2%)		11 (5.3%)	0 (0%)		9 (4.6%)	2 (5.9%)	
FIGO										
I–IIA	102 (44.3%)	62 (46.3%)	40 (41.7%)	0.488	85 (41.3%)	17 (70.8%)	0.006 *	87 (60.2%)	15 (50.0%)	0.265
IIB–IV	128 (55.7%)	55 (53.7%)	40 (58.3%)		121 (58.7%)	7 (29.2%)		109 (39.8%)	19 (50.0%)	
Grade										
1	19 (8.3%)	10 (7.8%)	9 (9.5%)		17 (8.9%)	2 (6.1%)		13 (6.7%)	4 (12.1%)	
2	129 (56.1%)	72 (56.3%)	58 (60.0%)	0.676	112 (58.9%)	17 (51.5%)	0.653	123 (63.1%)	12 (36.4%)	0.243
3	75 (32.6%)	46 (35.9%)	29 (30.5%)		61 (32.1%)	14 (42.4%)		59 (30.3%)	17 (51.50%)	
NA	7 (3.0%)									

Table 1. *Cont.*

Clinicopathological Characteristics	Total (%)	IRS of CCL22 in CC Cells		*p*	Quantity of CCL22+ (n%)		*p*	Quantity of FOXP3+ (n%)		*p*
		Low (IRS < 4)	High (IRS ≥ 4)		Small ($n \leq 11$)	Large ($n > 11$)		Small ($n \leq 29$)	Large ($n > 29$)	
Subtype										
Squamous carcinoma	187 (81.3%)	95 (70.9%)	92 (95.8%)	0.001 *	171 (83.0%)	16 (66.7%)	0.091	155 (79.1%)	32 (94.1%)	0.038 *
Adenocarcinoma	43 (18.7%)	39 (29.1%)	4 (4.2%)		35 (17.0%)	8 (33.3%)		41 (20.9%)	2 (5.9%)	
Progression										
No	175 (76.1%)	99 (75.0%)	76 (80.0%)	0.377	160 (78.8%)	15 (62.5%)	0.072	149 (76.8%)	26 (78.8%)	0.802
Yes	52 (22.6%)	33 (25.0%)	19 (20.0%)		43 (21.2%)	9 (37.5%)		45 (23.2%)	7 (21.2%)	
NA	3 (1.3%)									
Therapeutic Strategy										
Surgery	96 (41.7%)	59 (44.0%)	37 (38.5%)	0.675	79 (38.3%)	17 (70.8%)	0.007 *	83 (42.3%)	13 (38.2%)	0.494
Preoperative chemoradiotherapy	6 (2.6%)	3 (2.2%)	3 (3.1%)		6 (2.9%)	0 (0.0%)		4 (2.0%)	2 (5.9%)	
Chemoradiotherapy	128 (55.7%)	72 (53.7%)	56 (58.3%)		121 (58.7%)	7 (29.2%)		109 (55.6%)	19 (55.9%)	
Survival State										
Alive	198 (86.1%)	114 (85.1%)	84 (87.5%)	0.600	183 (88.8%)	15 (62.5%)	0.002 *	170 (86.7%)	28 (82.4%)	0.507
Death	32 (13.9%)	20 (14.9%)	12 (12.5%)		23 (11.2%)	9 (37.5%)		26 (13.3%)	6 (17.6%)	

NA, not applicable as data not available. * $p < 0.05$.

2.3. Higher Number of CCL22+ Cells Predicts Poor Prognosis of Patients with Cervical Cancer

We compared the overall survival rate (OS) and progression free survival (PFS) between group $CCL22^{low}$ and group $CCL22^{high}$ and the combined groups of CCL22 and FOXP3. The results of this study revealed that the OS of group $CCL22^{high}$ was significantly lower than that of group $CCL22^{low}$ ($p = 0.001$) (Figure 2A, left). The OS of group $CCL22^{high}FOXP3^{low}$ was significantly lower than that of group $CCL22^{low}FOXP3^{low}$ ($p = 0.022$), while the OS of group $CCL22^{high}FOXP3^{high}$ was significantly lower than that of group $CCL22^{low}FOXP3^{low}$ ($p = 0.003$). The OS of group $CCL22^{high}$ $FOXP3^{high}$ was significantly lower than that of group $CCL22^{low}$ $FOXP3^{high}$ ($p = 0.019$) (Figure 2B, left, Table 2). There was no significant difference in PFS between group $CCL22^{low}$ and group $CCL22^{high}$ (Figure 2A, right), but PFS of group $CCL22^{high}FOXP3^{high}$ was significantly lower than that of group $CCL22^{low}FOXP3^{high}$ (Figure 2B, right, Table 3).

We further compared the OS and PFS of the four groups in low and high FIGO stages, respectively. We found that the OS of $CCL22^{high}FOXP3^{low}$ and $CCL22^{high}FOXP3^{high}$ groups were significantly lower than those of the $CCL22^{low}FOXP3^{low}$ group in FIGO stage I–IIA ($p = 0.001$, $p = 0.013$, respectively) (Figure 2C, left, Table 4). The OS of the $CCL22^{high}FOXP3^{high}$ group was significantly lower than that of the $CCL22^{low}FOXP3^{low}$ group in FIGO stage IIB–IV ($p = 0.029$) (Figure 2C, right, Table 4). However, there was no significant difference in PFS among different groups in both low and high FIGO stages ($p > 0.05$) (Figure 2D, Table 5).

Due to the significant difference in the distribution of FOXP3(+) cells in cervical squamous carcinoma and adenocarcinoma (Table 1), we further compared the OS and PFS of the four groups in the two disease types, respectively. We found that the OS of the $CCL22^{high}FOXP3^{high}$ group was significantly lower than that of the $CCL22^{low}FOXP3^{high}$ and $CCL22^{low}FOXP3^{low}$ groups in cervical squamous carcinoma ($p = 0.023$, $p = 0.020$, respectively) (Figure 2E, left, Table 6). The OS of group $CCL22^{high}FOXP3^{high}$ was significantly lower than that of group $CCL22^{low}$ $FOXP3^{low}$ in cervical adenocarcinoma ($p = 0.043$) (Figure 2E, right, Table 6). There was no significant difference in PFS in cervical squamous carcinoma ($p > 0.05$) (Figure 2F, left, Table 7). The PFS of group $CCL22^{high}FOXP3^{high}$ was significantly lower than that of group $CCL22^{low}FOXP3^{low}$ in cervical adenocarcinoma ($p = 0.041$) (Figure 2F, right, Table 7).

Subsequently, a multivariate analysis was done using the COX proportional hazards model for variables that were significant in the univariate analysis was performed. For the OS analysis, we constructed two models with $CCL22^{low}$ vs. $CCL22^{high}$ or with $CCL22^{low}FOXP3^{low}$ vs. $CCL22^{high}FOXP3^{high}$. For the PFS, one model with $CCL22^{low}FOXP3^{low}$ vs. $CCL22^{high}FOXP3^{high}$ was constructed. The results showed that $CCL22^{high}$ and $CCL22^{high}FOXP3^{high}$ were independent predictors of shorter OS (HR 4.985, $p = 0.0001$; HR 5.284, $p = 0.009$; respectively). Although there were significant differences in PFS between group $CCL22^{high}FOXP3^{high}$ and group $CCL22^{low}FOXP3^{low}$, $CCL22^{high}FOXP3^{high}$ was not an independent predictor of PFS (HR, 3.018; $p = 0.068$) (Table 8).

Table 2. Pairwise comparison of overall survival rate.

Group		$CCL22^{low}$ $FOXP3^{low}$		$CCL22^{high}$ $FOXP3^{low}$		$CCL22^{low}$ $FOXP3^{high}$		$CCL22^{high}$ $FOXP3^{high}$	
		X^2	*p*-Value	X^2	*p*-Value	X^2	*p*-Value	X^2	*p*-Value
Log Rank (Mantel–Cox)	$CCL22^{low}$ $FOXP3^{low}$	–	–	5.250	0.022 *	0.005	0.946	8.732	0.003 *
	$CCL22^{high}$ $FOXP3^{low}$	5.250	0.022 *	–	–	2.466	0.116	0.469	0.494
	$CCL22^{low}$ $FOXP3^{high}$	0.005	0.946	2.466	0.116	–	–	5.486	0.019 *
	$CCL22^{high}$ $FOXP3^{high}$	8.732	0.003 *	0.469	0.494	5.486	0.019 *	–	–

* $p < 0.05$.

Table 3. Pairwise comparison of progression-free survival.

Group		CCL22^{low} FOXP3^{low}		CCL22^{high} FOXP3^{low}		CCL22^{low} FOXP3^{high}		CCL22^{high} FOXP3^{high}	
		X^2	*p*-Value	X^2	*p*-Value	X^2	*p*-Value	X^2	*p*-Value
Log Rank (Mantel–Cox)	CCL22^{low} FOXP3^{low}	–	–	0.519	0.471	0.490	0.484	3.320	0.068
	CCL22^{high} FOXP3^{low}	0.519	0.471	–	–	1.431	0.232	0.353	0.552
	CCL22^{low} FOXP3^{high}	0.490	0.484	1.431	0.232	–	–	4.069	0.044 *
	CCL22^{high} FOXP3^{high}	3.320	0.068	0.353	0.552	4.069	0.044 *	–	–

* $p < 0.05$.

Table 4. Pairwise comparison of overall survival rate in different FIGO stages.

Group			CCL22^{low} FOXP3^{low}		CCL22^{high} FOXP3^{low}		CCL22^{low} FOXP3^{high}		CCL22^{high} FOXP3^{high}	
			X^2	*p*-Value	X^2	*p*-Value	X^2	*p*-Value	X^2	*p*-Value
I–IIa	Log Rank (Mantel–Cox)	CCL22^{low} FOXP3^{low}	–	–	10.547	0.001 *	0.263	0.608	6.107	0.013 *
		CCL22^{high} FOXP3^{low}	10.547	0.001 *	–	–	3.122	0.077	0.010	0.920
		CCL22^{low} FOXP3^{high}	0.263	0.608	3.122	0.077	–	–	3.000	0.083
		CCL22^{high} FOXP3^{high}	6.107	0.013 *	0.010	0.920	3.000	0.083	–	–
IIb-IV	Log Rank (Mantel–Cox)	CCL22^{low} FOXP3^{low}	–	–	2.575	0.109	0.013	0.911	4.761	0.029 *
		CCL22^{high} FOXP3^{low}	2.575	0.109	–	–	0.896	0.344	0.119	0.730
		CCL22^{low} FOXP3^{high}	0.013	0.911	0.896	0.344	–	–	1.891	0.169
		CCL22^{high} FOXP3^{high}	4.761	0.029 *	0.119	0.730	1.891	0.169	–	–

* $p < 0.05$.

Table 5. Pairwise comparison of progression-free survival rate in different FIGO stages.

Group			CCL22^{low} FOXP3^{low}		CCL22^{high} FOXP3^{low}		CCL22^{low} FOXP3^{high}		CCL22^{high} FOXP3^{high}	
			X^2	*p*-Value	X^2	*p*-Value	X^2	*p*-Value	X^2	*p*-Value
I–IIa	Log Rank (Mantel–Cox)	CCL22^{low} FOXP3^{low}	–	–	1.967	0.161	0.301	0.583	1.413	0.235
		CCL22^{high} FOXP3^{low}	1.967	0.161	–	–	2.888	0.089	0.029	0.864
		CCL22^{low} FOXP3^{high}	0.301	0.583	2.888	0.089	–	–	3.000	0.083
		CCL22^{high} FOXP3^{high}	1.413	0.235	0.029	0.864	3.000	0.083	–	–
IIb–IV	Log Rank (Mantel–Cox)	CCL22^{low} FOXP3^{low}	–	–	0.603	0.437	0.004	0.950	2.515	0.113
		CCL22^{high} FOXP3^{low}	0.603	0.437	–	–	0.367	0.544	0.119	0.730
		CCL22^{low} FOXP3^{high}	0.004	0.950	0.367	0.544	–	–	1.160	0.282
		CCL22^{high} FOXP3^{high}	2.515	0.113	0.119	0.730	1.160	0.282	–	–

Table 6. Pairwise comparison of overall survival rate in different disease subtypes.

Group			$CCL22^{low}$ $FOXP3^{low}$		$CCL22^{high}$ $FOXP3^{low}$		$CCL22^{low}$ $FOXP3^{high}$		$CCL22^{high}$ $FOXP3^{high}$	
			X^2	*p*-Value	X^2	*p*-Value	X^2	*p*-Value	X^2	*p*-Value
Squamous carcinoma	Log Rank (Mantel–Cox)	$CCL22^{low}$ $FOXP3^{low}$	–	–	2.133	0.144	0.011	0.917	5.399	0.020
		$CCL22^{high}$ $FOXP3^{low}$	2.133	0.144	–	–	1.387	0.239	0.208	0.648
		$CCL22^{low}$ $FOXP3^{high}$	0.011	0.917	1.387	0.239	–	–	5.139	0.023 *
		$CCL22^{high}$ $FOXP3^{high}$	5.399	0.020 *	0.208	0.648	5.139	0.023	–	–
Adenocarcinoma	Log Rank (Mantel–Cox)	$CCL22^{low}$ $FOXP3^{low}$	–	–	1.802	0.179	1.363	0.243	4.093	0.043 *
		$CCL22^{high}$ $FOXP3^{low}$	1.802	0.179	–	–	0.264	0.608	1.824	0.177
		$CCL22^{low}$ $FOXP3^{high}$	1.363	0.243	0.264	0.608	–	–	1.000	0.317
		$CCL22^{high}$ $FOXP3^{high}$	4.093	0.043 *	1.824	0.177	1.000	0.317	–	–

* $p < 0.05$.

Table 7. Pairwise comparison of progression-free survival in different disease subtypes.

Group			$CCL22^{low}$ $FOXP3^{low}$		$CCL22^{high}$ $FOXP3^{low}$		$CCL22^{low}$ $FOXP3^{high}$		$CCL22^{high}$ $FOXP3^{high}$	
			X^2	*p*-Value	X^2	*p*-Value	X^2	*p*-Value	X^2	*p*-Value
Squamous carcinoma	Log Rank (Mantel–Cox)	$CCL22^{low}$ $FOXP3^{low}$	–	–	0.011	0.918	0.739	0.390	1.327	0.249
		$CCL22^{high}$ $FOXP3^{low}$	0.011	0.918	–	–	0.687	0.407	0.246	0.620
		$CCL22^{low}$ $FOXP3^{high}$	0.739	0.390	0.687	0.407	–	–	3.438	0.064
		$CCL22^{high}$ $FOXP3^{high}$	1.327	0.249	0.246	0.620	3.438	0.064	–	–
Adenocarcinoma	Log Rank (Mantel–Cox)	$CCL22^{low}$ $FOXP3^{low}$	–	–	0.770	0.380	0.796	0.372	4.175	0.041 *
		$CCL22^{high}$ $FOXP3^{low}$	0.770	0.380	–	–	0.264	0.608	1.824	0.177
		$CCL22^{low}$ $FOXP3^{high}$	0.796	0.372	0.264	0.608	–	–	1.000	0.317
		$CCL22^{high}$ $FOXP3^{high}$	4.175	0.041 *	1.824	0.177	1.000	0.317	–	–

* $p < 0.05$.

Table 8. Univariate and multivariate Cox regression analysis.

Clinicopathological Variables	Univariate Analysis		Multivariate Analysis		
	PFS	OS	PFS	OS (model 1)	OS (model 2)
Age (≤50 years vs. >50 years)					
HR	1.384	1.804	-	-	-
95%CI	0.804–2.385	0.897–3.629	-	-	-
p	0.241	0.098	-	-	-
Tumor Size (≤4 cm vs. >4 cm)					
HR	3.063	4.188	2.652	5.564	5.487
95%CI	1.710–5.486	1.924–9.112	1.063–6.617	1.538–20.130	1.504–20.011
p	0.001 *	0.001 *	0.037 *	0.009 *	0.010 *
PN (Without Lymph Node Metastasis vs. Lymph Lode Metastasis)					
HR	1.851	2.355	1.555	2.609	2.547
95%CI	1.065–3.218	1.162–4.774	0.756–3.200	1.032–6.596	0.988–6.562
p	0.029 *	0.017 *	0.231	0.043 *	0.053
PM (Without Metastasis vs. Metastasis)					
HR	1.710	3.303	-	-	-
95%CI	0.531–5.508	0.999–10.924	-	-	-
p	0.369	0.050	-	-	-
FIGO (I–IIa vs. IIb–IV)					
HR	2.630	2.913	1.088	0.584	0.599
95%CI	1.439–4.808	1.340–6.332	0.360–3.288	0.134–2.536	0.136–2.633
p	0.002 *	0.007 *	0.881	0.473	0.498
Grade (I vs. II–III)					
HR	1.672	1.054	-	-	-
95%CI	0.520–5.375	0.320–3.472	-	-	-
p	0.388	0.931	-	-	-
Disease Subtype (Squamous Carcinoma vs. Adenocarcinoma)					
HR	1.901	2.882	1.918	2.824	2.830
95%CI	1.043–3.466	1.408–5.899	1.038–3.545	1.359–5.869	1.361–5.883
p	0.036 *	0.004 *	0.038 *	0.005 *	0.005 *
Number of CCL22+ cells (CCL22low vs. CCL22high)					
HR	-	3.41	-	4.985	-
95%CI	-	1.567–7.419	-	2.206–11.266	-
p	-	0.002 *	-	0.0001 *	-
Number of CCL22+FOXP3+ cells (CCL22lowFOXP3low vs. CCL22highFOXP3high)					
HR	2.806	5.355	3.018	-	5.284
95%CI	0.864–9.115	1.580–18.154	0.923–9.869	-	1.513–18.456
p	0.086	0.007 *	0.068	-	0.009 *

* $p < 0.05$

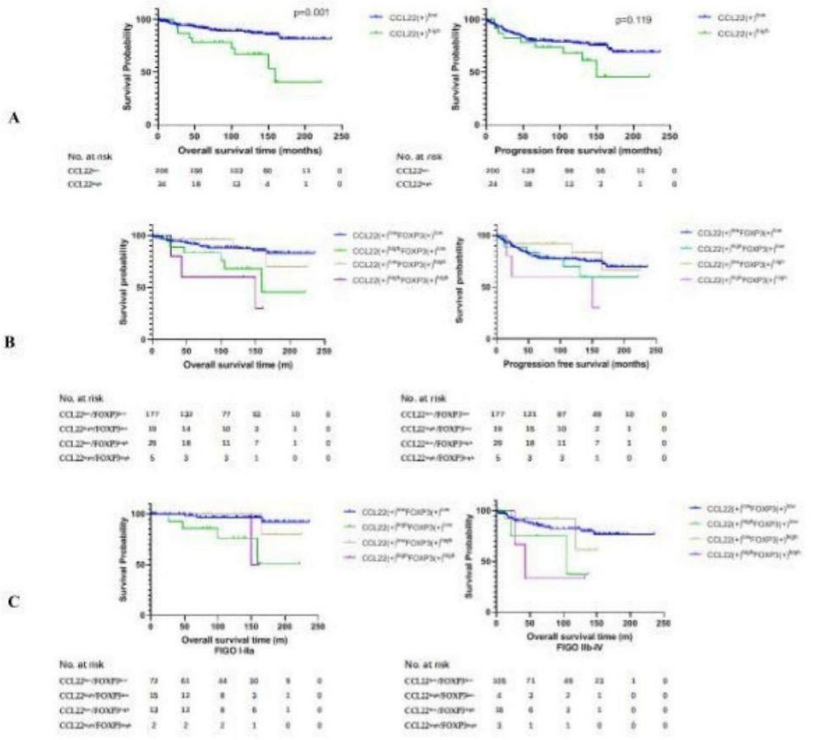

Figure 2. *Cont.*

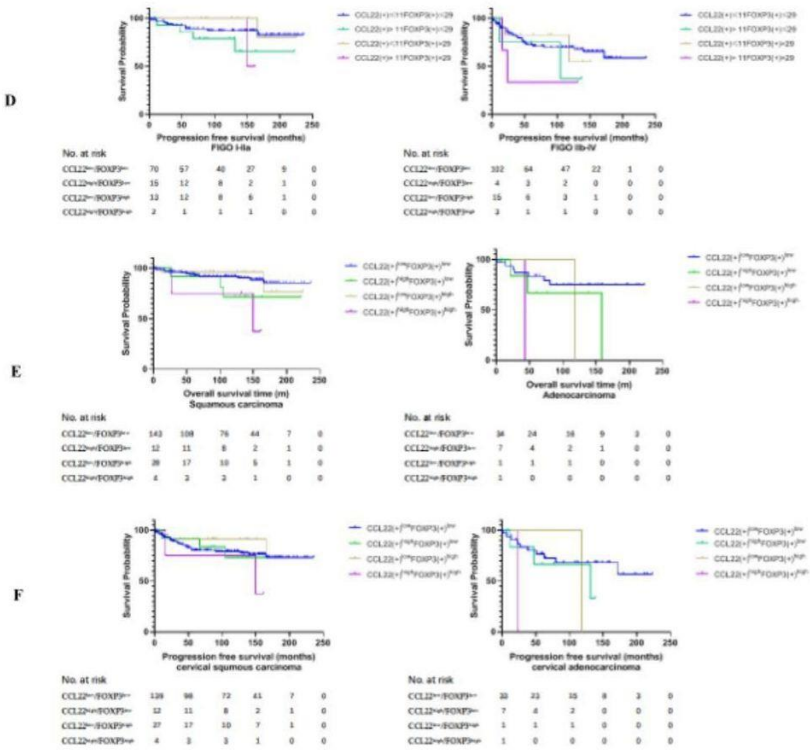

Figure 2. Kaplan–Meier estimates of overall survival rate and progression-free survival. (**A**) Overall survival rate (OS) (left) and progression free survival (PFS) (right) of group $CCL22^{low}$ and $CCL22^{high}$. (**B**) OS (left) and PFS (right) of the combined groups. (**C**) OS of the combined groups at different FIGO stages. (**D**) PFS of the combined groups at different FIGO stages. (**E**) OS of the combined groups in different disease subtypes. (**F**) PFS of the combined groups in different disease subtypes.

2.4. Correlation Analysis between CCL22+ Expression and FOXP3+ Cells

FoxP3 has been employed as a marker of regulatory T-cells. We postulated that the number of CCL22+ cells or the CCL22 expression in cervical cancer cells is correlated to the number of FOXP3+ cells in cervical cancer specimens. This hypothesis was tested by determining the expression of CCL22 and FOXP3 proteins by tissue microarray with IHC (Figure 3). A spearman correlation analysis indicated that both the number of CCL22+ cells and the CCL22 expression in cervical cancer cells were positively correlated with that of FOXP3+ cells ($r = 0.210$, $p = 0.002$; $r = 0.144$, $p = 0.027$, respectively) (Figure 4).

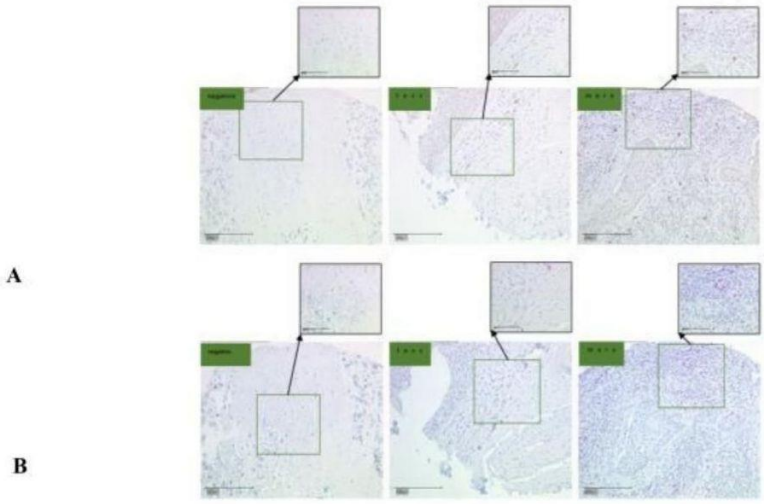

Figure 3. CCL22 and FOXP3 expression in cervical cancer (CC) tissue microarray as determined by IHC. (**A**) IHC for CCL22. The scale is 100 and 200 µm, respectively; (**B**) IHC for FOXP3. The scale is 100 and 200 µm, respectively. The number of CCL22+ and FOXP3+ cells was counted and classified as either negative, less, or more.

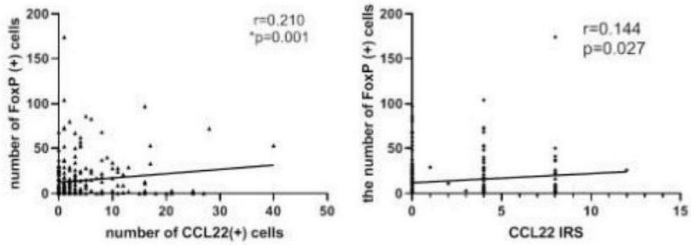

Figure 4. Left: number of CCL22+ cells is associated with that of FOXP3+ cells ($r = 0.210$, $p = 0.001$). Right: IRS of CCL22 expressed in cervical cancer cells is associated with the number of FOXP3+ cells ($r = 0.144$, $p = 0.027$). The number of cells was counted at a magnification of 25× lens and calculated three times each in three different areas of the tissue microarray (TMA). The IRS of CCL22 in cervical cancer cells was evaluated at a magnification of 25× and evaluated by two independent researchers.

2.5. Identification of CCL22 Expressing Cells in Cervical Cancer

Placenta tissue was used as a positive control for CCL22 and CD68, and appendix tissue as a positive control tissue for CD163. Negative control regents with normal IgG were applied to check CCL22 (rabbit IgG), CD68 (mouse IgG), and CD163 (mouse IgG) antibody specificity (Figures 5 and 6).

A previous study reported that CCL22 is expressed in myeloid cells such as dendritic cells and macrophages in the steady state [38]. This study, therefore, performed double immunofluorescence staining for CCL22, CD68, and CD163 to ascertain the expression of CCL22 in CC macrophages. CD68 and CD163 are specific markers for macrophages and M2-like macrophages, respectively [39]. We

analyzed the percentage of CD68+/CCL22-, CD68+/CCL22+ and CD163+/CCL22-, CD163+/CCL22+ cells with eight slides. Our results showed that 55.22% (±14.32%) CCL22+CD68+ cells were found on CD68+ cells, but 82.55% (±22.23%) CCL22+CD163+ cells were found on CD163+ cells ($p = 0.014$, Student's t test). The results of our study indicate that M2-like macrophages primarily secrete CCL22.

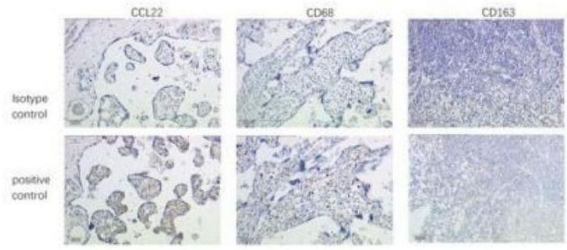

Figure 5. Validation of antibody specificity by IHC. Placenta as positive control tissue for CCL22 and CD68, and appendix as positive control tissue for CD163. The scale is 200 µm.

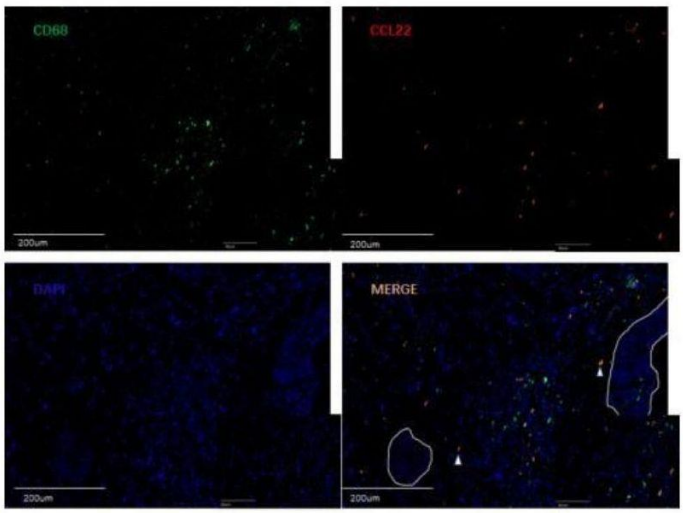

Figure 6. *Cont.*

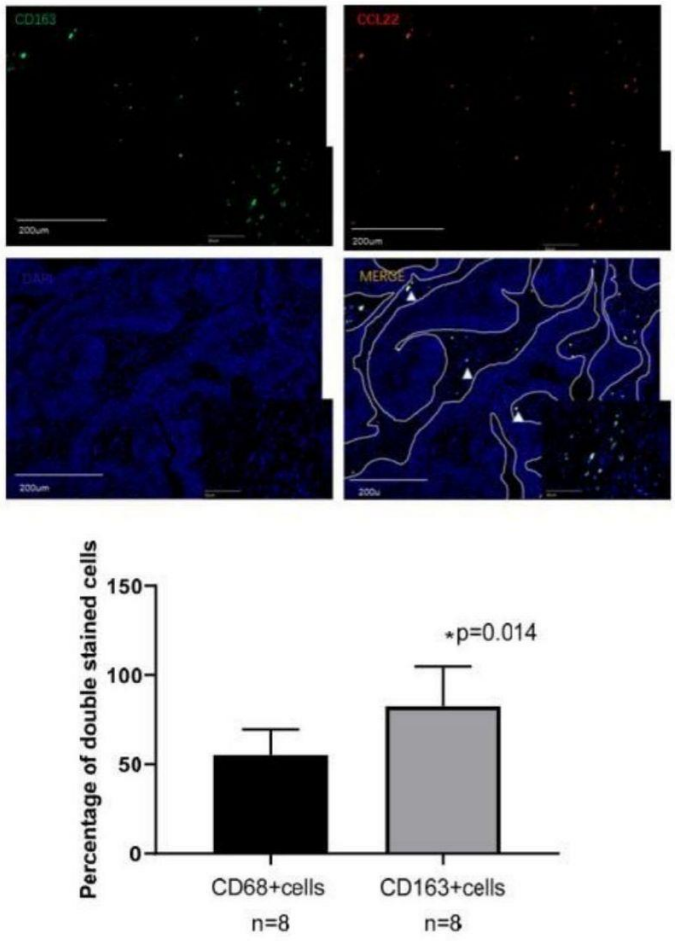

Figure 6. Double fluorescence staining of cervical cancer detecting CD68+CCL22+ cells and CD163+CCL22+cells. Immunofluorescent staining of CCL22+ cells (in red) expressing CD68 (macrophages in green) and CD163 (M2 macrophages in green). These two sets of pictures of different cervical tumor samples are representative of eight tumors analyzed. Arrowheads in the merged picture (lower right) designate double-positive cells located in the stroma. 55.22% (±14.32%) CCL22+CD68+ cells were found on CD68+ cells, but 82.55% (±22.23%) CCL22+CD163+ cells were found on CD163+ cells ($p = 0.014$, Student's t test). The solid line in white indicates a barrier between stroma and tumor nest. The image was shown in original magnification of 10× and 40×.

2.6. Cervical Cancer Cells Induced CCL22 in Monocytes

We cocultured monocytes with cervical cancer cells in a noncontact transwell system, which allowed the exchange of soluble factors, but prevented direct cell-cell contact. After coculture, ELISA assay demonstrated that the concentration of CCL22 in the supernatant of the lower chamber of cocultures was significantly higher (1405.4 ± 15.8, $p < 0.05$; 293.2 ± 13.3, $p < 0.05$; with Caski cells and Hela cells, respectively) than that of monocytes (0.000007 ± 0.0000004) or cervical cancer cells alone (73.3 ± 13.7, $p < 0.05$; 10.4 ± 18.1, $p < 0.05$; Caski and HeLa cells, respectively) (Figure 7). These results indicated that cervical cancer cells could induce CCL22 in monocytes.

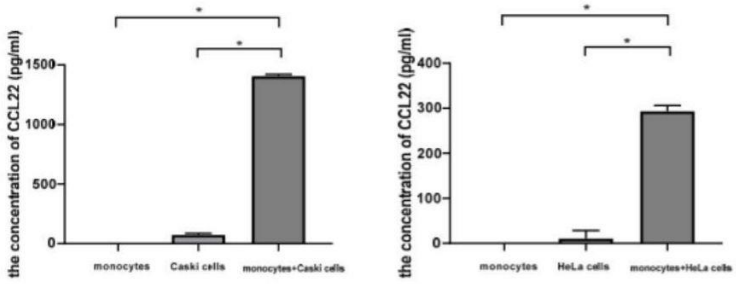

Figure 7. Cervical cancer cells induced CCL22 in monocytes. The left column graph representing the concentration of CCL22 in the supernatant from monocytes, Caski cells, and the cocultures of monocytes and Caski cells, respectively. The right column graph represents the concentration of CCL22 in the supernatant from monocytes, HeLa cells, and the cocultures of monocytes and HeLa cells, respectively. Each experiment was triplicated. * $p < 0.05$.

3. Materials and Methods

3.1. Bioinformatics

The GEPIA database was used to identify the expression profile of CCL22 (http://gepia.cancer-pku.cn/) [34]. Transcript expression analysis for CCL22 was carried out in a total of 316 samples including 13 normal and 303 CESC tissues across TCGA normal and GTEx data. Next, using ANOVA method, 1 as the Log2FC cutoff value, 0.01 as the cutoff value of the significance level, the expressing difference of CCL22 in CESC tissue was obtained. TIMER database was used to identify the correlation between T-regs, TAM2, and CCL22 (https://cistrome.shinyapps.io/timer/) [35]. UALCAN database was used to analyze survival rate in groups with differently expressed CCL22 in CESC dataset from TCGA (http://ualcan.path.uab.edu/index.html) [37].

3.2. Clinical Sample

The Institutional Review Board of the Ludwig-Maximilian University, Munich, (Number of approval: 337-06, 29 December 2006) approved this study. All patients provided written informed consent. Human cervical cancer tissue microarrays contained 230 samples from the patients diagnosed with CC between January 1994 and September 2002 consecutively from the Department of Obstetrics and Gynecology, LMU Munich. The age was from 22 to 83 years with a median age of 49 years. Clinicopathologic characteristics of patients are available in Table 1. Staging was performed according to the FIGO staging system. Primary treatment of CC consisted of type 3 radical hysterectomy with pelvic lymph-node dissection. Data including age, stage, lymph node metastasis, distant metastasis, and survival status were obtained from medical records. Data on tumor size, tumor grade, and lymph-node metastases were reviewed from pathology reports.

3.3. Tissue Microarray Construction

TMAs were constructed from 230 formalin-fixed, paraffin-embedded cervical cancer tissue specimens, including 187 cervical squamous cancer and 43 cervical adenocarcinoma. Briefly, to define representative tumor areas, an institutional pathologist reviewed the hematoxylin and eosin (HE)-stained whole-mount sections to define representative tumor areas. Subsequently, after retrieval of four 1.0-mm diameter tissue cores from the formalin-fixed paraffin-embedded tissue blocks of which consisted tumor specimens, they were arrayed on a 38 × 25 recipient paraffin block using an MTA-1 manual tissue array (Beecher Instruments Inc., Silver Spring, MD, USA). Then, 3 µm sections were cut on a microtome and placed on glass slides for two replicates. One series was for staining CCL22 and the other was for staining FoxP3. The presence of tumor tissue on the sections was verified by HE staining.

3.4. Immunohistochemistry

The TMA sections were deparaffinized in xylol for 20 min and rinsed in 100% ethanol. Then, 20 min H_2O_2 incubation was performed to inhibit endogenous peroxidase reaction. Afterwards, the specimens were rehydrated in deescalating alcohol gradients, starting with 100% ethanol and ending with distilled water. The pressure pot contained a sodium citrate buffer (pH = 6.0), which consisted of 0.1 m citric acid and 0.1 mM sodium citrate in distilled water. Then, samples were washed in PBS twice and incubated with a blocking solution (Regent 1, ZytoChem Plus HRP Polymer System (Mouse/Rabbit), Zytomed, Berlin, Germany) for 5 min. Incubation with the primary antibody was performed at 4 °C for 16 h. All antibodies used are listed in Table 4. Samples were washed twice in PBS (pH = 7.4) following every subsequent step. The blocking solutions (Regent 2) was applied for 20 min and HRP-Polymer (Regent 3) for 30 min. The chromogen-substrate staining was carried out using the Liquid DAB+ Substrate Chromogen System (Dako Scientifi, Glostrup, Denmark). The reaction was stopped by applying distilled water. Finally, the slides were counterstained with Hemalaun for 2 min and blued in tap water. The slides were dehydrated in an ascending alcohol gradient and cover slipped with Eukitt quick hardening mounting medium (Sigma Aldrich, St.Lousis, MO, USA). Human tonsil tissue was applied as positive control. All slides were analyzed using the microscope Leitz Wetzlar (Wetzlar, Germany; Type 307-148.001 514686). The immunoreactive score (IRS) was used for evaluation of the intensity and distribution pattern of antigen expression. The semiquantitative score was calculated as follows: the optical staining intensity (grades: 0 = none, 1 = weak, 2 = moderate, 3 = strong staining) was multiplied by the total percentage of positively stained cells (0 = none, 1 = 10%, 2 = 11–50%, 3 = 51–80%, and 4 = 81% of the cells). This multiplication has a minimum of 0 and a maximum of 12. Two experience staff members analyzed the slides independently. Total number of CCL22+ cells and FOXP3+ cells were counted in a magnification field of 40× lens three times each in three different areas of each slide. The cutoff value was calculated by ROC curve. Cutoff values of 11 and 27 were applied for CCL22+ cells and FOXP3+ cells, respectively.

3.4.1. Evaluation of CCL22+ Cells as Macrophages

For the visualization of CCL22 expressing cells in CC infiltrating cells, the same tissue samples with TMA were used. The antibodies are shown in Table 4. Double immunofluorescence staining for CCL22 and CD68 as a specific macrophage marker was performed to identify the CCL22 expression in macrophages.

3.4.2. Evaluation of CCL22+ Cells as M2-Like Macrophages

In order to identify which subtype of macrophages express CCL22, the same tissue samples with TMA were used. The antibodies are shown in Table 9. Double immunofluorescence staining for CCL22 and CD163 as a specific M2-like macrophage marker was performed.

Table 9. Antibodies used for immunohistochemical characterization and double immunofluorescence of cervical cancer samples.

Antibody	Isotype	Clone	Dilution	Source
CCL22	rabbit IgG	polyclonal	1:400 in PBS [a] 1:400 in Dako [b]	Perprotech; DAKO(S322); Carpentera, CA, USA
FoxP3	mouse IgG	monoklonal	1:300 in PBS [a]	Abcam
CD68	mouse IgG	polyclonal	1:1000 in PBS [a] 1:1000 in Dako [b]	Sigma; DAKO(S322); Carpentera, CA, USA
CD163	mouse IgG	monoklonal	1:800 in PBS [a] 1:800 in Dako [b]	Abcam; DAKO(S322); Carpentera, CA, USA
Cy-3 [b]	goat IgG anti-rabbit	polyclonal	1:500 [b] in Dako [b]	Dianova, Hamburg, Germany
Cy-2 [b]	goat IgG anti-mouse	polyclonal	1:100 [b] in Dako [b]	Dianova, Hamburg, Germany

[a] antibodies used for immunohistochemistry, [b] antibodies used for immunofluorescence.

3.5. Cell Coculture

To determine the effect of cervical cancer cells on the induction of CCL22 in macrophages, monocytes were cocultured with HeLa cells and Caski cells, respectively. Transwell core size was 0.4 μm. First, we picked up the ordered buffy coat and purified the PBMCs using the Ficoll–Hypaque method. We counted the PBMCs and seeded 0.2 million PBMCs per well into 24-well plates. Then plastic adherence was in the incubator overnight. The next day, adhered monocytes were washed gently with 1 × PBS, digested by 0.25% trypsin with 0.25% EDTA and ended by complete medium. Monocytes were plated in the lower chamber and 10^7 cervical cells were plated in the upper chamber in 24 wells. They were cultured in 500 μL culture medium in each chamber with RPMI 1640 medium and 10% fetal calf serum. Cocultures were incubated for 48 h and the supernatant of the lower chambers were harvested followed by Elisa. 0.2 million monocytes with inserts and 10^7 Caski and 10^7 HeLa cells with inserts cultured with RPMI 1640 medium with 10% fetal cow serum were as the control. Elisa was performed after 48 h.

3.6. Elisa

Serum of all groups were collected and stored in −80 °C before analysis. ELISA assay was performed according to the manufacturer's instructions of the ELISA kits (Catalog No. DMD00, R&D Systems, Minneapolis, MN, USA). The OD value at 450 nm was measured. The concentrations of CCL22 was calculated according to the standard curve.

3.7. Statistical Analysis

Clinical data are presented as number (percentage of the amount of relevant clinicopathology). Statistical analysis of the number of CCL22+ and FOXP3+ cells were performed using chi-square test. Correlation analysis of the number of CCL22+ and FOXP3+ cells were performed using Spearman correlation. The Kaplan–Meier method was used to calculate the OS curve and further survival analysis was performed using the log-rank test. The Cox proportional hazard model was used to estimate hazard ratios and 95% confidence intervals in both univariate and multivariate models. CCL22 concentration was presented as mean ± standard deviation. ANOVA analysis was performed using Welch ANOVA and Games-Howell. Statistical analyses were performed using SPSS version 23.0 (SPSS Inc., Chicago, IL, USA). $p < 0.05$ was considered statically significant.

4. Discussion

Our study revealed a correlation between the expression of CCL22 and FOXP3 in cervical cancer. This study is the first to report the relationship between CCL22 expression and the prognosis of cervical cancer (CC) patients. The group with a higher number of CCL22+ infiltrating cells shows a lower overall survival rate (OS) than that of the group of lower number of CCL22+ infiltrating cells in cervical

cancer. However, the expression of CCL22 in cervical cancer cells seems not to affect the survival rate of CC patients. Moreover, the OS of the group combining higher CCL22+ and FOXP3+ infiltrating cells is lower than that of the group with a combined lower number of CCL22+ and FOXP3+ infiltrating cells.

In recent years, several studies have investigated the prognostic value of new immune checkpoints such as CCL22. CCL22 belongs to a family of secreted proteins that play various roles in immunoregulatory and inflammatory processes [27]. Previous research has reported that CCL22 is a prognostic predictor of various cancers. For instance, a report by Li et al. indicated that tumor secretion by CCL22 is an independent prognostic predictor of breast cancer [40]. Another study proved that the levels of serum macrophage-derived CCL22 are associated with glioma risk and survival period [41]. Besides, CCL22 predicts postoperative prognosis in patients with stage II/III gastric cancer [42]. The prognostic value of CCL22 in cervical cancer has, however, not been investigated. This study reveals that the $CCL22^{high}$ group had a lower OS, compared to the $CCL22^{low}$ group ($p = 0.001$). $CCL22^{high}$ was an independent predictor of shorter OS (HR, 4.985; $p = 0.0001$). The OS of the combination group $CCL22^{high}FOXP3^{high}$ was significantly lower than that of the combination group $CCL22^{low}FOXP3^{low}$ regardless of the FIGO stage and disease subtype. $CCL22^{high}FOXP3^{high}$ was an independent indictor of shorter OS (HR, 5.284; $p = 0.009$). The PFS of group $CCL22^{high}FOXP3^{high}$ was significantly lower than that of group $CCL22^{low}FOXP3^{low}$ in cervical adenocarcinoma, but $CCL22^{high}FOXP3^{high}$ was not an independent indicator (HR, 3.018; $p = 0.068$). Therefore, the CCL22+ infiltrating cells or the combination of CCL22 (+) and FOXP3 (+) cells are novel biomarkers that can be potentially used for cervical cancer prognosis. Since this study only had 5/230 samples with both a high number of CCL22+ and FOXP3+ infiltrating cells, increasing the sample size might provide a more reliable result.

Previous studies reported that CCL22 could recruit FOXP3 (+) regulatory T-cells. Increased CCL22 mRNA levels are correlated with increased FoxP3 mRNA levels in oral cancer specimens [43]. In a B16F10 melanoma model, imiquimod (IQM) has been shown to reduce T-regs at the tumor site by the downregulation of CCL22 production [44]. In cervical cancer, the *CCL22* mRNA levels of neoplastic foci and tumor periphery is positively correlated with FOXP3 [45]. In cervical cancer, however, the correlation between protein expression levels of CCL22 and FOXP3, and the cell source of CCL22 have not been determined. This study revealed a similar trend, that the protein level of CCL22 from both cervical cancer cells and infiltrating cells was positively correlated with FOXP3. This correlation was defined by calculating the IRS of CCL22 expression in cervical cancer cells and counting the number of CCL22+ and FOXP3+ cells. The association of the latter was better than the former. Therefore, both cervical cancer cell-derived and infiltrating cell-derived cells might recruit T-regs, and the role of CCL22 from infiltrating cells was found to be more significant than that of CCL22 from cervical cancer cells.

Several studies have investigated the source of CCL22. For instance, Huang et al. proved that CCL22 was overexpressed in head and neck cancer cells [43]. CCL22 was found in macrophages of tongue squamous cell carcinoma [46]. Additionally, the secretion of CCL22 by M2-like macrophages in colorectal cancer was proven [32]. However, CCL22 expression in cervical cancer has not been previously determined. By performing a tissue microarray (TMA) using immunohistochemistry (IHC), we showed that CCL22 could be secreted by cervical cancer cells. Besides, double immunofluorescence of CD163 and CCL22 showed that 82.55% (±22.23%) of CD163(+) cells were overlapped with CCL22 (+) infiltrating cells. Therefore, CCL22 is secreted by M2-like macrophages and cervical cancer cells in cervical cancer. Moreover, many studies proved that cervical cancer cells could induce monocytes into M2 macrophages [18,42] which was consistent with the result in our study to some degree that CCL22 in monocytes could be induced by cervical cancer cells. However, further studies need to be performed to show the effect of cervical cancer cells on M2 macrophages and the regulatory mechanisms of CCL22 needs to be studied in the future. In conclusion, our findings suggest that the increase in CCL22 (+) infiltrating M2-like macrophage cells may recruit more T-regs in CC tissue and cause a poor prognosis for cervical cancer patients. CCL22 could be a prognostic predictor and therapeutic target to identify and treat cervical cancer patients with poorer clinical outcomes.

5. Conclusions

Our study demonstrates that high CCL22(+) infiltrating cells particularly M2-like macrophage cells, is associated with a poor outcome of cervical cancer patients. CCL22 expression is positively correlated with FoxP3 expression in cervical cancer. Thus, CCL22 may be a novel prognostic marker and therapeutic target for the treatment of cervical cancer.

Supplementary Materials: The following are available online at http://www.mdpi.com/2072-6694/11/12/2004/s1, Figure S1: Correlation analysis of CCL22, MRC1 and FOXP3 in CESC tissue as explored by the TIMER database.

Author Contributions: H.H.H.: project development, data collection. Q.W.: experiments, manuscript writing. H.H.H., B.P.K. and A.V.: data collection, manuscript editing. H.H.H. and Q.W. and T.V.: data analyses. E.S., D.M. and U.J.: supervision, data analyses. C.K. and Q.W.: experiments, methodology. S.M.: data analyses, supervision.

Funding: The China Scholarship Council (CSC) funded this study for Qun Wang.

Conflicts of Interest: S.M. reports grants and personal fees from AstraZeneca, personal fees from Clovis, grants and personal fees from Medac, grants and personal fees from MSD. He also reports personal fees from Novartis, grants and personal fees from PharmaMar, grants and personal fees from Roche, personal fees from Sensor Kinesis, grants and personal fees from Tesaro, grants and personal fees from Teva, outside the submitted work. All other authors declare no conflict of interest.

References

1. Torre, L.A.; Bray, F.; Siegel, R.L.; Ferlay, J.; Lortet-Tieulent, J.; Jemal, A. Global cancer statistics, 2012. *CA Cancer J. Clin.* **2015**, *65*, 87–108. [CrossRef] [PubMed]
2. Ch, P.N.; Gurram, L.; Chopra, S.; Mahantshetty, U. The management of locally advanced cervical cancer. *Curr. Opin. Oncol.* **2018**, *30*, 323–329. [CrossRef]
3. Kessler, T.A. Cervical Cancer: Prevention and Early Detection. *Semin. Oncol. Nurs.* **2017**, *33*, 172–183. [CrossRef] [PubMed]
4. Walboomers, J.M.; Jacobs, M.V.; Manos, M.M.; Bosch, F.X.; Kummer, J.A.; Shah, K.V.; Snijders, P.J.F.; Peto, J.; Meijer, C.J.L.M.; Munoz, N. Human papillomavirus is a necessary cause of invasive cervical cancer worldwide. *J. Pathol.* **1999**, *189*, 12–19. [CrossRef]
5. Clifford, G.M.; Tully, S.; Franceschi, S. Carcinogenicity of Human Papillomavirus (HPV) Types in HIV-Positive Women: A Meta-Analysis From HPV Infection to Cervical Cancer. *Clin. Infect. Dis.* **2017**, *64*, 1228–1235. [CrossRef] [PubMed]
6. Feldman, C.H.; Liu, J.; Feldman, S.; Solomon, D.H.; Kim, S.C. Risk of high-grade cervical dysplasia and cervical cancer in women with systemic lupus erythematosus receiving immunosuppressive drugs. *Lupus* **2017**, *26*, 682–689. [CrossRef]
7. Duenas-Gonzalez, A.; Campbell, S. Global strategies for the treatment of early-stage and advanced cervical cancer. *Curr. Opin. Obs. Gynecol.* **2016**, *28*, 11–17. [CrossRef]
8. Borcoman, E.; Le Tourneau, C. Pembrolizumab in cervical cancer: Latest evidence and clinical usefulness. *Adv. Med. Oncol.* **2017**, *9*, 431–439. [CrossRef]
9. Toker, A.; Ohashi, P.S. Expression of costimulatory and inhibitory receptors in FOXP3(+) regulatory T cells within the tumor microenvironment: Implications for combination immunotherapy approaches. *Adv. Cancer Res.* **2019**, *144*, 193–261. [CrossRef]
10. Miyara, M.; Sakaguchi, S. Natural regulatory T cells: Mechanisms of suppression. *Trends Mol. Med.* **2007**, *13*, 108–116. [CrossRef]
11. Loddenkemper, C.; Hoffmann, C.; Stanke, J.; Nagorsen, D.; Baron, U.; Olek, S.; Huehn, J.; Ritz, J.-P.; Stein, H.; Kaufmann, A.M.; et al. Regulatory (FOXP3+) T cells as target for immune therapy of cervical intraepithelial neoplasia and cervical cancer. *Cancer Sci.* **2009**, *100*, 1112–1117. [CrossRef]
12. Visser, J.; Nijman, H.W.; Hoogenboom, B.N.; Jager, P.; Van Baarle, D.; Schuuring, E.; Abdulahad, W.; Miedema, F.; Van Der Zee, A.G.; Daemen, T. Frequencies and role of regulatory T cells in patients with (pre)malignant cervical neoplasia. *Clin. Exp. Immunol.* **2007**, *150*, 199–209. [CrossRef] [PubMed]

13. Heusinkveld, M.; De Vos van Steenwijk, P.J.; Goedemans, R.; Ramwadhdoebe, T.H.; Gorter, A.; Welters, M.J.; Van Hall, T.; Van der Burg, S.H. M2 macrophages induced by prostaglandin E2 and IL-6 from cervical carcinoma are switched to activated M1 macrophages by CD4+ Th1 cells. *J. Immunol.* **2011**, *187*, 1157–1165. [CrossRef] [PubMed]
14. Sierra-Filardi, E.; Nieto, C.; Dominguez-Soto, A.; Barroso, R.; Sanchez-Mateos, P.; Puig-Kroger, A.; Lopez-Bravo, M.; Joven, J.; Ardavin, C.; Rodrguez-Fernandez, J.L.; et al. CCL2 shapes macrophage polarization by GM-CSF and M-CSF: Identification of CCL2/CCR2-dependent gene expression profile. *J. Immunol.* **2014**, *192*, 3858–3867. [CrossRef] [PubMed]
15. Riley, J.K.; Takeda, K.; Akira, S.; Schreiber, R.D. Interleukin-10 receptor signaling through the JAK-STAT pathway. Requirement for two distinct receptor-derived signals for anti-inflammatory action. *J. Biol. Chem.* **1999**, *274*, 16513–16521. [CrossRef]
16. Kim, J.; Bae, J.S. Tumor-Associated Macrophages and Neutrophils in Tumor Microenvironment. *Mediat. Inflamm.* **2016**, *2016*, 6058147. [CrossRef]
17. Davidson, B.; Goldberg, I.; Kopolovic, J. Inflammatory response in cervical intraepithelial neoplasia and squamous cell carcinoma of the uterine cervix. *Pathol. Res. Pract.* **1997**, *193*, 491–495. [CrossRef]
18. Rigo, A.; Gottardi, M.; Zamo, A.; Mauri, P.; Bonifacio, M.; Krampera, M.; Damiani, E.; Pizzolo, G.; Vinante, F. Macrophages may promote cancer growth via a GM-CSF/HB-EGF paracrine loop that is enhanced by CXCL12. *Mol. Cancer* **2010**, *9*, 273. [CrossRef]
19. Punt, S.; Thijssen, V.L.; Vrolijk, J.; De Kroon, C.D.; Gorter, A.; Jordanova, E.S. Galectin-1, -3 and -9 Expression and Clinical Significance in Squamous Cervical Cancer. *PLoS ONE* **2015**, *10*, e0129119. [CrossRef]
20. Chen, X.J.; Han, L.F.; Wu, X.G.; Wei, W.F.; Wu, L.F.; Yi, H.Y.; Yan, R.-M.; Bai, X.; Zhong, M.; Yu, Y.; et al. Clinical Significance of CD163+ and CD68+ Tumor-associated Macrophages in High-risk HPV-related Cervical Cancer. *J. Cancer* **2017**, *8*, 3868–3875. [CrossRef]
21. Hartwig, T.; Montinaro, A.; Von Karstedt, S.; Sevko, A.; Surinova, S.; Chakravarthy, A.; Taraborrelli, L.; Draber, P.; Lafont, E.; Vargas, F.A.; et al. The TRAIL-Induced Cancer Secretome Promotes a Tumor-Supportive Immune Microenvironment via CCR2. *Mol. Cell* **2017**, *65*, 730–742. [CrossRef] [PubMed]
22. Lepique, A.P.; Daghastanli, K.R.; Cuccovia, I.M.; Villa, L.L. HPV16 tumor associated macrophages suppress antitumor T cell responses. *Clin. Cancer Res.* **2009**, *15*, 4391–4400. [CrossRef] [PubMed]
23. Hilders, C.G.; Munoz, I.M.; Nooyen, Y.; Fleuren, G.J. Altered HLA expression by metastatic cervical carcinoma cells as a factor in impaired immune surveillance. *Gynecol. Oncol.* **1995**, *57*, 366–375. [CrossRef] [PubMed]
24. Walentowicz-Sadlecka, M.; Koper, A.; Krystyna, G.; Koper, K.; Basta, P.; Mach, P.; Skret-Magierlo, J.; Dutsch-Wicherek, M.; Sikora, J.; Grabiec, M.; et al. The analysis of metallothionein immunoreactivity in stromal fibroblasts and macrophages in cases of uterine cervical carcinoma with respect to both the local and distant spread of the disease. *Am. J. Reprod. Immunol.* **2013**, *70*, 253–261. [CrossRef] [PubMed]
25. Melichar, B.; Solichova, D.; Freedman, R.S. Neopterin as an indicator of immune activation and prognosis in patients with gynecological malignancies. *Int. J. Gynecol. Cancer* **2006**, *16*, 240–252. [CrossRef] [PubMed]
26. Bolpetti, A.; Silva, J.S.; Villa, L.L.; Lepique, A.P. Interleukin-10 production by tumor infiltrating macrophages plays a role in Human Papillomavirus 16 tumor growth. *BMC Immunol.* **2010**, *11*, 27. [CrossRef]
27. Godiska, R.; Chantry, D.; Raport, C.J.; Sozzani, S.; Allavena, P.; Leviten, D.; Mantovani, A.; Gray, P.W. Human macrophage-derived chemokine (MDC), a novel chemoattractant for monocytes, monocyte-derived dendritic cells, and natural killer cells. *J. Exp. Med.* **1997**, *185*, 1595–1604. [CrossRef]
28. Chang, M.; McNinch, J.; Elias, C., 3rd; Manthey, C.L.; Grosshans, D.; Meng, T.; Boone, T.; Andrew, D. Molecular cloning and functional characterization of a novel CC chemokine, stimulated T cell chemotactic protein (STCP-1) that specifically acts on activated T lymphocytes. *J. Biol. Chem.* **1997**, *272*, 25229–25237. [CrossRef]
29. Schaniel, C.; Pardali, E.; Sallusto, F.; Speletas, M.; Ruedl, C.; Shimizu, T.; Seidl, T.; Andersson, J.; Melchers, F.; Rolink, A.G.; et al. Activated murine B lymphocytes and dendritic cells produce a novel CC chemokine which acts selectively on activated T cells. *J. Exp. Med.* **1998**, *188*, 451–463. [CrossRef]
30. Mantovani, A.; Gray, P.A.; Van Damme, J.; Sozzani, S. Macrophage-derived chemokine (MDC). *J. Leukoc. Biol.* **2000**, *68*, 400–404.
31. Curiel, T.J.; Coukos, G.; Zou, L.; Alvarez, X.; Cheng, P.; Mottram, P.; Evdemon-Hogan, M.; Conejo-Garcia, J.R.; Zhang, L.; Burow, M.; et al. Specific recruitment of regulatory T cells in ovarian carcinoma fosters immune privilege and predicts reduced survival. *Nat. Med.* **2004**, *10*, 942–949. [CrossRef] [PubMed]

32. Wei, C.; Yang, C.; Wang, S.; Shi, D.; Zhang, C.; Lin, X.; Xiong, B. M2 macrophages confer resistance to 5-fluorouracil in colorectal cancer through the activation of CCL22/PI3K/AKT signaling. *OncoTargets Ther.* **2019**, *12*, 3051–3063. [CrossRef] [PubMed]
33. Zhao, M.; Li, Y.; Wei, X.; Zhang, Q.; Jia, H.; Quan, S.; Cao, D.; Wang, L.; Yang, T.; Zhao, J.; et al. Negative immune factors might predominate local tumor immune status and promote carcinogenesis in cervical carcinoma. *Virol. J.* **2017**, *14*, 5. [CrossRef] [PubMed]
34. Tang, Z.; Li, C.; Kang, B.; Gao, G.; Li, C.; Zhang, Z. GEPIA: A web server for cancer and normal gene expression profiling and interactive analyses. *Nucleic Acids Res.* **2017**, *45*, W98–W102. [CrossRef] [PubMed]
35. Li, T.; Fan, J.; Wang, B.; Traugh, N.; Chen, Q.; Liu, J.S.; Li, B.; Liu, X.S. TIMER: A Web Server for Comprehensive Analysis of Tumor-Infiltrating Immune Cells. *Cancer Res.* **2017**, *77*, e108–e110. [CrossRef] [PubMed]
36. Pedraza-Brindis, E.J.; Sanchez-Reyes, K.; Hernandez-Flores, G.; Bravo-Cuellar, A.; Jave-Suarez, L.F.; Aguilar-Lemarroy, A.; Gomez-Lomeli, P.; Lpez-Lopez, B.A.; Ortiz-Lazareno, P.C. Culture supernatants of cervical cancer cells induce an M2 phenotypic profile in THP-1 macrophages. *Cell. Immunol.* **2016**, *310*, 42–52. [CrossRef]
37. Chandrashekar, D.S.; Bashel, B.; Balasubramanya, S.A.H.; Creighton, C.J.; Ponce-Rodriguez, I.; Chakravarthi, B.; Varambally, S. UALCAN: A Portal for Facilitating Tumor Subgroup Gene Expression and Survival Analyses. *Neoplasia* **2017**, *19*, 649–658. [CrossRef]
38. Vissers, J.L.; Hartgers, F.C.; Lindhout, E.; Teunissen, M.B.; Figdor, C.G.; Adema, G.J. Quantitative analysis of chemokine expression by dendritic cell subsets in vitro and in vivo. *J. Leukoc. Biol.* **2001**, *69*, 785–793.
39. Jiang, S.; Yang, Y.; Fang, M.; Li, X.; Yuan, X.; Yuan, J. Co-evolution of tumor-associated macrophages and tumor neo-vessels during cervical cancer invasion. *Oncol. Lett.* **2016**, *12*, 2625–2631. [CrossRef]
40. Li, Y.Q.; Liu, F.F.; Zhang, X.M.; Guo, X.J.; Ren, M.J.; Fu, L. Tumor secretion of CCL22 activates intratumoral Treg infiltration and is independent prognostic predictor of breast cancer. *PLoS ONE* **2013**, *8*, e76379. [CrossRef]
41. Zhou, M.; Bracci, P.M.; McCoy, L.S.; Hsuang, G.; Wiemels, J.L.; Rice, T.; Zheng, S.; Kelsey, K.T.; Wrensch, M.R.; Wiencke, J.K. Serum macrophage-derived chemokine/CCL22 levels are associated with glioma risk, CD4 T cell lymphopenia and survival time. *Int. J. Cancer* **2015**, *137*, 826–836. [CrossRef] [PubMed]
42. Wu, S.; He, H.; Liu, H.; Cao, Y.; Li, R.; Zhang, H.; Li, H.; Shen, Z.; Qin, J.; Xu, J. C-C motif chemokine 22 predicts postoperative prognosis and adjuvant chemotherapeutic benefits in patients with stage II/III gastric cancer. *Oncoimmunology* **2018**, *7*, e1433517. [CrossRef]
43. Huang, Y.H.; Chang, C.Y.; Kuo, Y.Z.; Fang, W.Y.; Kao, H.Y.; Tsai, S.T.; Wu, L.-W. Cancer-associated fibroblast-derived interleukin-1beta activates the pro-tumor CCL22 signaling in head and neck cancer. *Cancer Sci.* **2019**, *110*, 2783–2793. [CrossRef] [PubMed]
44. Furudate, S.; Fujimura, T.; Kambayashi, Y.; Kakizaki, A.; Hidaka, T.; Aiba, S. Immunomodulatory Effect of Imiquimod Through CCL22 Produced by Tumor-associated Macrophages in B16F10 Melanomas. *Anticancer Res.* **2017**, *37*, 3461–3471. [CrossRef] [PubMed]
45. Zhao, M.Y.; Zhao, J.; Yang, T.; Wang, L.; Pei, M.L.; Tian, S.J.; Yu, Y.; Yang, X.-F. Aberrant Expressions of Immune Factors Facilitate the Disequilibrium of Immune Status in Cervical Cancer. *Zhongguo Yi Xue Ke Xue Yuan Xue Bao* **2016**, *38*, 522–527. [CrossRef] [PubMed]
46. Kimura, S.; Nanbu, U.; Noguchi, H.; Harada, Y.; Kumamoto, K.; Sasaguri, Y.; Nakayama, T. Macrophage CCL22 expression in the tumor microenvironment and implications for survival in patients with squamous cell carcinoma of the tongue. *J. Oral Pathol. Med.* **2019**, *48*, 677–685. [CrossRef]

© 2019 by the authors. Licensee MDPI, Basel, Switzerland. This article is an open access article distributed under the terms and conditions of the Creative Commons Attribution (CC BY) license (http://creativecommons.org/licenses/by/4.0/).

References

[1] Paget S. The distribution of secondary growths in cancer of the breast. 1889. Cancer Metastasis Rev. 1989; 8:98–101.

[2] Qian B, Deng Y, Im JH, Muschel RJ, Zou Y, Li J, Lang RA, Pollard JW. A distinct macrophage population mediates metastatic breast cancer cell extravasation, establishment and growth. PLoS One. 2009.4:e6562.

[3] Schreiber RD, Old LJ, Smyth MJ (2011) Cancer immunoediting: integrating immunity's roles in cancer suppression and promotion. Science 331:1565–1570.

[4] Maude SL, Frey N, Shaw PA, et al. Chimeric antigen receptor T cells for sustained remissions in leukemia. N Engl J Med 2014;371:1507–17

[5] Morrissey, K. M., Yuraszeck, T. M., Li, C. C., Zhang, Y. & Kasichayanula, S. Immunotherapy and novel combinations in oncology: current landscape, challenges, and opportunities. Clin. Transl. Sci. 9, 89–104 (2016).

[6] Qin L, Zhao R, Chen D, et al. Chimeric antigen receptor T cells targeting PD-L1 suppress tumor growth. Biomark Res 2020;8:19–31.

[7] Kambhampati S, Gray L, Fakhri B, et al. Immune-related adverse events associated with checkpoint inhibition in the setting of CAR T cell therapy: a case series. Clin Lymphoma Myeloma Leuk 2020;20:e118–23.

[8] Hyman DM, Taylor BS, and Baselga J (2017) Implementing genome-driven oncology. Cell 168:584–599.

[9] Telang S, Rasku M A, Clem A L, et al. Phase Ⅱ trial of the regulatory T cell-depleting agent, denileukin diftitox, in patients with unresectable stage Ⅳ melanoma. BMC Cancer, 2011, 11: 515

[10] Tandon AK, Clark GM, Chamnes GC, et al. HER-2/neu oncogene protein and prognosis in breast cancer. J Clin Ocol, 1989,7 (8): 1120-1128.

[11] Chapman PB, Hauschld A, Robert C, et al. Improved srvival with vemurafenib in melanoma with BRAF V600E mutation. N Engl J Med, 2011, 364 (26): 2507-2516.

[12] Lynch TJ, Bell DW, Sordella R, et al. Activating mutations in the epidermal growth fator receptor underlying responsiveness of non-small-cell lung cancer to gefitinib. N Eng J Med.2004,350(21): 2129-2139.

[13] Druker BJ, Guilhot F, Brien SG, et al. Five years follow-up of patients receiving imatinib for chronic myeloid leukemia. N Engl J Med, 2006, 35 (23): 2408-2417.

[14] Llovet JM, Ricci S, Mazzaferro V, et al. Sorafenib in advanced hepatocellular carcinoa. N Engl J Med, 2008, 359 (4): 378-390.

[15] Richardson PG, Sonneveld P, Schuster M, et al. Extended follow-up of a phase 3 trial in relapsed multiple myeloma: final time-to-event results of the APEX trial. Blood, 2007, 110 (10): 3557-3560.

[16] Zighelboim I, Wright JD, Gao F, et al. Multicenter phase II trial of topotecan, cisplatin and bevacizumab for recurrent or persistent cervical cancer. Gynecol Oncol, 2013, 130 (1)：64-68

[17] Symonds RP，Gourley C，Davidson S，et al. Cediranib combined with carboplatin and paclitaxel in patients with metastatic or recurrent cervical cancer (CIRCCa): a randomised, double -blind, placebo - controlled phase 2 trial. Lancet Oncol，2015，16（15）：1515-1524.

[18] Farley J，Sill MW，Birrer M，et al. Phase II study of cisplatin plus cetuximab in advanced, recurrent, and previously treated cancers of the cervix and evaluation of epidermal growth factor receptor immunohistochemical expression: a Gynecologic Oncology Group study. Gynecol Oncol, 2011, 121(2):303-308.

[19] Sharma DN，Rath GK，Julka PK，et al. Role of gefitinib in patients with recurrent or metastatic cervical carcinoma ineligible or refractory to systemic chemotherapy: first study from Asia. Int J Gynecol Cancer，2013，23(4)：705-709.

[20] Nogueira-Rodrigues A，Moralez G，Grazziotin R，et al. Phase 2 trial of erlotinib combined with cisplatin and radiotherapy in patients with locally advanced cervical cancer. Cancer，2014，120（8）：1187- 1193

[21] P. J. Lou et al., PMMA particle-mediated DNA vaccine for cervical cancer. J Biomed Mater Res A.2009. 88, 849-857.

[22]S. Jantova et al, Immunobiological efficacy and immunotoxicity of novel synthetically prepared fluoroquinolone ethyl 6-fluoro-8-nitro-4-oxo-1,4-dihydroquinoline-3-carboxylate. Immunobiology. 2018. 223, 81-93.

[23] Y. Ohshika, N. Umesaki, T. Sugawa, Immunomodulating capacity of the monocyte-macrophage system in patients with uterine cervical cancer. Nihon Sanka Fujinka Gakkai Zasshi. 1998. 40, 601-608.

[24] J. T. Chen et al., [Sizofiran and recombinant interferon gamma stimulate peritoneal macrophages obtained from patients with gynecologic malignancies--increased secretion of tumor necrosis factor, IL-1 and interferon-gamma]. Gan To Kagaku Ryoho. 1990. 17, 1365-1369.

[25] K. Hasegawa et al., [Electron microscopic and immunological studies concerning the effect on the antitumor activity of sizofiran (SPG) combined with radiotherapy for cervical cancer]. Nihon Gan Chiryo Gakkai Shi. 1990. 25, 2549-2561.

[26] T. C. van der Sluis et al., Therapeutic Peptide Vaccine-Induced CD8 T Cells Strongly Modulate Intratumoral Macrophages Required for Tumor Regression. Cancer Immunol Res. 2015. 3, 1042-1051.

[27] C. Rosales, V. V. Graham, G. A. Rosas, H. Merchant, R. Rosales, A recombinant vaccinia virus containing the papilloma E2 protein promotes tumor regression by stimulating macrophage antibody-dependent cytotoxicity. Cancer Immunol Immunother. 2000. 49, 347-360.

[28] Thomas H, Coley HM, et al. Overcoming multidrug resistance in cancer: an update on the clinical strategy of inhibiting p-glycoprotein. Cancer Control, 2003,10(2): 159-165

[29] Shuklas, Chen ZS, Ambudkar SV, et al. Tyrosine kinase inhibitors as modulators of ABC transporter mediated drug resistance. Drug Tesist Updat, 2012, 15 (1-2) : 70-80.

[30] Shih JY, Gow Ch, Yang PC, et al. EGFR mutation conferring primary resistance to gefitinib in non-small-cell lung cancer. N Engl J Med, 2005, 353 (2): 207-208.

[31] Mcdermott U, Settleman J. Personalized cancer therapy with selective kinase inhibitors: an emerging paradigm in medical oncology. J Clin Oncol, 2009, 27 (33): 5650-5659.

[32] Huang S, Holzel M, Knijnenburg T, et al. Med12 controls the response to multiple cancer drugs through regulation of TGF-beta receptor signaling. Cell, 2012, 151 (5): 937-950.

[33] Wilson TR, Fridlyand J, Yan Y, et al. Widespread potential for growth-factor-driven resistance to anticancer kinase inhibitors. Nature, 2012, 487 (7408): 505-509

[34] Crawford Y, Kasman I , Yu L, et al. PDGF-C mediates the angiogenic and tumorigenic properties of fibroblasts assoicated with tumors refractory to anti VEGF treatment. Cancer Cell, 2009, 15 (1) : 21-34.

[35] Lei L, Xiao-Li W, Qian L, et al. Comprehensive immunogenomic landscape analysis of prognosis-related genes in head and neck cancer. Sci Rep. 2020 Apr 14;10(1):6395.

[36] Yuan-Lin S, Yang Z, Yu-Chen G, et al. A Prognostic Model Based on the Immune-related Genes in Colon Adenocarcinoma. Int J Med Sci. 2020 Jul 19;17(13):1879-1896.

[37] Hao Zh, Haijian Zh, Muqi Sh, et al. A robust signature associated with patient prognosis and tumor immune microenvironment based on immune-related genes in lung squamous cell carcinoma. Int Immunopharmacol. 2020 Nov;88:106856.

[38] Jie Zh, Han W, Ting M, et al. Identification of immune-related genes as prognostic factors in bladder cancer. Sci Rep. 2020 Nov 12;10(1):19695.

[39] Wu H.Y., Li Q.Q., Liang L., Qiu L.L., Wei H.W., Huang B.Y., Chen G., He R.Q., Huang Z.G., Hou W., et al. Prognostic alternative splicing signature in cervical squamous cell carcinoma. IET Syst. Biol. 2020;14:314–322.

[40] Eun J.K., Mi H.H., Jeon Y.J., Yun H.K. Identification and Complete Validation of Prognostic Gene Signatures for Human Papillomavirus-Associated Cancers: Integrated Approach Covering Different Anatomical Locations. J. Virol. 2020:JVI.02354-20.

[41] Cai L.Y., Hu C., Yu S.S., Liu L.X., Yu X.B., Chen J.H., Liu X., Lin F., Zhang C., Li X.Y. Identification and validation of a six-gene signature associated with glycolysis to predict the prognosis of patients with cervical cancer. BMC Cancer. 2020;20:1133.

[42] Zhao S., Yu M.X. Identification of MMP1 as a Potential Prognostic Biomarker and Correlating with Immune Infiltrates in Cervical Squamous Cell Carcinoma. DNA Cell Biol. 2020;39:255–272. doi: 10.1089/dna.2019.5129.

[43] Chen Q., Hu L., Huang D., Chen K., Qiu X., Qiu B. Six-lncRNA Immune Prognostic Signature for Cervical Cancer. Front. Genet. 2020;11:533628.

[44] Chen H., Deng Q., Wang W., Tao H., Gao Y. Identification of an autophagy-related gene signature for survival prediction in patients with cervical cancer. J. Ovaian Res. 2020;13:131.

[45] Gu Z., Wang H., Xia J., Yang Y., Jin Z., Xu H., Shi J., De Domenico I., Tricot G., Zhan F. Decreased ferroportin promotes myeloma cell growth and osteoclast differentiation. Cancer Res. 2015;75:2211–2221.

[46] Song J.Y., Lee J.K., Lee N.W., Jung H.H., Kim S.H., Lee K.W. Microarray analysis of normal cervix, carcinoma in situ, and invasive cervical cancer: Identification of candidate genes in pathogenesis of invasion in cervical. Int. J. Gynecol. Cancer. 2008;18:1051–1059.

[47] Castro F.A., Haimila K., Sareneva I., Schmitt M., Lorenzo J., Kunkel N., Kumar R., Försti A., Kjellberg L., Hallmans G., et al. Association of HLA-DRB1, interleukin-6 and cyclin D1 polymorphisms with cervical cancer in the Swedish population--a candidate gene approach. Int. J. Cancer. 2009;125:1851–1858.

[48] Bodelon C., Madeleine M.M., Johnson L.G., Du Q., Galloway D.A., Malkki M., Petersdorf E.W., Schwartz S.M. Genetic variation in the TLR and NF-kappaB pathways and cervical and vulvar cancer risk: A population-based case-control study. Int. J. Cancer. 2014;134:437–444.

[49] Hugo de Almeida V., Guimaraes I.D.S., Almendra L.R., Rondon A.M.R., Tilli T.M., de Melo A.C., Sternberg C., Monteiro R.Q. Positive crosstalk between EGFR and the TF-PAR2 pathway mediates resistance to cisplatin and poor survival in cervical cancer. Oncotarget. 2018;9:30594–30609.

[50] Shanshan H., Lan X., Xia L., Huang W., Meifang Z., Ling Y. Inhibition of protease-activated receptor-2 induces apoptosis in cervical cancer by inhibiting signal transducer and activator of transcription-3 signaling. J. Int. Med. Res. 2019;47:1330–1338.

[51] Leo C., Horn L.C., Einenkel J., Hentschel B., Hockel M. Tumor hypoxia and expression of c-met in cervical cancer. Gynecol. Oncol. 2007;104:181–185.

[52] Liu D., Zhou P., Zhang L., Gong W., Huang G., Zheng Y., He F. HDAC1/DNMT3A-containing complex is associated with suppression of Oct4 in cervical cancer cells. Biochemistry. 2012;77:934–940.

[53] Lu J., Li X., Tu K., Guan Y., Fung K.P., Liu F. Verticillin A suppresses HGF-induced migration and invasion via repression of the c-Met/FAK/Src pathway in human gastric and cervical cancer cells. Onco. Targets Ther. 2019;12:5823–5833.

[54] Liu C.Y., Chao T.K., Su P.H., Lee H.Y., Shih Y.L., Su H.Y., Chu T.-Y., Yu M.-H., Lin Y.-W., Lai H.-C. Characterization of LMX-1A as a metastasis suppressor in cervical cancer. J. Pathol. 2009;219:222–231.

[55] Ye F., Yu Y., Hu Y., Lu W., Xie X. Alterations of dendritic cell subsets in the peripheral circulation of patients with cervical carcinoma. J. Exp. Clin. Cancer Res. 2010;29:78.

[56] Battaglia A., Buzzonetti A., Martinelli E., Fanelli M., Petrillo M., Ferrandina G., Scambia G., Fattorossi A. Selective changes in the immune profile of tumor-draining lymph nodes after different neoadjuvant chemoradiation regimens for locally advanced cervical cancer. Int. J. Radiat. Oncol. Biol. Phys. 2010;76:1546–1553.

[57] Zhu X., Lv J., Yu L., Zhu X., Wu J., Zou S., Jiang S. Proteomic identification of differentially-expressed proteins in squamous cervical cancer. Gynecol. Oncol. 2009;112:248–256.

[58] Tao X.H., Shen J.G., Pan W.L., Dong Y.E., Meng Q., Honn K.V., Jin R. Significance of SHP-1 and SHP-2 expression in human papillomavirus infected Condyloma acuminatum and cervical cancer. Pathol. Oncol. Res. 2008;14:365–371.

[59] Zhang H., Zhang S. The expression of Foxp3 and TLR4 in cervical cancer: Association with immune escape and clinical pathology. Arch. Gynecol. Obstet. 2017;295:705–712.

[60] Tang J., Yang Z., Wang Z., Li Z., Li H., Yin J., Deng M., Zhu W., Zeng C. Foxp3 is correlated with VEGF-C expression and lymphangiogenesis in cervical cancer. World J. Surg. Oncol. 2017;15:173.

[61] Luo Q., Zhang S., Wei H., Pang X., Zhang H. Roles of Foxp3 in the occurrence and development of cervical cancer. Int. J. Clin. Exp. Pathol. 2015;8:8717–8730.

[62] Li R., Yan Q., Tian P., Wang Y., Wang J., Tao N., Li N., Lin X., Ding L., Liu J.W., et al. CBX7 Inhibits Cell Growth and Motility and Induces Apoptosis in Cervical Cancer Cells. Mol. Ther. Oncolytics. 2019;15:108–116.

[63] Zhai N.C., Chi X.M., Li T.Y., Song H.X., Li H.J., Jin X., Ian N.C., Su L.S., Niu J.Q., Tu Z.K. Hepatitis C virus core protein triggers expansion and activation of CD4(+)CD25(+) regulatory T cells in chronic hepatitis C patients. Cell Mol. Immunol. 2015;12:743–749.

[64] Davidson, B.; Goldberg, I.; Kopolovic, J. Inflammatory response in cervical intraepithelial neoplasia and squamous cell carcinoma of the uterine cervix. Pathol. Res. Pract. 1997, 193, 491–495.

[65] Al-Saleh, W.; Delvenne, P.; Arrese, J.E.; Boniver, J.; Nikkels, A.F. Inverse modulation of intraepithelial Langerhans' cells and stromal macrophage/dendrocyte populations in human papillomavirus-associated squamous intraepithelial lesions of the cervix. Virchows Arch. 1995, 427, 41–48.

[66] Heller, D.S.; Hameed, M.; Cracchiolo, B.; Wiederkehr, M.; Scott, D.; Skurnick, J.; Ammar, N.; Lambert, W.C. Presence and quantification of macrophages in squamous cell carcinoma of the cervix. Int. J. Gynecol. Cancer 2003, 13, 67–70.

[67] Davidson, B.; Goldberg, I.; Gotlieb, W.H.; Lerner-Geva, L.; Ben-Baruch, G.; Agulansky, L.; Novikov, I.; Kopolovic, J. Macrophage infiltration and angiogenesis in cervical squamous cell carcinoma— Clinicopathologic correlation. Acta Obstet. Gynecol. Scand. 1999, 78, 240–244

[68] Ring, K. L., Yemelyanova, A. V., Soliman, P. T., Frumovitz, M. M. & Jazaeri, A. A. Potential immunotherapy targets in recurrent cervical cancer. Gynecologic oncology 145, 462–468; 10.1016/j.ygyno.2017.02.027 (2017).

[69] Le Buanec, H. et al. HPV-16 E7 but not E6 oncogenic protein triggers both cellular immunosuppression and angiogenic processes. Biomedicine & pharmacotherapy = Biomedecine & pharmacotherapie 53, 424–431; 10.1016/S0753-3322(99)80122-X (1999).

[70] Wang Q, Wei, Y. & Zhang, J. Combined Knockdown of D-dopachrome Tautomerase and Migration Inhibitory Factor Inhibits the Proliferation, Migration, and Invasion in Human Cervical Cancer. International journal of gynecological cancer : official journal of the International Gynecological Cancer Society 27, 634–642;

[71] Chen, X.J.; Han, L.F.; Wu, X.G.; Wei, W.F.; Wu, L.F.; Yi, H.Y.; Yan, R.M.; Bai, X.Y.; Zhong, M.; Yu, Y.H.; et al. Clinical significance of CD163+ and CD68+ tumor-associated macrophages in high-risk HPV-related cervical cancer. J. Cancer 2017, 8, 3868–3875.

[72] Kawachi, A.; Yoshida, H.; Kitano, S.; Ino, Y.; Kato, T.; Hiraoka, N. Tumor-associated CD204(+) M2 macrophages are unfavorable prognostic indicators in uterine cervical adenocarcinoma. Cancer Sci. 2018, 109, 863–870.

[73] Li, Y.; Huang, G.; Zhang, S. Associations between intratumoral and peritumoral M2 macrophage counts and cervical squamous cell carcinoma invasion patterns. Int. J. Gynaecol. Obstet. 2017, 139, 346–351.

[74] F. C. B. Berti, A. P. L. Pereira, G. C. M. Cebinelli, K. P. Trugilo, K. Brajao de Oliveira, The role of interleukin 10 in human papilloma virus infection and progression to cervical carcinoma. Cytokine Growth Factor Rev 34, 1-13 (2017).

[75] J. M. Oh et al., Human papillomavirus E5 protein induces expression of the EP4 subtype of prostaglandin E2 receptor in cyclic AMP response element-dependent pathways in cervical cancer cells. Carcinogenesis 30, 141-149 (2009).

[76]K. Subbaramaiah, A. J. Dannenberg, Cyclooxygenase-2 transcription is regulated by human papillomavirus 16 E6 and E7 oncoproteins: evidence of a corepressor/coactivator exchange. Cancer Res 67, 3976-3985 (2007).

[77] A. Mantovani et al., The chemokine system in diverse forms of macrophage activation and polarization. Trends Immunol 25, 677-686 (2004).

[78] J. K. Riley, K. Takeda, S. Akira, R. D. Schreiber, Interleukin-10 receptor signaling through the JAK-STAT pathway. Requirement for two distinct receptor-derived signals for anti-inflammatory action. J Biol Chem 274, 16513-16521 (1999).

[79] M. Heusinkveld et al., M2 macrophages induced by prostaglandin E2 and IL-6 from cervical carcinoma are switched to activated M1 macrophages by CD4+ Th1 cells. J Immunol 187, 1157-1165 (2011).

[80] K. J. Sales, A. A. Katz, R. P. Millar, H. N. Jabbour, Seminal plasma activates cyclooxygenase-2 and prostaglandin E2 receptor expression and signalling in cervical adenocarcinoma cells. Mol Hum Reprod 8, 1065-1070 (2002).

[81]M. Muller, K. J. Sales, A. A. Katz, H. N. Jabbour, Seminal plasma promotes the expression of tumorigenic and angiogenic genes in cervical adenocarcinoma cells via the E-series prostanoid 4 receptor. Endocrinology 147, 3356-3365 (2006).

[82]C. L. Rametse et al., Inflammatory Cytokine Profiles of Semen Influence Cytokine Responses of Cervicovaginal Epithelial Cells. Front Immunol 9, 2721 (2018).

[83] X. J. Chen et al., The role of the hypoxia-Nrp-1 axis in the activation of M2-like tumor-associated macrophages in the tumor microenvironment of cervical cancer. Mol Carcinogen 58, 388-397 (2019).

[84] Liu L, Shi W, Xiao X, et al. BCG immunotherapy inhibits cancer progression by promoting the M1 macrophage differentiation of THP‑1 cells via the Rb/E2F1 pathway in cervical carcinoma. Oncol Rep. 2021 Nov;46(5):245.

[85] Jiang S, Yang Y, Fang M, et al. Co-evolution of tumor-associated macrophages and tumor neo-vessels during cervical cancer invasion. Oncol Lett. 2016 Oct;12(4):2625-2631.

[86] Mantovani A, Sica A, Locati M. New vistas on macrophage differentiation and activation. Eur J Immunol. 2007;37(1):14–16.

[87] Mantovani A, Sica A, Locati M. Macrophage polarization comes of age. Immunity. 2005;23(4):344–346.

[88] Mosser,D.M.(2003)Themanyfacesofmacrophageactivation.J.Leukoc. Biol. 73, 209–212.

[89] Stein, M., Keshav, S., Harris, N., and Gordon, S. (1992) Interleukin 4 potently enhances murine macrophage mannose receptor activity: A marker of alternative immunologic macrophage activation. J. Exp. Med. 176, 287–292

[90] Anderson, C. F., and Mosser, D. M. (2002) A novel phenotype for an activated macrophage: The type 2 activated macrophage. J. Leukoc. Biol. 72, 101–106

[91] Hong S, Qian J, Yang J, Li H, Kwak LW, Yi Q. Roles of idiotype-specific T cells in myeloma cell growth and survival: Th1 and CTL cells are tumoricidal while Th2 cells promote tumor growth. Cancer Res 2008;68:8456–64.

[92] Shen Y, Fujimoto S. A tumor-specific Th2 clone initiating tumor rejection via primed CD8+ cytotoxic T-lymphocyte activation in mice. Cancer Res 1996;56:5005–11.

[93] Mattes J, Hulett M, Xie W, Hogan S, Rothenberg ME, Foster P, et al. Immunotherapy of cytotoxic T cell-resistant tumors by T helper 2 cells: an eotaxin and STAT6-dependent process. J Exp Med 2003;197:387–93.

[94] Mantovani A, Sica A, Sozzani S, Allavena P, Vecchi A, et al. (2004) The chemokine system in diverse forms of macrophage activation and polarization. Trends in immunology 25: 677–686.

[95] Little AC, Pathanjeli P, Wu Z, Bao L, Goo LE, Yates JA, Oliver CR, Soellner MB, Merajver SD. IL-4/IL-13 Stimulated Macrophages Enhance Breast Cancer Invasion Via Rho-GTPase Regulation of Synergistic VEGF/CCL-18 Signaling. Front Oncol. 2019 May 31;9:456.

[96] Tanaka, K. [Effect of gynecologic cancer sera on functions of monocyte from healthy volunteers]. Nihon Sanka Fujinka Gakkai Zasshi 1982, 34, 1528–1534.

[97] De Vos van Steenwijk, P.J.; Ramwadhdoebe, T.H.; Goedemans, R.; Doorduijn, E.M.; van Ham, J.J.; Gorter, A.; van Hall, T.; Kuijjer, M.L.; van Poelgeest, M.I.; van der Burg, S.H.; et al. Tumor-infiltrating CD14-positive myeloid cells and CD8-positive T-cells prolong survival in patients with cervical carcinoma. Int. J. Cancer 2013, 133, 2884–2894.

[98] Pedraza-Brindis, E.J.; Sánchez-Reyes, K.; Hernández-Flores, G.; Bravo-Cuellar, A.; Jave-Suárez, L.F.; Aguilar-Lemarroy, A.; Gómez-Lomelí, P.; López-López, B.A.; Ortiz-Lazareno, P.C. Culture supernatants of cervical cancer cells induce an M2 phenotypic profile in THP-1 macrophages. Cell Immunol. 2016, 310, 42–52.

[99] Li, L.; Yu, S.; Zang, C. Low necroptosis process predicts poor treatment outcome of human papillomavirus positive cervical cancers by decreasing tumor-associated macrophages M1 polarization. Gynecol. Obstet. Investig. 2018, 83, 259–267.

[100] M. Heusinkveld et al., M2 macrophages induced by prostaglandin E2 and IL-6 from cervical carcinoma are switched to activated M1 macrophages by CD4+ Th1 cells. J Immunol 187, 1157-1165 (2011).

[101] T. Saito, M. E. Berens, C. E. Welander, Direct and indirect effects of human recombinant gamma-interferon on tumor cells in a clonogenic assay. Cancer Res 46, 1142-1147 (1986).

[102] Chen MM, Xiao X, Lao XM, et al. Polarization of tissue-resident TFH-like cells in human hepatoma bridges innate monocyte inflammation and M2b macrophage polarization. Cancer Discov. 2016;6: 1182–1195.

[103] Kim D, Koh J, Ko JS, Kim HY, Lee H, Chung DH. Ubiquitin E3 Ligase Pellino-1 Inhibits IL-10-mediated M2c Polarization of Macrophages, Thereby Suppressing Tumor Growth.

[104] Pathria P, Louis TL, Varner JA. Targeting tumor-associated macrophages in cancer. Trends Immunol. 2019;40(4):310–327.

[105] Zhang W, Zhu X D, Sun H C, et al. Depletion of tumor-associated macrophages enhances the effect of sorafenib in metastatic liver cancer models by antimetastatic and antiangiogenic effects. Clinical Cancer Research, 2010, 16(13): 3420-3430.

[106] Bianchini G, Gianni L. The immune system and response to HER2-targeted treatment in breast cancer. The Lancet Oncology, 2014, 15(2): e58-e68

[107] Wei J, Besner GE. M1 to M2 macrophage polarization in heparin binding epidermal growth factor-like growth factor therapy for necrotizing enterocolitis. J Surg Res, 2015, 197(1):126-138.

[108] Kawachi A, Yoshida H, Kitano S, et al. Tumor-associated CD204 (+) M2 macrophages are unfavorable prognostic indicators in uterine cervical adenocarcinoma. Cancer Sci, 2018, 109(3): 863-870.

[109] Owen KL, Brockwell NK, Parker BS. JAK-STAT Signaling: A Double-Edged Sword of Immune Regulation and Cancer Progression. Cancers (Basel), 2019, 11(12):138-142.

[110] Ren C, Cheng X, Lu B, et al. Activation of interleukin-6/signal transducer and activator of transcription 3 by human papillomavirus early proteins 6 induces fibroblast senescence to promote cervical tumourigenesis through autocrine and paracrine pathways in tumour microenvironment. Eur J Cancer, 2013, 49(18): 3889-3899.

[111] Siegel RL, Miller KD, Jemal A. Cancer statistics, 2020. CA Cancer J Clin. 2020;70(1):7–30.

[112] Hanikezi T, Shaadaiti W, Mayinuer A, Zhao J, Guzainuer M, Mourboul A, et al. Impacts of isoliquiritigenin on proliferation and apoptosis of human cervical cancer cells. Eur J Gynaecol Oncol. 2019;40(3):425–30.

[113] SmallW, BaconMA, BajajA, et al. Cervical cancer: a global health crisis [J]. Cancer, 2017, 123(13): 2404-2412.

[114] Lin M, Ye M, Zhou J, Wang ZP, Zhu X. Recent advances on the molecular mechanism of cervical carcinogenesis based on systems biology technologies. Comput Struct Biotechnol J. 2019;17:241–50.

[115] Huang Y.H., Chang C.Y., Kuo Y.Z., Fang W.Y., Kao H.Y., Tsai S.T., Wu L.-W. Cancer-associated fibroblast-derived interleukin-1beta activates the pro-tumor CCL22 signaling in head and neck cancer. Cancer Sci. 2019;110:2783–2793.

[116] Kimura S., Nanbu U., Noguchi H., Harada Y., Kumamoto K., Sasaguri Y., Nakayama T. Macrophage CCL22 expression in the tumor microenvironment and implications for survival in patients with squamous cell carcinoma of the tongue. J. Oral Pathol. Med. 2019;48:677–685.

[117] Wei C., Yang C., Wang S., Shi D., Zhang C., Lin X., Xiong B. M2 macrophages confer resistance to 5-fluorouracil in colorectal cancer through the activation of CCL22/PI3K/AKT signaling. OncoTargets Ther. 2019;12:3051–306

[118] Schmid MP, Franckena M, Kirchheiner K, Sturdza A, Georg P, Dörr W, et al. Distant metastasis in patients with cervical cancer after primary radiotherapy with or without chemotherapy and image guided adaptive brachytherapy. Gynecol Oncol. 2014;133(2):256–62

[119] ChungHC, SchellensJHM, DelordJP, et al. Pembrolizumab treatment of advanced cervical cancer: updated results from the phase 2 KEYNOTE-158 study [J]. J Clin Oncol, 2018, 36(15Suppl): 5522.

[120] MaciagPC, RadulovicS, RothmanJ, et al. The first clinical use of a live-attenuated listeria monocytogenes vaccine: a phase Ⅰ safety study of Lm-LLO-E7 in patients with advanced carcinoma of the cervix [J]. Vaccine, 2009, 27(30): 3975-3983.

[121] Yamashita U, Kuroda E, et al. Regulation of macrophage-derived chemokine (MDC, CCL22) production. Crit Rev Immunol. 2002;22:105–14.

[122] Wang G, Yu D, Tan W, et al. Genetic polymorphism in chemokine CCL22 and susceptibility to Helicobacter pylori infection‐related gastric carcinoma. Cancer. 2009;115:2430‐7.

[123] Nishikawa H, Sakaguchi S, et al. Regulatory T cells in tumor immunity. Int J Cancer. 2010;127:759-67.

[124] Godiska, R.; Chantry, D.; Raport, C.J.; Sozzani, S.; Allavena, P.; Leviten, D.; Mantovani, A.; Gray, P.W. Human macrophage-derived chemokine (MDC), a novel chemoattractant for monocytes, monocyte-derived dendritic cells, and natural killer cells. J. Exp. Med. 1997, 185, 1595–1604.

[125] Chang, M.; McNinch, J.; Elias, C., 3rd; Manthey, C.L.; Grosshans, D.; Meng, T.; Boone, T.; Andrew, D. Molecular cloning and functional characterization of a novel CC chemokine, stimulated T cell chemotactic protein (STCP-1) that specifically acts on activated T lymphocytes. J. Biol. Chem. 1997, 272, 25229–25237.

[126] Schaniel, C.; Pardali, E.; Sallusto, F.; Speletas, M.; Ruedl, C.; Shimizu, T.; Seidl, T.; Andersson, J.; Melchers, F.; Rolink, A.G.; et al. Activated murine B lymphocytes and dendritic cells produce a novel CC chemokine which acts selectively on activated T cells. J. Exp. Med. 1998, 188, 451–463.

[127] Li Y.Q., Liu F.F., Zhang X.M., Guo X.J., Ren M.J., Fu L. Tumor secretion of CCL22 activates intratumoral Treg infiltration and is independent prognostic predictor of breast cancer. PLoS ONE. 2013;8:e76379.

[128] Zhou M., Bracci P.M., McCoy L.S., Hsuang G., Wiemels J.L., Rice T., Zheng S., Kelsey K.T., Wrensch M.R., Wiencke J.K. Serum macrophage-derived chemokine/CCL22 levels are associated with glioma risk, CD4 T cell lymphopenia and survival time. Int. J. Cancer. 2015;137:826–836.

[129] Wu S., He H., Liu H., Cao Y., Li R., Zhang H., Li H., Shen Z., Qin J., Xu J. C-C motif chemokine 22 predicts postoperative prognosis and adjuvant chemotherapeutic benefits in patients with stage II/III gastric cancer. Oncoimmunology. 2018;7:e1433517.

[130] Wang X., Xie Y., Wang J. Overexpression of MicroRNA-34a-5p Inhibits Proliferation and Promotes Apoptosis of Human Cervical Cancer Cells by Downregulation of Bcl-2. Oncol. Res. 2018;26:977–985.

[131] Sobti R.C., Singh N., Hussain S., Suri V., Bharti A.C., Das B.C. Overexpression of STAT3 in HPV-mediated cervical cancer in a north Indian population. Mol. Cell Biochem. 2009;330:193–199. doi: 10.1007/s11010-009-0133-2. [PubMed] [CrossRef] [Google Scholar]

[132] Takemoto S., Ushijima K., Kawano K., Yamaguchi T., Terada A., Fujiyoshi N., Nishio S., Tsuda N., Ijichi M., Kakuma T., et al. Expression of activated signal transducer and activator of transcription-3 predicts poor prognosis in cervical squamous-cell carcinoma. Br. J. Cancer. 2009;101:967–972. doi: 10.1038/sj.bjc.6605212. [PMC free article] [PubMed] [CrossRef] [Google Scholar]

[133] Sobti R.C., Singh N., Hussain S., Suri V., Bharadwaj M., Das B.C. Deregulation of STAT-5 isoforms in the development of HPV-mediated cervical carcinogenesis. J. Recept. Signal Transduct. Res. 2010;30:178–188.

[134] Shanshan H., Lan X., Xia L., Huang W., Meifang Z., Ling Y. Inhibition of protease-activated receptor-2 induces apoptosis in cervical cancer by inhibiting signal transducer and activator of transcription-3 signaling. J. Int. Med. Res. 2019;47:1330–1338

Acknowledgements

I would like to express my thanks to everyone I meet in Munich, the opportunity being in the lab full of joy, warmness and happiness, and the financial supports from China Scholarship Council.

Firstly, I would like to express my great appreciations to Prof. Udo Jeschke for supervision of my doctoral study. I appreciate him for his support, patience, advice and trust in my research work. Apart from his brilliant scientific knowledge, I also learned practical skills from him no matter in scientific work or in life out of lab. I would like to acknowledge many thanks to Dr. Helene Hildegard Heidegger for her kindness and research support so I can adapt to the new environment quickly and my research work can keep going smoothly. I also thank both of them for giving me the opportunity to work in the Walter-Brendel Center for cooperation. I would also express many thanks to Dr. rer. nat. Kessler, Mirjana and the post Doctor Kritika Sudan for offering feasible advices for my research and M.D. Heather Mullikin for revising my manuscripts and instructing on my English writing.

Great thanks to the technicians Christina Kuhn, Gabriele Weimer, Cornelia Herbst, Sabine Fink, and Martina Rahmeh. I want to thank them for answering my questions patiently, showing me tiny detailed parts of experiments, and instructing me how to polish experimental techniques. Many thanks to my other colleagues Fangfang Chen, Yue Liao, Nan Han, Lili Lin, Ma Zhi, Mingjun Zheng, Huixia Yang and Yao Ye. I am grateful for being a member of such a supportive and cooperative working team.

I really appreciated Prof. Christian Schulz for encouraging and supporting me during learning Flow Cytometry in the Walter-Brendel Center. Lastly, I would like to thank my family for loving and supporting me in life. I also grateful to have my excellent friends (Haijun Xue and Xuankun Wang) for accompanying with me during my hard time and exploring different things together out of the lab.